OULU 2010
C 368

ACTA UNIVERSITATIS OULUENSIS

Johanna Vartiainen

CONCENTRATED SIGNAL EXTRACTION USING CONSECUTIVE MEAN EXCISION ALGORITHMS

UNIVERSITY OF OULU,
FACULTY OF TECHNOLOGY,
DEPARTMENT OF ELECTRICAL AND INFORMATION ENGINEERING;
UNIVERSITY OF OULU,
CENTRE FOR WIRELESS COMMUNICATIONS,
INFOTECH OULU

ACTA UNIVERSITATIS OULUENSIS
C Technica 368

JOHANNA VARTIAINEN

CONCENTRATED SIGNAL EXTRACTION USING CONSECUTIVE MEAN EXCISION ALGORITHMS

Academic dissertation to be presented with the assent of the Faculty of Technology of the University of Oulu for public defence in OP-sali (Auditorium L10), Linnanmaa, on 19 November 2010, at 12 noon

UNIVERSITY OF OULU, OULU 2010

Acta Univ. Oul. C 368, 2010

Supervised by
Professor Markku Juntti

Reviewed by
Professor Peter Händel
Professor Mikko Valkama

ISBN 978-951-42-6348-4 (Paperback)
ISBN 978-951-42-6349-1 (PDF)
http://herkules.oulu.fi/isbn9789514263491/
ISSN 0355-3213 (Printed)
ISSN 1796-2226 (Online)
http://herkules.oulu.fi/issn03553213/

Cover Design
Raimo Ahonen

JUVENES PRINT
TAMPERE 2010

Vartiainen, Johanna, Concentrated signal extraction using consecutive mean excision algorithms
University of Oulu, Faculty of Technology, Department of Electrical and Information Engineering, P.O.Box 4500, FI-90014 University of Oulu, Finland; University of Oulu, Centre for Wireless Communications, Infotech Oulu, P.O. Box 4500, FI-90014 University of Oulu, Finland
Acta Univ. Oul. C 368, 2010
Oulu, Finland

Abstract

Spread spectrum communication systems may be affected by other types of signals called outliers. These coexisting signals are typically narrow (or *concentrated*) in the considered domain. This thesis considers two areas of outlier detection, namely the concentrated interference suppression (IS) and concentrated signal detection. The focus is on concentrated signal extraction using blind, iterative and low-complex consecutive mean excision (CME) -based algorithms that can be applied to both IS and detection.

A summary of results obtained from studying the performance of the existing IS methods, namely the CME, the forward CME (FCME) and the transform selective IS algorithms (TSISA), is presented. Accurate threshold parameter values for the FCME algorithm are defined. These accurate values are able to control the false alarm rate. The signal detection capability of the CME algorithms is studied and analyzed. It is noticed that the CME algorithms are able to detect signals, but they are not able to estimate signal parameters such as the bandwidth. The presented generic shape-based analysis leads to the limits of detection in which the concentrated signals can be detected. These limits enable checking fast whether the signal is detectable or not without time consuming computer simulations. The performance of the TSISA method is evaluated. Simulation results demonstrate that the TSISA method is able to suppress several types of concentrated interfering signals with a reasonable computational complexity.

Finally, new CME-based methods are proposed and evaluated. The proposed methods are the extended TSISA method for IS and the localization algorithm based on double-thresholding (LAD), LAD with normalized thresholds (LAD NT), LAD with adjacent cluster combining (LAD ACC) and two-dimensional (2-D) LAD methods for detection. The simulations indicate that the extended TSISA method has a good performance against several types of concentrated interfering signals. The narrowband signal detection capability of the LAD methods is studied. Numerical results show that the proposed LAD methods are able to detect and localize signals in their domain, and they are able to estimate the number of narrowband signals and their parameters, including, for example, bandwidths and signal-to-noise ratio (SNR) values. The simulations show that the LAD methods outperform the CME algorithms, and ACC and 2-D LAD methods outperform the original LAD method. The LAD methods are also proposed to be used for spectrum sensing purposes in cognitive radios.

Keywords: interference suppression, signal detection, spectrum sensing

To my late grandparents Laina and Onni Vuorenmaa

Preface

"For I am a Bear of Very Little Brain and long words Bother me."
-Winnie the Pooh

The research work for this doctoral thesis has been carried out in the Centre for Wireless Communications (CWC), Department of Electrical and Information Engineering, University of Oulu, Oulu, Finland, during the years 2002-2009. Most of the research has been conducted in projects of the Future Radio Access (FUTURA), Packet Access Networks with Flexible Spectrum Use (PANU) and Cognitive and Opportunistic Wireless Communication Networks (COGNAC). The financial support provided by Finnish Defence Forces, Finnish Defence Forces Technical Research Centre, Nokia, Nokia Siemens Networks, Elektrobit Ltd., Instrumentointi, the Finnish Funding Agency for Technology and Innovation (TEKES), Academy of Finland and Infotech Oulu Graduate School is gratefully acknowledged. I am also grateful to the following Finnish foundations: Nokia foundation, Tauno Tönningin säätiö, Seppo Säynäjäkankaan tiedesäätiö, Takasen säätiö, Pohjois-Pohjanmaan kulttuurirahasto and Ahti Pekkalan säätiö for their financial support.

I would like to thank my supervisor Prof. Markku Juntti and Dr. Harri Saarnisaari for their support and guidance throughout this project. They have guided me through all the difficulties that I have had during this process. I also thank Dr. Janne Lehtomäki for his comments and guidance.

My special thanks belong to Prof. Pentti Leppänen for giving me the possibility to work at the CWC. I would also like to thank all my project managers throughout these years, especially the aforementioned Dr. Harri Saarnisaari, Dr. Pekka Pirinen and Dr. Timo Bräysy. I also thank all the coauthors. The contribution of the godfather of the LAD, M. Sc. Sami Aromaa, is gratefully acknowledged. I would also like to thank Alli Huovinen from the department of Mathematical Sciences.

My thanks go to the whole CWC and Telecommunication Laboratory staff including the administrative personnel. Especially I wish to thank Elina Komminaho and Antero Kangas for their kindness and Jari Sillanpää for his patience. Jari, I really don't know why all these strange things (burned mouse, etc.) happened to my computer.

I am very grateful to the reviewers of this thesis, Prof. Peter Händel and Prof. Mikko Valkama.

I also thank Kaija Nissinen for the language revision.

I would like to express my gratitude to my family, especially to my parents Pentti Vartiainen and Marjaliisa Vuorenmaa, for their support and encouragement. I am always thankful to my late grandparents Laina and Onni Vuorenmaa for being my grandparents. I also thank Olavi Pelkonen for pushing me to finish this thesis. I would like to thank all my friends - including Harriet Gullsten, Minna Isomursu, Mika Kellokoski and Maarit Pylkkö, Heljä Korkeala, Kari and Satu Lapinlampi, Sonja Latvakoski, Masa and Malla Mäkäräinen, Sami Niemelä, Anna Pankarinkangas, Pasi and Pia Parkkila, Maija Piippo, Marko Pistemaa, Heidi and Tapsa Rautio as well as Erja and Hannu Rönkkömäki. The families of Teija Meklin and Tarja Pelkonen are acknowledged. I also thank all my friends I have got to know within my hobbies.

My warmest and deepest gratitude belongs to my common-law husband Marko Nivalainen who has lived with me for over 18 years. Without his love, support, patience and delicious meals this work would never have been finished.

"The hardest part is what to leave behind, ... It's time to let go!"
- Winnie the Pooh

Oulu, September 6, 2010 Johanna Vartiainen

List of symbols and abbreviations

a	order parameter in FrFT/coefficient (LAD NT)
b	coefficient (LAD NT)
$\mathbf{C}$	shape parameter (usually the covariance)
E_b	the energy of the desired signal per bit
H	conjugate transpose
H_0	noise-only hypothesis
H_1	signal-present hypothesis
I	power of the concentrated signal
I_k	received frequency domain samples belonging to the kth estimated NB signal set
$i_i(n)$	ith concentrated signal
K	noise set size
M	number of transform domains
M_a	arithmetic mean
M_g	geometric mean
m	number of unknown concentrated signals
m'	estimated number of narrowband signal sets
N	set size
N_0	noise power spectral density
N_k	number of samples in the kth estimated NB signal set
N_{con}	number of corrupted samples
N_{tot}	total number of samples
n	adjacent samples below the lower threshold (LAD ACC)
P_D	probability of detection
P_{FA}	probability of false alarm
$P_{\text{FA,DES}}$	desired clean sample rejection rate
P_{lo}	fixing coefficient (LAD NT)
P_M	miss probability
P_{up}	fixing coefficient (LAD NT)
Q	set size
$\mathbf{r}$	vector

$\bar{\mathbf{r}}$	the location parameter (usually the mean)
$r(n)$	received discrete-time signal sample
$r_t(n)$	received time domain signal sample
$r_f(n)$	received windowed signal sample in the transform domain
S	power of the wideband signal
S_i	height of the ith signal lobe
$s(n)$	wideband direct sequence spread spectrum signal
T	threshold value
T_1	upper threshold parameter
T_2	lower threshold parameter
T_{CME}	threshold parameter
T_h	threshold
T_{l}	lower threshold
T_{l}'	lower threshold (LAD NT)
T_{new}	threshold (LAD NT)
T_{u}	upper threshold
T_{u}'	upper threshold (LAD NT)
T_x	threshold parameter (LAD NT)
W	width of the base signal
W_i	width of the ith signal lobe
$\{W(n)\}$	received frequency domain noise+wideband signal samples
x_i	zero-mean, independent, i.i.d. Gaussian distributed complex random variable
$\bar{x}$	average sample mean
$\overline{x^2}$	average sample mean (or energy)
β_i	relative width of the ith signal lobe
γ	the ratio of signal energy to noise power density
$\hat{\gamma}_k$	SNR estimate for the kth estimated narrowband signal
$\hat{\delta}$	estimate of the Rayleigh parameter of the received vector
ε	ratio of the number of corrupted samples to the total number of samples
ϵ	coefficient of variation
ζ	average sample mean
ζ_{new}	average sample mean (LAD NT)
$\eta(n)$	noise process

ξ	interference-to-signal ratio
ρ	normalization coefficient
ϱ	compression gain
$\hat{\sigma}$	estimate of the standard deviation

AWGN	additive white Gaussian noise
ACM	approximate conditional mean
BER	bit error rate
BPSK	binary phase shift keying
BW	bandwidth
CA	cell-averaging
CDMA	code division multiple access
CFAR	constant false alarm rate
CG	compression gain
CME	consecutive mean excision
CV	coefficient of variation
DFT	discrete Fourier transform
DS	direct sequence
DSSS	direct sequence spread spectrum
DTV	digital television
DUDE	dynamic undersea detection extractor
DVB-T	digital video broadcasting - terrestrial
FCME	forward consecutive mean excision
FCC	Federal Communications Commission
FFT	fast Fourier transform
FH	frequency hopping
FPGA	field-programmable gate array
FrFT	fractional Fourier transform
FSK	frequency shift keying
FT	Fourier transform
GHz	Gigahertz
GPS	global positioning system
HMM	hidden Markov model
IFrFT	inverse fractional Fourier transform
IFT	inverse Fourier transform

IS	interference suppression
ISR	interference-to-signal ratio
LAD	localization algorithm based on double-thresholding
LAD ACC	LAD with adjacent cluster combining
LAD NT	LAD with normalized thresholds
2-D LAD	two-dimensional LAD
LCME	limiter consecutive mean excision algorithm
LMS	least mean squares
LOS	line-of-sight
LPI/D	low probability of interception/detection
MF	matched filter
MFSK	M-ary frequency shift keying
MHz	Megahertz
MSD	Mahalanobis squared distance
MVE	minimum volume ellipsoid
NB	narrowband
NMSE	normalized mean square error
OFDM	orthogonal frequency division multiplexing
Ofcom	Office of Communications
PN	pseudo noise
PRC	percentile
PSD	power spectral density
PU	primary user
RC	raised cosine
RLS	recursive least squares
RMSE	root mean square error
SAW	surface acoustic wave
SINR	signal-to-interference plus noise ratio
SNR	signal-to-noise ratio
S/P	serial-to-parallel
SS	spread spectrum
SU	secondary user
TSISA	transform selective interference suppression algorithm
TV	television
UWB	ultra wideband

VSB	vestigial sideband
WARP	wireless open-access research platform
WLAN	wireless local area network
WRAN	wireless regional area network
XPS	Xilinx platform studio

List of original articles

This template is based on the following articles, which are referred to in the text by their Roman numerals (I–IX):

I Vartiainen J, Aromaa S, Saarnisaari H & Juntti M (2004) Performance Evaluation of Transform Selective Interference Suppression. IEEE Military Communications Conference MILCOM 2004, Monterey, CA, USA.
II Vartiainen J, Lehtomäki J, Saarnisaari H & Juntti M (2005) Interference Suppression in Several Transform Domains. IEEE Military Communication Conference MILCOM 2005, Atlantic City, USA.
III Vartiainen J., Lehtomäki J., Saarnisaari H & Henttu P (2004) Estimation of Signal Detection Threshold by CME algorithms. IEEE Vehicular Technology Conference VTC 2004 spring, Milan, Italy.
IV Lehtomäki J, Vartiainen J, Juntti M & Saarnisaari H (2007) CFAR Outlier Detection with Forward Methods. IEEE Transactions on Signal Processing 55(9): 4702–4706.
V Vartiainen J, Lehtomäki J, Saarnisaari H & Juntti M (2010) Limits of Detection for the Consecutive Mean Excision Algorithms. 5th International Conference on Cognitive Radio Oriented Wireless Networks and Communications CrownCom 2010, Cannes, France.
VI Vartiainen J, Lehtomäki J & Saarnisaari H (2005) Double-Threshold based Narrowband Signal Extraction. IEEE 61st Semiannual Vehicular Technology conference VTC 2005 spring, Stockholm, Sweden.
VII Vartiainen J, Saarnisaari H, Lehtomäki J & Juntti M (2006) A Blind Signal Localization and SNR Estimation Method. IEEE Military Communication Conference MILCOM 2006, Washington DC, USA.
VIII Vartiainen J, Sarvanko H, Lehtomäki J, Juntti M & Latva-aho M (2007) Spectrum Sensing with LAD based Methods. IEEE International Symposium on Personal, Indoor and Mobile Radio Communications PIMRC 2007, Athens, Greece.
IX Vartiainen J, Lehtomäki J, Saarnisaari H, Juntti M & Umebayashi K (2010) Two-Dimensional Signal Localization Algorithm for Spectrum Sensing. IEICE Transactions on Communications E93-B(11).

The contents of the papers can be divided into two categories which both are applications of outlier detection. Papers I and II are focused on interference suppression, whereas in Papers III-IX the focus is on signal detection. In Paper I, the performance of a filter-bank type interference suppression method called the TSISA is studied. The TSISA searches several transform domains and performs interference suppression in the transform in which the interference is the most narrow. The extended version of the TSISA is considered in Paper II. Therein, several transform domain selection methods are proposed. Both the TSISA and its extended version utilize the same interference suppression method called the FCME algorithm. The FCME algorithm belongs to the family of CME algorithms which includes iterative notch-type outlier detection methods that are able to find interfering narrow signals blindly, i.e., without *a priori* knowledge of their environment. The CME algorithms can be used in time, frequency, or in some other transform domain as long as the signal is narrow (i.e., concentrated) in the studied domain. Paper III introduces the idea of using the low-complex but effective CME algorithms as a narrowband signal detection method. In Paper IV, the false alarm probability of the FCME algorithm is analyzed. It is proposed that forward CA technique can be applied for outlier detection. The analysis of the CME algorithms is presented in Paper V, and in [148]. Therein, detection limits at which the CME algorithms are able to find concentrated signals are derived. In Paper VI, an enhancement of the FCME algorithm called the LAD method is proposed. The LAD method is a narrowband signal detection method that uses two thresholds and is able to localize the narrowband signal samples in the frequency. It is shown in Paper VII that because of a good localization ability, the LAD method is also able to estimate SNR values. Paper VIII proposes two new versions of the LAD method. In addition, it proposes the use of LAD methods in finding unoccupied frequencies in future cognitive radio systems. Finally, Paper IX proposes an extension of the LAD method that utilizes both time and frequency domain processing.

Contents

1 Introduction

"Keep it simple."

Since smoke signals, homing pigeons, telegraphic and landline telephones, data transmission methods have been vastly improved. Nowadays, wireless communication enables transforming information even long distances without the use of physical wires. In the modern wireless world, spread spectrum (SS) communication techniques are widely used [20, 28, 97, 102, 170]. In an SS system, the signal is spread in the frequency (Fourier) domain, so the used transmission bandwidth is significantly larger than the source information rate. The roots of SS techniques lie in World War II. In 1942, the actress Heddy Lamarr and the musician George Antheil patented the first form of an SS system called the "Secret Communications System" [123]. The system was developed to control armed torpedoes without the threat of intentional interference, i.e., jamming. The first SS systems were developed for military use. It was found out later that SS techniques are also attractive in commercial communications systems because the SS waveforms have several advantages over traditional ones. The benefits include the possibility of code division multiple access (CDMA), low probability of interception and detection (LPI/D), privacy, tolerance to co-channel interference as well as to multipath effects [133]. SS systems are also able to share a frequency band with non-spread systems. Nowadays, SS signals are used in several applications in both the military and civilian worlds. These include communications systems (e.g. Bluetooth [9]), wireless local area networks (WLAN) [9] and positioning systems (e.g. the global positioning system GPS).

SS information signals coexist usually with other types of signals. These signals can be, for example, narrowband (NB) or impulsive signals. A narrowband signal is a signal whose bandwidth in the frequency domain is much narrower than that of the SS signal. An impulsive or short duration signal is "narrow" in the time domain, i.e., it only covers a small fraction of the symbol interval of an SS system. Herein, a *concentrated signal* denotes a signal which is narrow either in the time or frequency domain or possibly in some other domain. The problem of identifying these coexisting signals can be seen as an *outlier detection problem*. From a statistical point of view, outliers can be defined to be samples that differ from the majority of data [160] as illustrated in Figure 1.

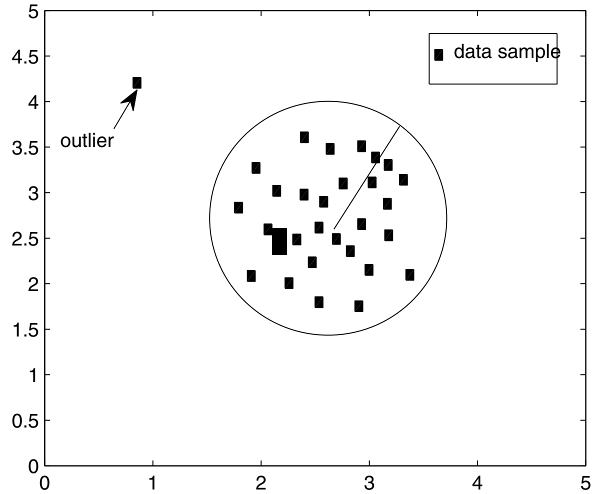

Fig. 1. An outlier is a data sample that differs from the majority of the data.

Outlier detection has numerous applications in several fields of science, and examples of outliers can be found almost everywhere. As a gardener classifies weeds as outliers and removes them by rooting up, the lowest and the highest style points in ski jumping are considered as outliers, and, thus, tossed out before calculating the sum of points. In the case of SS communication, an outlier, aka, concentrated signal sample has a large numerical value (usually the energy of a sample) when compared to the majority of the data samples (i.e., the clean data). This thesis considers two problems that both belong to the field of outlier detection, namely the concentrated interference suppression (IS) and concentrated signal detection. In the first one, interfering outliers are removed after the detection, whereas the second means pure detection. Even though the focus in this thesis is on NB signals, some other kind of concentrated signals are also considered.

1.1 Interference suppression

Interference or an interfering signal denotes a signal which is at the same time in the same transform domain as the information signal. Different communication systems, other electronic devices and natural phenomena such as lightning cause unintentional electromagnetic interference [86]. An environment with interference is illustrated in

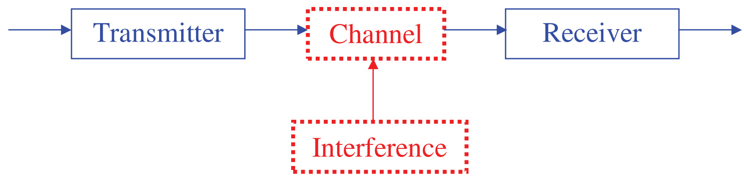

Fig. 2. A spread spectrum (SS) system with interference.

Figure 2. A narrow bandwidth or short duration and small power (i.e., time average of energy) are common to unintentional interference. In contrast, the power of intentional interference, jamming, may be large and the bandwidth wide. Interference causes performance degradation and may even prevent the recovery of the information from the received SS signal, especially if both the power and the bandwidth or the duration of interfering signal are large [27]. The SS systems have some implicit capability to reject the effects of interference. It is common to increase the tolerance to interference by increasing the signal power, using the frequency hopping (FH) technique, coding techniques or directional antennas. However, these methods are not necessarily sufficient, especially when the interfering signal is intentional. In these cases, the impact of interference should be minimized in order to improve the interference rejection capability of SS systems to guarantee reliable data transmission. This minimization can be done by limiting or zeroing the interfered samples.

A good IS method is blind and robust. A blind IS method needs no knowledge of the interfering signal or noise level. Robustness means that the method is able to handle several types of interfering signals. In addition, the computational complexity of a good IS method should be low. An effective IS filter should also be adaptive, since the characteristics of the interfering signals are usually not known, and change with time. Interference suppression causes performance loss. The amount of the performance loss depends on the interference suppression method used. For example, the losses for different types of notch filters have been evaluated in [162]. The loss can be compensated, for example, by increasing the signal-to-noise ratio (SNR) via increasing the transmitter power, using longer integration time, or using stronger coding.

1.2 Signal detection

In signal detection, the presence or absence of a signal is determined. In concentrated signal detection a wideband information signal may also be present with noise. In such a case, concentrated signal detection involves decision-making between two hypotheses: either there is only noise and possibly a wideband signal, or there is a concentrated signal embedded in the noise and possibly a wideband signal [65]. In many practical situations, this kind of simple binary detection is not sufficient. While binary detection simply decides if there is a signal or not, localization gives detailed information about the signal. In this context, localization means that the NB signal is localized in its domain, e.g., the frequency band of the NB signal is searched. Localization information may be used to characterize the detected signal. In frequency localization, the center frequency and bandwidth of a NB signal are estimated. Localization can also be done in other transform domains, for example, in the time domain, but this aspect is not considered in this thesis.

Localization information can be used, for example, when finding unoccupied frequency bands in future cognitive radios. The concept of cognitive radio was first proposed by Mitola III in the late 1990s [92, 94]. Since then, cognitive radio has been discussed in a number of papers, e.g., [14, 18, 53, 93, 122]. In this thesis, cognitive radio is defined as an intelligent device which is able to find out vacant channels for transmission and, if required, is able to change its transmission channels while avoiding interference with other users. According to [53], the key elements are awareness, intelligence, learning, adaptivity, reliability and efficiency. The cognitive radio approach is one possible solution to the problem of insufficient amount of frequencies suitable for wireless communication transmission. The cognitive network concept can be divided into three categories called underlay, overlay and interweave techniques [46]. In underlay systems, the cognitive radio is allowed to operate simultaneously with the non-cognitive users if the interference caused by the cognitive radio is below an acceptable threshold. This can be achieved, for example, using ultra wideband (UWB) communication signals. Overlay systems require information about the non-cognitive users' codebooks and messages. The cognitive radio may even help non-cognitive users transmission [46]. Interweave systems are based on the original idea of the cognitive radio [92, 94]. Therein, the main purpose is to find unoccupied frequency bands, i.e., "white spaces" or spectrum holes, for transmission. There, unlicensed or so called secondary users (SU) are allowed to use temporarily unoccupied frequency bands statically allo-

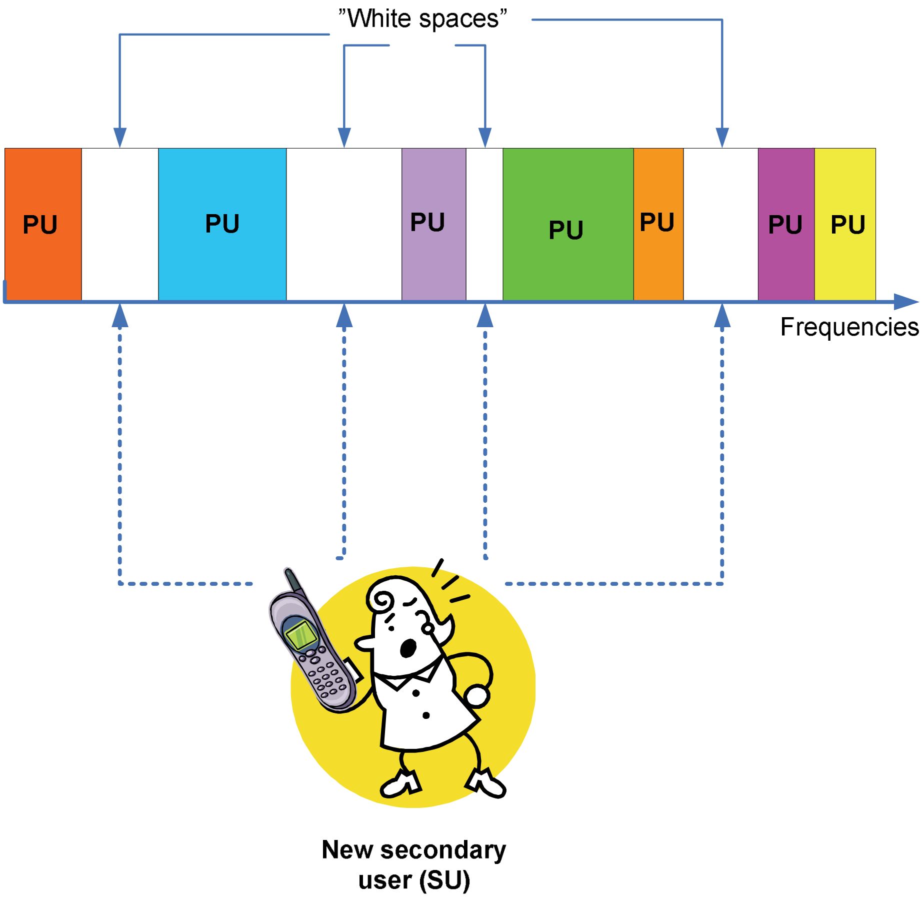

Fig. 3. Cognitive radio system. PU denotes primary user as SU denotes secondary user. "White space" denotes unoccupied frequencies what new SU is able to use.

cated to licensed or so called primary users (PU) if they do not cause any harm to the licensed users. In this thesis, mainly cognitive radio systems based on spectrum sensing are considered. The cognitive radio system is illustrated in Figure 3. The number of these unoccupied frequency bands varies over frequencies, time and geographic locations. However, because of inflexible spectrum allocation, it is widely known that the spectrum resources are not efficiently used [33–35, 37, 40]. Suggested channel candidates for cognitive radio operation are television (TV) broadcasting bands [37]. In Europe, the digital television (DTV) signal is based on orthogonal frequency division multiplexing (OFDM) [32] whereas in the Northern America, DTV signal is a Vestigial

Sideband (VSB) modulated signal [4]. The standardization of cognitive radio operation has already been started. For example, the Institute of Electrical and Electronics Engineers (IEEE) 802.22 wireless regional area network (WRAN) group established to develop a standard for WRAN cognitive radio devices in 2004. In 2006, the Federal Communications Commission (FCC) reported that fixed low-power devices could operate in unused TV channels [36]. In the United Kingdom, the Office of Communications (Ofcom) considered in 2007 the cognitive usage of TV bands [98]. In 2008, the FCC approved that unlicensed radios are able to operate in the TV bands under some specific rules [38]. The most important restriction is that secondary users are not allowed to interfere with primary users. This calls for a reliable location of unoccupied bands. The FCC resolved technical issues concerning "white spaces" in TV spectrum in September 2010 [39]. One of the most interesting issue is that devices incorporating geolocation and database access do not have to sense TV signals or low-power auxiliary service stations. Even though sensing is not required, it can be used, for example, to sense other secondary users. However, it should be kept in mind that this is the situation at the present moment in the specific frequencies in the United States. It is not known yet how the communications regulators in other countries react. In the end, time will tell what the role of sensing will be.

Signal detection methods, as well as many IS algorithms, are based on the use of a detection threshold [118]. The threshold can be fixed or adaptive. Adaptive thresholds are typically used under non-stationary conditions. The threshold calculation is based, for example, on the statistical properties of the noise-only case. The threshold is used to separate the samples into two sets. One set is assumed to be caused by noise (and a possible wideband information signal), and another set is caused by the concentrated signal. The setting of the threshold is a critical task. The signal energy at a certain frequency within the frequency band of the signal may temporarily drop below the threshold during the signal. This causes needless separation of the signal into two or more signals. Also, noise (and the possible wideband signal) may temporarily exceed the threshold and cause falsely detected signals. If the threshold is too high, the signal may be separated into several parts or the signal is not detected at all, but false detections are avoided. If, however, the threshold is too small, false detections become common but needless separation of the signal is avoided. Needless separation of signals as well as falsely detected signals cause problems especially when localization information of the signal, for example, the center frequency and bandwidth, is estimated.

1.3 The aim and outline of the thesis

The focus of this thesis is in two areas, namely concentrated interference suppression and concentrated signal detection. Both of these are applications of outlier detection. The goal is to consider low-complexity concentrated interference suppression and concentrated signal detection methods that are efficient but easy and possible to implement. The two main contributions are to investigate existing IS methods and to introduce new IS and detection methods.

The performance of the IS methods, namely the consecutive mean excision (CME) algorithm [57], the forward CME (FCME) algorithm [117] and the transform selective IS algorithm (TSISA) [3], is studied. From a practical point of view, it was noticed that it may be advantageous to use the same algorithm for IS and detection. Hence, another goal of this thesis is to show that the CME algorithms are also able to detect NB signals. In addition, a new FCME-based method called the localization algorithm based on double-thresholding (LAD) and its three versions are introduced for NB signal extraction and localization. Although the LAD methods are primarily used for detecting NB signals in the frequency domain, they may also be applied for detecting other concentrated signals in other domains.

This thesis is organized as follows. Chapter 2 presents a literature review of outlier detection and its two applications, interference suppression and signal detection. Section 2.1 gives an introduction to outlier detection. The existing interference suppression methods are reviewed in Section 2.2. Section 2.3 reviews briefly the concept of signal detection, focusing on the detection of unoccupied frequencies in future cognitive radios. In Section 2.4, the threshold setting problem is discussed briefly. The studied methods are presented and a summary of original papers is given in Chapter 3. Section 3.1 presents the system model. The CME algorithms, the TSISA method and the LAD methods are considered in Sections 3.2, 3.3 and 3.4, respectively. Therein, their performance reported in the original papers is also considered. Methods and performance considerations are presented in Chapter 3 in detail for readability and clarity. In addition, supplementary papers contributed by the author of this thesis are briefly reviewed to offer a more comprehensive general view. These supplementary papers are referred to in the text as all other references. Finally, a brief summary and discussion is presented in Chapter 4. The original papers are reprinted in Appendices.

1.4 Author's contribution to the publications

This thesis is mainly based on nine original papers. The papers are included as appendices. The author of this thesis has been the main author in all the papers but Paper IV, where the first author provided the main part of the analysis and numerical results for the article. The author of this thesis provided part of the analysis, and wrote the most of Paper IV. Co-author, professor Markku Juntti, gave comments and supervised the writing process of Paper IV. Co-author Dr. Harri Saarnisaari gave comments, criticism and support. In other papers, the author of this thesis has invented the ideas as well as carried out the analysis, derivations, analysis of the results, and drawing the conclusions. The author of this thesis has been the only inventor of the extended TSISA and the LAD methods proposed in the papers. In the original papers, the co-authors have provided valuable guidance and support, comments and criticism, as well as help with running the computer simulations.

A number of supplementary papers related with this thesis have also been published. The author of this thesis has also been the main author in Papers [138, 140–149] and a co-author in Papers [49, 61, 63, 68, 71–75, 77, 78]. These papers are referred to in the text as all other references. In addition to the published papers, a patent of the LAD method was granted in 2007 [139].

2 Literature review

This chapter provides a literature overview of outlier detection with applications to interference suppression and signal detection in wireless communications. The purpose is to present a general overview and survey of the relevant literature without mathematical details. Chapter 3 introduces methods used in this thesis in more detail. Section 2.1 introduces outlier types and gives an overview of the outlier detection concept. Section 2.2 reviews the literature of interference suppression. Narrowband signal detection methods are considered in Section 2.3. Its application in cognitive radios is described in Section 2.3.1. Finally, Section 2.4 presents a short overview of the threshold setting problem.

2.1 Outlier detection

In statistical signal processing outlier detection is usually divided into two categories. These are robust signal processing and diagnostic methods [26, 62, 64, 80, 86, 99, 126, 127, 136, 154, 157, 160]. In robust signal processing, the outlier detection and mitigation are performed jointly. With diagnostic methods the outlier mitigation is performed after outliers are first detected. Here, the review is limited to diagnostic methods.

The diagnostic methods can be further divided into backward search methods [6] and forward search methods [7, 47, 59]. While backward methods use the whole data set for finding outliers, forward methods use a small appropriate part of data to fix the detection parameters. Even though the forward methods outperform the backward search methods, these are also more complex [160]. The classification of outlier detection methods is illustrated in Figure 4.

The probability of detecting outliers is a sum of several factors. Dimension (the number of antennas in wireless communications), number of data samples, contamination ratio (i.e., the ratio of the number of outlier samples to total samples) and the type of contamination as well as parameters needed in the algorithm have a major influence on the outlier detection. They also depend on each other. Outlier detection is impossible if both the contamination and the dimension of the data are high. In addition, the more data and the more time, the more outliers can be handled. It has also been noticed that the difficulties of detecting outliers increase as the dimension of the data increases, so

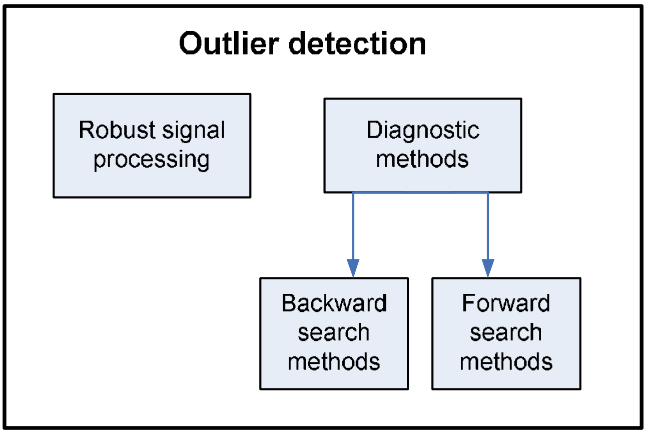

Fig. 4. Classification of the outlier detection methods.

the estimation of multivariate shape and location is difficult [114]. The outlier type has also an impact on successful detection. The hardest outliers to find are outliers with the same shape as the main data, very compact (i.e., closely spaced) as well as shifted outliers. Shifted outliers have the same but shifted distribution as the set of clean samples. Other outlier types include, for example, shifted as well as reduced outliers (in scale) [114].

An outlier detection metric is used to decide if a sample is an outlier or not. In the diagnostic methods, the outlier detection is usually based on the Mahalanobis squared distance (MSD) [50, 82, 131]. That is, all large observations are assumed to be caused by outliers. Mathematically, a sample from vector $\mathbf{r}$ is caused by outliers if the MSD

$$\chi_i = (\mathbf{r} - \bar{\mathbf{r}})^H \mathbf{C}^{-1} (\mathbf{r} - \bar{\mathbf{r}}) > T, \tag{1}$$

where H denotes the conjugate transpose (or Hermitian transpose), $\mathbf{C}$ is the shape parameter (usually the covariance matrix of $\mathbf{r}$) and $\bar{\mathbf{r}}$ is the location parameter (usually the mean of $\mathbf{r}$). Thus, the sample vector $\mathbf{r}$ is classified as an outlier if the MSD is larger than some predetermined threshold value T, i.e., the cutoff point. A threshold that separates the outliers from other samples can be solved from Eq. (1). The threshold setting problem is considered in more detail in Section 2.4.

The main problem with the MSD is that the mean and covariance are usually unknown, so these have to be estimated reliably. However, these estimates are not necessarily robust but sensitive to outliers resulting in undesired effects like swamping and masking. Swamping means that all large MSD values are not necessarily caused by outliers. Masking means that all the outliers do not necessarily have a large MSD value, because the outliers may affect the estimates of the mean and the covariance. For example, an outlier may mask another outlier. [47]

The swamping and masking problems can be alleviated or avoided, for example, by using iterative and/or robust parameter estimation. One possible method is to use minimum volume ellipsoid (MVE) [114]. The MVE is efficient, but the computational complexity is high. Hence, algorithms for approximating the MVE have been suggested. For example, an effective and computationally simple forward-type procedure for approximating the MVE has been proposed in [47]. The method starts by rearranging the samples in an ascending order according to a robust distance. The MSD is used to calculate a robust distance but robust location and covariance are used instead of the basic mean and covariance. The data set of size N is divided into two sets: a basic set (starting set) contains the first $p+1$ samples which are assumed to be clean, and a non-basic set (complementary of the basic set) contains the rest $N-(p+1)$ samples including both clean and outlier samples. Here, p denotes the dimension. Next, the arithmetic mean (i.e., centre) of the basic set is computed and the distance between the mean and data points are calculated. The distances are calculated relative to the sample covariance matrix of the basic set. After that, all the N samples are rearranged again in an ascending order and divided into two sets. Now, the first $p+2$ samples belong to the updated basic set and the rest $N-(p+2)$ samples belong to the updated non-basic set. The process continues until a pre-determined stopping criterion is reached. Thus, if performed properly, the last updated basic set contains all the clean samples as the last updated non-basic set contains all the outlier samples. This is basically a forward type diagnostic method.

When the number of outliers is one, the outlier detection is a simple task. Instead, detecting clusters of outliers is a more difficult task and requires robust estimators [114]. To ensure outlier detection, there has to be enough clean samples. In addition to robustness, a good estimator is also able to reject outliers that are far away from the centre of the data, is able to converge to a good solution, and has a reasonable computational complexity. [113, 114]

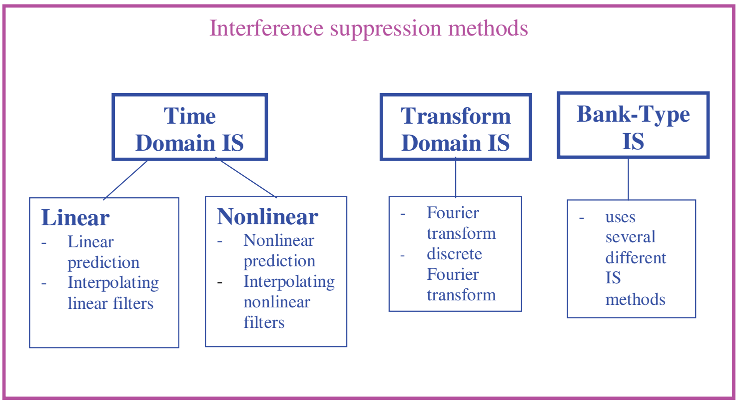

Fig. 5. One classification of the interference suppression (IS) methods.

2.2 Interference suppression

Interference suppression (IS) techniques and the effects of IS have been widely studied since the 1970s. Several methods have been considered for detecting the interfering signals, see, e.g., [25, 44, 56, 60, 67, 79, 89, 90, 104, 112, 120, 162]. IS methods can be classified into three groups: time domain, transform domain and bank-type methods. The classification is illustrated in Figure 5.

2.2.1 Time domain interference suppression

Time domain techniques can be further divided into linear and nonlinear methods [17, 88]. In the linear (or estimator) methods, estimates of the received signal are obtained using a transversal filter. The estimates are based on both model assumptions and previous samples. Existing time domain IS methods are mainly based on predictive techniques. This means that the present sample of interference can be predicted from the previous and future samples. Predictive methods are based on the idea that in the received signal only the concentrated signal is primarily predictable, whereas the wideband SS signal and noise are not [84]. The first IS filters, called linear prediction filters, were proposed in the 1980s. Linear predictive filters can be made adaptive, for example, by using the Widrow-Hopf least mean squares (LMS) algorithm [158] as in [88]. Therein, no external reference waveform is needed, in contrast to many other applications of the LMS algorithm, where an external reference waveform is used to adjust the tap weights.

A linear estimator, such as the Kalman filter, may have serious problems if the densities are non-Gaussian. However, in practice, densities are seldom purely Gaussian. The optimum filter for predicting an interfering signal in the presence of an identically distributed binary sequence, the direct sequence (DS) signal, is nonlinear. Nonlinear IS is based on the work by Masreliez [83], who proposed an approximation to the optimal non-Gaussian filtering assuming linear state and observation relations in 1975. According to [83], the observation noise does not have to be Gaussian, but the distribution is still Gaussian for the conditional mean. For that reason, the proposed filter is called the approximate conditional mean (ACM) filter. The ACM filter is widely considered in the literature, and it has been extended to the nonlinear IS [115, 151]. In [43], nonlinear filters in DSSS systems were studied for rejecting NB interference in impulsive noise channels. It was noticed that the performances of the nonlinear adaptive filters were better than that of the LMS filter.

Conventionally, the nonlinear filters have been made adaptive using the LMS algorithm. A drawback of the LMS algorithm is its rather slow convergence rate which limits its IS capability in a time-varying case. Many other techniques have, therefore, been proposed to make the system adaptive. These are based on recursive least squares (RLS) or conjugate gradient methods [52]. The adaptive RLS filter has many advantages, e.g., the convergence rate is faster than that of the LMS algorithm. However, the RLS algorithm is computationally complex. The overall complexity is of order $O(N^2)$, where N is the length of the input vector.

2.2.2 Transform domain interference suppression

NB signals can also be suppressed in the frequency domain or in some other transform domain [89, 90]. Transform domain methods transform the received signal to the transform domain before the IS. The most often used domain is the frequency domain, to which the signal is transformed using the Fourier transform (FT). The transform domain systems have an advantage over the LMS based receivers when rapid adaptivity is needed: the transform domain systems can be made adaptive without the need for an adaptive algorithm since they are usually block-based. [88]

Transform domain interference suppressors consist of three parts as illustrated in Figure 6. In part one, the received signal is windowed in the time domain to reduce

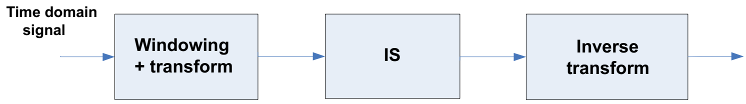

Fig. 6. Transform domain interference suppressor (IS).

the spectrum leakage. After the windowing, the transform is performed. In the 1970s and 1980s, a continuous-time Fourier transform was used in the literature analysis. The discrete Fourier transform (DFT) and the fast Fourier transform (FFT) are currently the main methods for calculating the frequency domain representation. In part two, after the transformation, the detected interfered samples are set to zero or limited. In part three, the signal is returned to the time domain using inverse transform. The main problem herein is to detect the interfered samples or decide which samples are interfered. This thesis will provide some interesting alternatives for this.

Notch filters have been considered, for example, in [1, 16, 88]. Adaptive notch filtering based on the DFT was considered in [67]. The considered IS filters were based on the parametric spectrum estimation algorithm and the nonparametric spectral estimation algorithm (the Welch method). The nonparametric spectral IS method discussed in [67] used the knowledge that the spectrum of the pseudo noise (PN) sequence is flat while the spectrum of the NB interference is peaked. Prior knowledge of the interference was not needed. The drawback is that adaptive notch filtering is ungainly against multiple sinusoidal interfering signals and adaptivity is slow. In [24, 112], the interference excision function was an on-off switch which implements a notching function in the frequency domain. The energy of NB interference was concentrated using a windowing function. Saulnier [120] considered frequency-domain adaptive filters for IS. A new tap-weight structure with the leakage factor was discussed. In [112], rectangularly windowed block DFT was studied. In the interference excision, the six cells surrounding the interference frequency were set to zero. It was shown that the use of ensemble averaging over both the interference frequencies and PN sequences enhances the bit error rate (BER) performance. In [162], several real-time DFT based frequency domain IS algorithms were considered in an environment where multiple sinusoidal interfering signals co-exist. It was also assumed that the receiver does not know the statistics of the interference. Impulse noise effects and mitigation in DVB-T (digital video broadcasting - terrestrial) systems have been considered, for example, in [54].

Henttu *et al.* [57] proposed an adaptive iterative notch-type interference excision method called the consecutive mean excision (CME) algorithm in 2002. The CME algorithm has low complexity and it does not need any *a priori* knowledge of the interfering signals. Similar approach has been later applied, for example, in [129]. Saarnisaari and Henttu [117] proposed two new versions of the CME algorithm, namely the limiter CME (LCME) and forward CME (FCME) algorithms for impulsive IS in 2003. It was noticed that the CME algorithms are special cases of classical diagnostic methods used to detect outliers in the statistical literature [47]. Even though proposed for impulse rejection in the time domain, the CME algorithms can also be used in any other transform domain, as in the Fourier domain. Threshold values of the CME algorithm were studied in [57]. It was noticed that a proper choice of clean sample rejection rate (i.e., the desired false alarm rate) is approximately 0.1%, thus meaning that in the noise-only case, 0.1% of the samples are classified as outliers. The clean sample rejection rates of both the CME and FCME algorithms were considered in [117]. It was noticed that the desired clean sample rejection rate should be set to be less than 1%, otherwise too many clean samples are rejected and the performance degrades. It was also noticed that the CME algorithm was able to detect random impulses if at most 20% of the samples were corrupted by impulses. For constant envelope impulses, the proportion was 40%, as the FCME algorithm detected impulses even when 90% of the samples were corrupted by impulses, regardless of the impulse type.

Both the CME and FCME algorithms were considered for narrowband interference suppression in [116]. Noniterative notch filters were used as a point of comparison. The root mean square error (RMSE) of the delay estimator was studied. The delay estimation is of interest, for example, in positioning. When the interference was very narrowband, i.e., 1% of the bandwidth of the desired signal, both the CME algorithms performed well. When compared to the case where no IS was used, the improvement the CME algorithms offered before their performance collapse was at least 60 dB. When the bandwidth of the interference was 25% of the bandwidth of the desired signal, the improvement the CME algorithms offered was approximately 40 dB. It was shown that the performance of the CME algorithm starts to decrease after that. Instead, the performance of the FCME algorithm starts to decrease after the bandwidth of the interference is 40% of the bandwidth of the desired signal. The improvement the FCME algorithm offered before the performance collapse was approximately 40 dB. It was also noticed that the wider the bandwidth of the interference is, the more important the averaging in delay estimation is. The theoretical impulse detection performance of the CME algorithms was analyzed and detection probabilities were presented in [118]. In [76], the CME algorithms were used with the cell-averaging (CA) scaling factors. The conventional CA-type detector uses the average of all reference cells when calculating the threshold [41].

The CME algorithms have also been studied, for example, in [10, 63, 75, 108, 109, 155, 167]. It has been observed that the CME algorithms outperform the notch filters. The FCME algorithm has somewhat higher computational complexity than the CME algorithm but it also has better performance [118]. The CME algorithm is efficient when the signal is very narrow. In general, the CME algorithms are able to offer good performance with low computational complexity. Thus, they can be said to be useful for suppressing narrow signals. The CME algorithms are discussed in more detail in Chapter 3.

2.2.3 Wideband signal detection in the presence of interference

Interference suppression techniques can also be applied to intercept receivers. The function of the receiver is to determine whether a DS signal is present or not when a DS signal may be superimposed by an NB signal. In an interfering environment, the IS is performed before the decision on the presence of the DS signal is made. In [44], a total power radiometer intercept receiver based on surface acoustic wave (SAW) was enhanced by proposing real-time transform domain processing for IS. A radiometer measures the power of the received signal, and compares it to a detection threshold. If the measured power exceeds the detection threshold, it can be assumed that there is a signal. The proper setting of the detection threshold was not considered in [44]. Two techniques for adaptive NB IS in the Fourier transform domain were considered. The first method detected the NB interference and excised it using an adaptive notch filter. The second method used a so called soft-limiter. In 1995, Masry [84] analyzed the interception receiver of [44] with the exception that multiple outputs of the analog compressive receiver were accumulated. The interference suppressor reduced the energy from the interference significantly. The performance of the radiometer under frequency and time domain interfering signals was discussed in [78]. A simple method for choosing if either the time domain or the frequency domain IS should be used by the receiver was proposed. In [78], the domain selection is based on the fact that the correct domain concentrates interference energy into a fewer samples. The selection is based on calculating 25% percentiles in each domain, i.e., 25% of the data is underneath the percentile. The domain with the smallest percentile is selected for IS. Unlike usual practice, the results of the IS were used when calculating the threshold of the radiometer. This allows better performance when compared to the conventional method that uses a fixed threshold. The proposed IS method gives some performance gain but the selection method is suitable only for specific types of interfering signals [78].

2.2.4 Bank-type interference suppression methods

Most of the existing IS methods are targeted against a specific type of interference. If the interference is another type of signal, these methods often fail. In order to improve the performance of IS systems, bank type IS methods have been studied. The goal is to achieve better performance against different types of concentrated interfering signals. A filter bank system may, for example, consist of several parallel estimators [17], independent IS systems [105] or transform domains [3] presented in Figure 7. In [17], a multiple NB IS system based on a bank of independent hidden Markov model (HMM) estimators was proposed to detect and estimate interfering signals. In [105], interference suppression was performed by four parallel branches, and finally only one IS output was chosen based on the maximum signal-to-interference plus noise ratio (SINR) [105]. The proposed IS bank consists of several IS methods, namely the pure matched filter (MF), the CME algorithm [57], the RLS algorithm [52, 58] and the polar algorithm [55]. The CME algorithm is discussed in more detail in Chapter 3. While the RLS filter is able to suppress interfering signals with amplitude variations, the polar suppressor can remove even very wideband *constant envelope* signals, covering even 100% of the bandwidth of the desired signal. According to [105], the proposed IS bank method is effective, but excessive computation is required due to the several algorithms. Aromaa *et al.* [3] proposed an efficient bank-type IS system. The proposed system, called the transform selective interference suppression algorithm (TSISA), is able to suppress several types of interfering signals – impulses, narrowband signals and sweeping or chirp signals – and its computational complexity is low. The transform domain selection is performed using the compression gain (CG) metric. The compression gain is commonly used, for example, in image processing, where it is called a coding gain. The TSISA is discussed in more detail in Chapter 3.

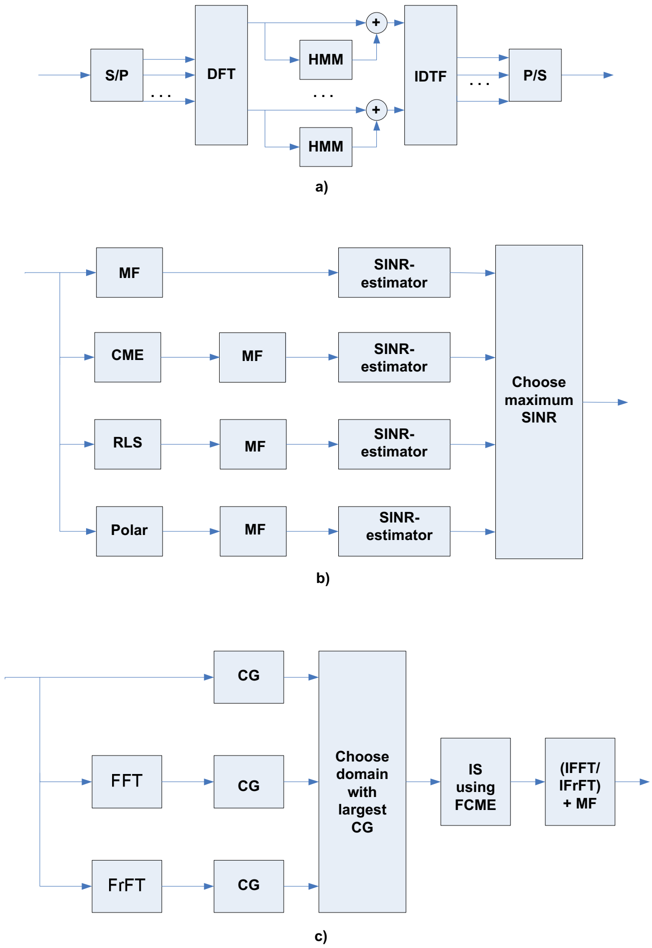

Fig. 7. Examples of filter bank systems. (a) Several parallel estimators. S/P denotes serial-to-parallel, DFT is discrete FT, HMM denotes hidden Markov model, IDFT is inverse DFT and P/S denotes parallel-to-serial. (b) Several independent interference suppression (IS) systems. MF denotes matched filter, CME denotes the consecutive mean excision algorithm, RLS means recursive least squares and SINR denotes signal-to-interference plus noise ratio. (c) Several transform domains. FFT is fast Fourier transform, FrFT is fractional Fourier transform, CG denotes compression gain and FCME is the forward consecutive mean excision algorithm.

2.2.5 The impact of temporal windowing

Windowing is widely used to improve the performance of IS methods that suppress interfering signals in some other than time domain. Therein, a window function is required to reduce spectrum leakage which transforms signal energy partly to other frequencies [106, 130]. The window to be used has to be chosen carefully. For example, when notch-type filters are used, a window with small values at tails is essential to prevent the performance failure. In the window functions, there is a trade-off between the width of the central peak in the spectrum and the falling of the tails. It is possible to have either a narrow central peak or tails that fall off as fast as possible. The length of the window is a trade-off between spectral resolution and statistical variance [106]. There exists several types of window functions. The rectangular window produces large sidelobes. These can be reduced by using weighting functions, but the disadvantage is that those distort the input signal. Consequently, different types of windows are needed [51, 88]. Hamming and Hanning (Hann) windows are commonly used window functions. Both of these are n-point symmetric windows. The Blackman window is also an n-point symmetric window. The central lobes are wider than those of the Hamming and Hanning windows, but the Blackman window has less sideband leakage. Another popular window is the 4-term Blackman-Harris window, which is an n-point minimum window, which means that the maximum sidelobes of the window are minimized. Windowing causes performance (SNR) losses which may be significant. In general, more concentrated windows cause larger losses. According to [163], performance loss due to the Hanning window is almost 2 dB and that of the 4-term Blackman-Harris window is approximately 3 dB. It has been noticed that the loss can be reduced using the *overlap-and-add* method [163]. For 50% overlap, the windowing loss is less than 1 dB for all the windows. It can be shown that the loss of the 4-term Blackman-Harris can be reduced to be less than 0.5 dB [163].

In this thesis, the CME algorithms and their applications are studied. The interference suppression capability of the backward and forward CME algorithms originally proposed in [57, 117] has been considered in the supplementary papers [140, 145, 146]. Therein, the focus lies in frequency domain interference suppression. The analysis of the CME algorithms has been presented in Papers IV, V, and in the supplementary paper [148]. The performance of the FCME-based TSISA method originally proposed in [3] has been evaluated in Paper I, and in the supplementary paper [141] under several types of interfering signals. In addition, the enhancement of the TSISA has been proposed in Paper II, and in the supplementary paper [147].

2.3 Signal detection

Signal detection is a decision-making problem: the presence or absence of a signal is decided [65, 103, 134]. Because there always exists noise, the decision is, in general, a comparison between two hypotheses: the noise-only hypothesis (H_0) and the signal-present hypothesis (H_1). This is called a binary hypothesis testing problem. Usually, the noise is assumed to be a zero-mean white Gaussian process with either known or unknown variance. The signal detection is usually based on some threshold testing [134]. Hypothesis H_1 is true if a received sample exceeds the threshold. Instead, if a received sample is below the threshold, hypothesis H_0 is true. In the well-known Bayes criterion, *a priori* known probability values are utilized to decide in which set samples are located [11]. Thus, the probability of the occurrence of each hypothesis is assumed to be known. The so called Neyman-Pearson criterion [2, 134] does not need to know *a priori* probabilities. Therein, the goal is to have a maximum probability of detection (P_D) while maintaining the probability of false alarm (P_{FA}) below some predetermined level. The probability of detection means the probability of a signal sample being classified as a signal sample, whereas the probability of false alarm means the probability of a noise-only sample being falsely classified as a signal sample. In the Neyman-Pearson sense, the best detector is defined to be the detector which is able to achieve the highest probability of detection subject to maximum false alarm probability constraint. It depends on the knowledge of the detected signal and/or noise what kind of detector is the best choice. When the noise is additive Gaussian noise and the detected signal is known, the optimum detector is the matched filter [88]. Usually, the noise level is not known or varies in time. In that case, it has to be estimated. When the detected signal is unknown, blind signal detection methods are needed since they require no *a priori* knowledge of the signal.

Signal detection can be classified into wideband and narrowband (or generally, concentrated) signal detection. Here, the main interest lies in the narrowband signal detection. Narrowband signal detection has many applications, for example, in radar, sonar and wireless communications [135, 150]. In the wide field of wireless communications, spectrum sensing in future cognitive radio transmissions is one of the most interesting and current topics. Next, signal detection is considered from that point of view.

2.3.1 Detection in cognitive radios

For cognitive operation purposes, the unoccupied frequency bands can be located using, for example, beacons, databases, location monitoring, or spectrum sensing [12, 22, 45, 61, 72, 119, 128, 142].

Spectrum sensing uses signal detection methods to decide if a signal or signals are present or not, i.e., if the investigated frequency band is occupied or available. The use of spectrum sensing has several benefits. These include, for example, that knowledge of other users is not necessarily required and all secondary users may operate individually.

The simplest approach for spectrum sensing is to use a low-complexity energy detector, aka, a radiometer, which measures the strength of the received signal and compares it to a threshold [65, 137]. Therein, if the threshold is exceeded, it is assumed that there is a signal present, so the channel is occupied as illustrated in Figure 8. The energy detector is said to be optimal if there is no information about the detected signals [65]. The channelized radiometer [14] integrates energy in several frequency bands simultaneously because it uses several parallel radiometer receivers. The benefit of a radiometer is that no *a priori* knowledge of signals or their parameters is required. The drawback of using an energy detector is that due to the noise level uncertainty, the performance may degrade [125]. These effects cause problems in the threshold setting procedure. When the noise power is unknown, constant false alarm rate (CFAR) techniques can be utilized [76]. In the CFAR type methods, the threshold setting is performed using a predetermined false alarm rate. In that case, the probability of false alarm stays constant. In general, the predetermined false alarm rate should be rather low. Otherwise, the performance of the system may drop in the interference-free case.

Cyclostationary feature detector [30, 42] uses cyclostationary properties of the signals. Thus, some *a priori* knowledge of the signal is required. In addition, a cyclostationary feature detector is complex for real-time spectrum sensing. In [21], a method based on fast Fourier transformation (FFT) was used to detect low power narrowband Part 74 devices, such as wireless microphones (IEEE 802.22 Standard [21, 23]). Partial matched filtering approach was used in [164]. Therein, some transmission parameters were estimated and compared to the *a priori* known parameters. Easy-to-implement OFDM spectrum sensing methods based on time-domain symbol cross-correlation were

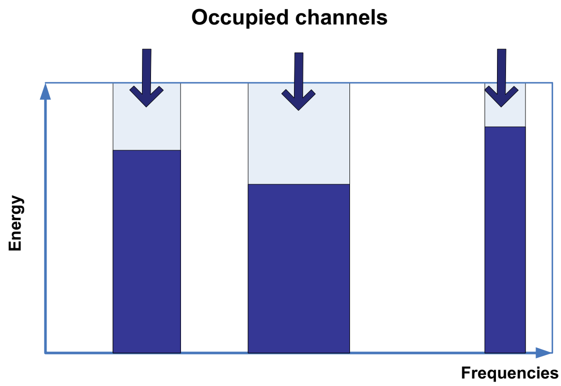

Fig. 8. Unoccupied channels can be found via detecting signals present (=occupied channels).

proposed in [19]. In [165], two eigenvalue-based sensing methods were proposed. The methods use the ratio of the maximum or average eigenvalue to the minimum eigenvalue. No knowledge of signal or noise power was required. So called goodness-of-fit testing was used in [153]. Therein, the presence of signal was detected via testing if the observed samples were independent from the noise distribution. No knowledge of the detected signal is required. The proposed method is said to outperform an energy detector especially at low SNR values. Wavelet based wideband "white space" detection has been studied in [132].

When there are several cognitive radios, the coexistence causes interference to each other. A so called hidden terminal problem means that the secondary user is not able to detect the primary user because it is far away from the primary transmitter, and, thus, the secondary user starts to transmit, causing interference to the primary user (i.e., to the receiver if TV signals are considered). This can be avoided, for example, with cooperation. Cooperative spectrum sensing means that multiple cognitive radios detect the spectrum holes collaboratively [74, 81, 168]. In [166], cooperative spectrum sensing with energy detection was used. In [169], a local blind source separation algorithm for cooperative sensing was proposed. Therein, no knowledge of the source signal or the channel was required. Usually, it is assumed that the communication between the cognitive radio devices and a base station is noise-free [45, 53, 91, 152]. However, this is not the case in realistic cognitive radio scenarios. The effects of imperfect channels have been studied, for example, in [110], where the goal was to minimize the interference to the primary user. The effects of correlated shadowing on the reporting channel were considered in [111]. A reporting channel is a channel which is used by cognitive radios when sending sensing results to the fusion center (or data collector). It was noticed in [111] that in realistic systems, correlated shadowing may cause performance degradation both in sensing and reporting channels. In [5], errors occurring during the transmission of local decisions were taken into account. Recently, the problem of selecting only the most suitable cognitive radios for cooperation was studied [68]. Three methods for selecting the cognitive radios with the best detection performance were proposed. Therein, the decisions were based only on binary decisions from the cognitive radios. Although cooperative spectrum sensing is an interesting topic, it is not within the scope of this thesis, and, therefore, not considered in more detail.

In this thesis, the CME algorithms and their applications have also been considered for signal detection purposes. The study of the CME algorithms has been extended to concentrated signal detection in Paper III, and in the supplementary paper [144]. The analysis of the CME algorithms has been presented in Papers IV, V, and in the supplementary paper [148]. A new narrowband signal detection method called the LAD method has been proposed in Paper VI, and in the supplementary paper [143], and extended in Paper VII. Two enhancements of the LAD method, namely the LAD NT and LAD ACC methods, have been proposed in Paper VIII. In Paper VIII, the LAD methods have also been proposed to be used for spectrum sensing purposes in cognitive radios. An extension of the LAD method called the 2-D LAD method has been proposed in Paper IX. The performance of the LAD methods has also been studied in the supplementary papers [71, 149], and the analysis of the LAD methods has also been presented in the supplementary paper [77].

2.4 Threshold setting problem

Setting the threshold is a demanding task. One of the simplest IS methods, the notch filter [88], calculates the threshold from the magnitude spectrum. The samples which exceed the threshold are outliers, and, thus, zeroed. The problem is how to select the proper threshold because adaptivity is required. The CME algorithms [57, 117] are iterative notch-type methods for setting an interference excision threshold. The adaptive threshold is set automatically based on a mean of sample energies and a threshold parameter. The used threshold parameter depends on the assumed distribution of noise. Because the CME algorithms use the CFAR principle used in the energy detection of unknown signals [65], the false alarm probability stays constant. The CFAR principle is widely used, for example, in radar applications [41]. The CME algorithms are computationally simple but effective methods and they are able to operate without any knowledge of the noise level or the signals to be suppressed. However, especially at low SNR levels, the CME algorithms suffer from two common problems we are interested herein: needless separation of a signal as well as falsely detected signals. These are problems especially in signal detection if the purpose is to estimate also signal parameters like the bandwidth of the signal.

Several threshold setting methods have been proposed for reducing these problems. The dynamic undersea detection extractor (DUDE) extracts and characterizes concentrated acoustic signals among the noise [66]. The DUDE consists of two parts. As the first part operates on single beam data, the second part considers multiple beams. The first part of the DUDE compares the frequency samples to the threshold. The threshold is a constant multiplied by a periodically updated noise estimate. The DUDE groups the adjacent samples assumed to be caused by a concentrated signal together to form a cluster. To avoid needless separation of the signal, the DUDE allows adjacent frequency samples in the cluster to drop below the threshold if the number of these samples is less than a predetermined constant, the *max ridge with skip* parameter. This situation is illustrated in Figure 9 a).

Wiley [159] described thresholding with hysteresis. The purpose is to avoid needless separation of the signal when thresholding noisy data. The threshold for the current sample is reduced if the previous sample is above the threshold. Consequently, the threshold for the current sample is increased if the previous sample is below the threshold. The reduction and accretion depends on the noise level. For that reason, the noise level has to be estimated. A threshold with hysteresis is illustrated in Figure 9 b). Thresholding with hysteresis is also used, for example, in Canny edge detector [15]. There, the edges in images are detected using two thresholds. Advanced hysteresis has been used in error diffusion in a digital audio recording in [31]. Output dependent threshold modulation changes the threshold to avoid certain output patterns. Both horizontal and vertical hysteresis constants were used to achieve better printability.

Mustafa *et al.* [95] proposed three algorithms for automatic detection of active radio stations. These algorithms are based on frequency domain information and both the bandwidths and the center frequencies of the detected radio stations are estimated. One of these algorithms calculates multiple thresholds. The statistical characteristics of the height and position of the spectrum components are used. The algorithm assumes

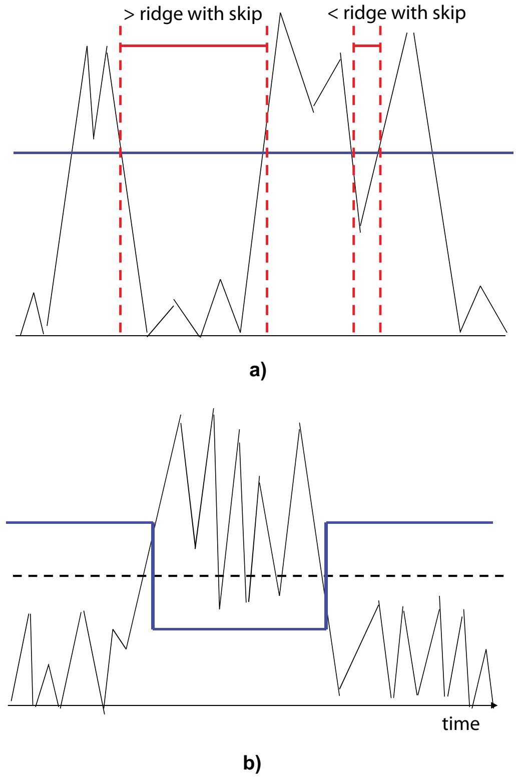

Fig. 9. (a) Threshold in the DUDE algorithm. The ridge with skip parameter defines how many adjacent frequency samples may be below the threshold without separating the signal. (b) Threshold with hysteresis. The threshold for the current sample is reduced/increased if the previous sample is above/below the threshold (dashed line).

that the maximum expected number of radio stations is known. The decisions can be based on the ranking of stations by the power. In such a case, the falsely detected radio stations are mainly avoided [95].

In this thesis, a novel simple but efficient threshold setting method called the LAD method is considered. The LAD method which is based on the FCME algorithm is discussed in more detail in Section 3.4.

3 Methods and their performance

This chapter introduces the investigated methods and summarizes their performance reported in the original publications I-IX. In addition, supplementary papers [49, 71, 73, 77, 140, 141, 143–149] are briefly reviewed. First, Section 3.1 presents the system model. Section 3.2 presents the CME and FCME algorithms. Both the interference suppression and detection performance of the CME algorithms are considered. The TSISA method and its extension are considered in Section 3.3. Finally, Section 3.4 considers the LAD methods and their performance. The methods considered and their relations to each other are presented in Figure 10.

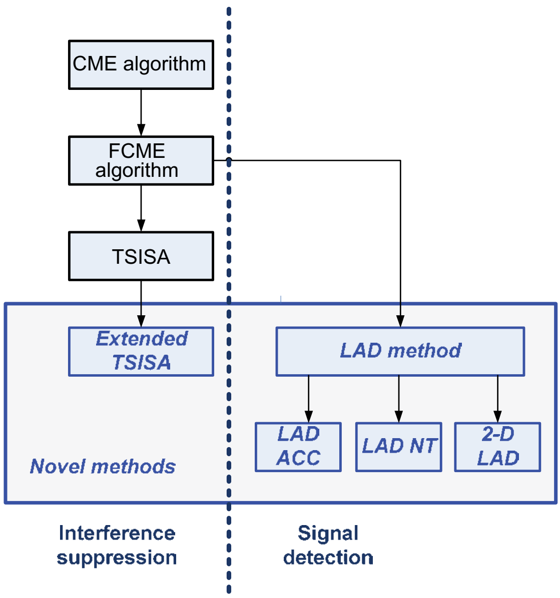

Fig. 10. Methods considered in this thesis.

3.1 System model

After front end filtering and sampling, the received discrete-time signal is assumed to be

$$r(n) = \sum_{i=1}^{m} i_i(n) + s(n) + \eta(n),\ n \in \mathbb{Z}, \tag{2}$$

where m is the number of unknown concentrated signals, $i_i(n)$ is the ith concentrated signal, $s(n)$ is a *possible* wideband direct sequence (DS) SS signal, and $\eta(n)$ is the noise process. The noise is assumed to be a zero mean complex white Gaussian process. The SS signal, the concentrated signal, and the noise are assumed to be mutually independent. In Papers I-IX, only single path channels are considered.

The signal-to-noise ratio (SNR) is the ratio of signal energy to noise power spectral density, i.e.,

$$\gamma = \frac{E_\mathrm{b}}{N_0}, \tag{3}$$

where E_b is the energy of the desired signal per bit and N_0 is the noise power density. In the presence of wideband signal, SNR denotes wideband signal-to-noise ratio. In the absence of wideband signal, SNR denotes concentrated signal-to-noise ratio. The interference-to-signal ratio (ISR) is defined as

$$\xi = \frac{I}{S}, \tag{4}$$

where I and S are the power of the concentrated and wideband signals, respectively. The concentrated signal can be interfering signal or signal to be detected. When there are multiple concentrated signals, it is assumed that independent signals are from different sources. Thus, the ISR is defined per concentrated signal.

The ratio of the number of corrupted samples N_con to the total number of samples N_tot is called the contamination ratio ε, i.e.,

$$\varepsilon = \frac{N_\mathrm{con}}{N_\mathrm{tot}}. \tag{5}$$

Next, some assumptions that are common to the papers considered in this thesis are reviewed. The data sequence is spread by a 63-chip Gold sequence meaning that the bandwidth of the spread spectrum signal is 63 times wider than the bandwidth of the information signal being sent. Furthermore, it is assumed that the signal is sampled once

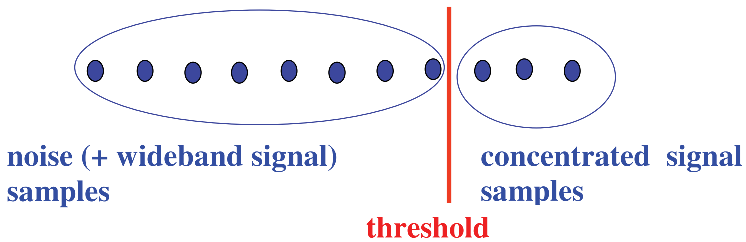

Fig. 11. The threshold setting. The threshold separates signal samples (dots) into noise and concentrated signal sample sets.

per chip. In the receiver, IS and/or detection precedes demodulation. The considered concentrated signals are impulsive signals, sinusoidal signals, chirps, or binary phase shift keying (BPSK) communication signals with different parameters. The BPSK signals are bandlimited by a root raised cosine (RC) filter with a roll-of factor of 0.22 [107]. A summary of the main assumptions in original publications is presented in Table 8 on page 94.

In Papers III, IV, V, VII, and VIII, the spectrum estimates have been calculated using the conventional periodogram [106]. In Papers I, II, and VI, 4-term Blackman-Harris window was used. In some papers, as in Paper IX, and in the supplementary paper [71], the Welch method [156] was used instead of the periodogram. In the Welch spectrum estimate, overlapping and windowing is used. Therein, the data is divided into different segments which are allowed to overlap. Herein, 50% overlapping is used. Each data segment is windowed separately.

3.2 Consecutive mean excision algorithms

The CME algorithms [57, 118, 138] are automated methods for setting a threshold in order to separate the samples into two sets: the concentrated signal set above the threshold containing the concentrated signal samples, and the desired signal set below the threshold containing the wideband information signal and the noise samples. This is illustrated in Figure 11. The threshold computation of the CME algorithms uses a threshold parameter which is calculated *a priori* using a desired clean sample rejection rate (i.e., the required false alarm rate) and the statistical properties of the noise [57, 87, 96]. The CME algorithms are blind methods in the sense that they do not need to know the noise level. In general, no side-information is required. That is, no *a priori* information about the signals or their parameters is required. The only requirement is that the signal/signals are narrow with respect to the studied bandwidth. The CME algorithms are good at excising samples that do not follow the statistics of the wideband signal and noise. They can be used either in the time domain or in some other transform domain. In the frequency domain, windowing is used to reduce the spectral leakage.

Both CME algorithms use the same threshold parameter. The threshold parameter used depends on the distribution of the noise. The most common distributions in the threshold setting are chi-squared and Rayleigh distributions, which follow if the noise is Gaussian. The CME algorithms assume that the samples x_i are zero mean, independent, i.i.d. Gaussian distributed complex random variables. Herein, the notation x_i is general and not specified to some particular domain, i.e., samples x_i can be in time, frequency or in some other domain. Zero mean assumption is usually valid in wireless communications. As a consequence, the variable $|x_i|^2$ has a chi-squared distribution with two degrees of freedom and $|x_i|$ follows a Rayleigh distribution. The threshold parameter can be solved from Eq. (1). Here, the mean $\overline{x_i} = 0$ and covariance reduces into the variance [117]. When the desired signal set has a chi-squared distribution, i.e., if the energy of samples is considered, the threshold for CME algorithms is [118]

$$T_h = -\overline{x^2}\ln(P_{\text{FA,DES}}) = \overline{x^2}T_{\text{CME}}, \tag{6}$$

where

$$\zeta = \overline{x^2} = \frac{1}{Q}\sum_{i=1}^{Q}|x_i|^2 \tag{7}$$

is the average sample mean (or energy), Q is the set size, $P_{\text{FA,DES}}$ is the desired clean sample rejection rate and

$$T_{\text{CME}} = -\ln(P_{\text{FA,DES}}) \tag{8}$$

is the threshold parameter. Example threshold parameter T_{CME} values in the chi-squared case are 4.6 (corresponding $P_{\text{FA,DES}} = 10^{-2} = 1\%$) and 6.9 ($P_{\text{FA,DES}} = 10^{-3} = 0.1\%$). When the desired signal set has a Rayleigh distribution, i.e., if the absolute value of samples is considered, the threshold is [57]

$$\begin{aligned} T_h &= \sqrt{2\hat{\delta}^2}\sqrt{-\ln(P_{\text{FA,DES}})} \\ &= \overline{|x|}\sqrt{\frac{4}{\pi}}\sqrt{-\ln(P_{\text{FA,DES}})} = \overline{|x|}T_{\text{CME}}, \end{aligned} \tag{9}$$

where

$$\hat{\delta} = \overline{|x|}\sqrt{\frac{2}{\pi}} \tag{10}$$

is an estimate of the Rayleigh parameter of the received vector, $P_{\mathrm{FA,DES}}$ is the desired clean sample rejection rate,

$$\zeta = \overline{|x|} = \frac{1}{Q}\sum_{i=1}^{Q}|x_i| \tag{11}$$

is the average sample mean, Q is the set size and

$$T_{\mathrm{CME}} = \sqrt{\frac{4}{\pi}}\sqrt{-\ln(P_{\mathrm{FA,DES}})} \tag{12}$$

is the threshold parameter. Example threshold parameter T_{CME} values in the Rayleigh distribution case are 2.97 (corresponding $P_{\mathrm{FA,DES}} = 10^{-3} = 0.1\%$), 2.42 ($P_{\mathrm{FA,DES}} = 10^{-2} = 1\%$) and 1.95 ($P_{\mathrm{FA,DES}} = 5\%$). In the IS, commonly used desired clean sample rejection rates are 0.1% and 1%, corresponding to the threshold parameters 2.97 and 2.42 [57]. Table 1 presents example threshold parameter values based on Eq. (8) (in the chi-square case) and Eq. (12) (in the Rayleigh case).

Table 1. Example threshold parameter T_{CME} values in chi-square and Rayleigh cases.

$P_{\mathrm{FA,DES}}$	T_{CME} (chi-square)	T_{CME} (Rayleigh)
$10^{-1} = 0.1$ (10%)	2.30	1.71
$10^{-2} = 0.01$ (1%)	4.60	2.42
$10^{-3} = 0.001$ (0.1%)	6.90	2.97

The used threshold parameter T_{CME} is calculated based on the desired clean sample rejection rate $P_{\mathrm{FA,DES}}$ which is to be decided. The resulting T_{CME} varies according to the assumed distribution. The larger the value of $P_{\mathrm{FA,DES}}$ is, the smaller is T_{CME}, the smaller is the threshold, and the larger is the amount of false alarms. Instead, small $P_{\mathrm{FA,DES}}$ leads to larger T_{CME}, larger threshold and, thus, a small amount of false alarms. The proper choice of $P_{\mathrm{FA,DES}}$ depends on the situation and on the application. In IS applications, there also exists a desired (information) signal which can be assumed to be wideband. In that case, a too low threshold may also suppress components from the desired signal. It was noticed in [117] that in IS purposes, $P_{\mathrm{FA,DES}} < 1\%$ in order to avoid performance degradation. In signal detection applications, a too low threshold causes falsely detected signals, whereas a too large threshold may lead to situation in which the signal is not detected at all. In addition, when using a too low threshold, the bandwidth estimate of the signal may be too wide because of the sidelobes above the

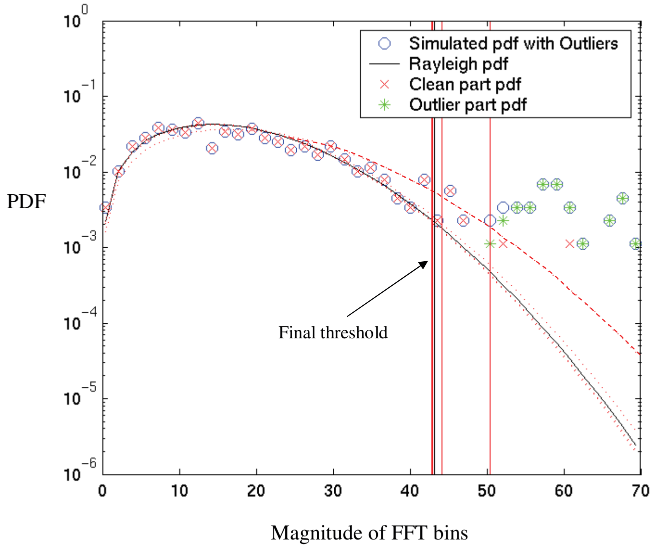

Fig. 12. One example outcome of the CME algorithm. Simulated frequency domain samples (O). The frequency domain samples are caused by the noise (and possible wideband information signal) ($\times$) or by the NB interfering signal ($*$).

threshold. In cognitive radio approach, the control of $P_{\mathrm{FA,DES}}$ is even more important, as $P_{\mathrm{FA,DES}}$ is directly related to the interference caused and the loss of spectral opportunities.

The original CME algorithm is a backward method, which means that in the first iteration the sample mean ζ is calculated from the whole set. After calculating the first threshold T_h, the samples above the threshold are selected for removal. The new value for ζ is calculated from the samples below the threshold. In general, the CME algorithm calculates iteratively a new value for ζ and, thus, a new threshold until samples that exceed the threshold (which are caused by the concentrated signal) are no longer found or a maximum number of iterations is reached [57]. The samples exceeding the threshold are assumed to be caused by a concentrated signal. One example outcome of the CME algorithm is presented in Figure 12.

The FCME algorithm is obtained by rearranging the samples in an ascending order according to their energies. Due to the rearrangement, the FCME algorithm requires sorting [106]. Commonly used sorting algorithms are Quicksort and Heapsort [106]. The running times of some sorting algorithms are presented in Table 2. After the sorting, the FCME algorithm calculates ζ of a small initial set [47, 160] which is assumed to be free of interference. The size of the initial set can vary from one element up to 10% of the size of the whole data set [57]. The larger the initial set, the simpler the algorithm is because less iterations are needed. However, the possibility that the initial set is not clean increases. On the other hand, the smaller the initial set is, the higher the possibility that the initial threshold is too small. In that case, it may be possible that the algorithm does not converge at all. Usually, the size of the initial set is 10% of all the samples. The FCME algorithm iteratively calculates a new value for ζ and a new threshold T_h until there are no new samples below the threshold [57]. While the threshold of the CME algorithm decreases in every iteration, the threshold calculated by the FCME algorithm increases. In general, the forward search methods have better performance than the backward methods [160]. The flowchart of the CME algorithm is presented in Figure 13 on page 52 and the flowchart of the FCME algorithm is presented in Figure 14 on page 53.

Table 2. Sorting algorithms; N = the number of elements. [106]

Sorting algorithm	Average running time	Worst case running time	Limitations
Straight insertion	N^2	N^2	$N < 20$
Shell's method	$N^{1.25}$	$N^{1.5}$	
Quicksort	$2\log_2 N$	N^2	
Heapsort	$N\log_2 N$	$N\log_2 N$	

Instead of zeroing the interfering samples, these can also be limited. Robust methods use limitation and it has been shown to have a good asymptotic performance [64]. For that reason, the limitation of outliers has also been adopted for the CME algorithms. Limiter CME (LCME) algorithm [118] limits the interfering samples to the lower level by normalizing, i.e., the interfering sample becomes $x_i = \frac{x_i\sqrt{T_h}}{||x_i||}$ instead of zero. The point is that every interfering signal sample also contains some energy from the information signal. While zeroing totally destroys the energy of the sample, limitation maintains some energy. This may be advantageous when there are a lot of interfering samples. However, the problem is that the energy after the limitation comes from both interfering and the information signal.

The CME algorithms are computationally simple. In the case of the CME algorithm, the most complex part is the Fourier transform which is required in frequency

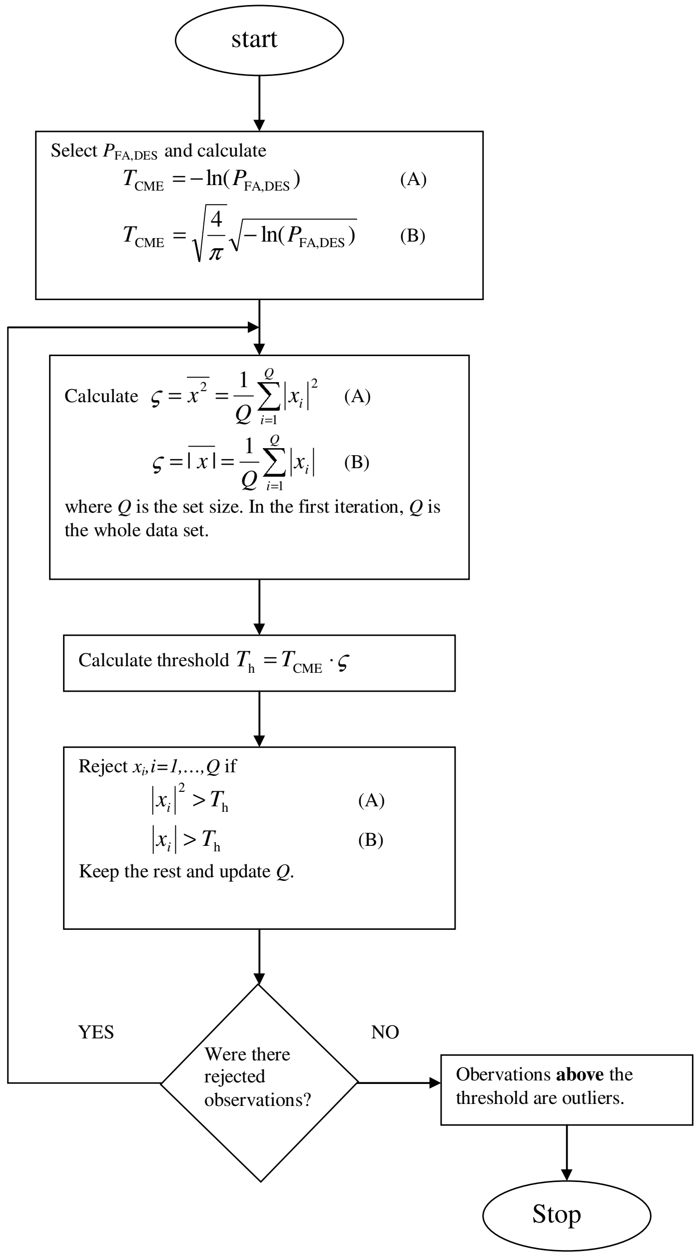

Fig. 13. The consecutive mean excision (CME) algorithm. (A) chi-squared distribution (B) Rayleigh distribution.

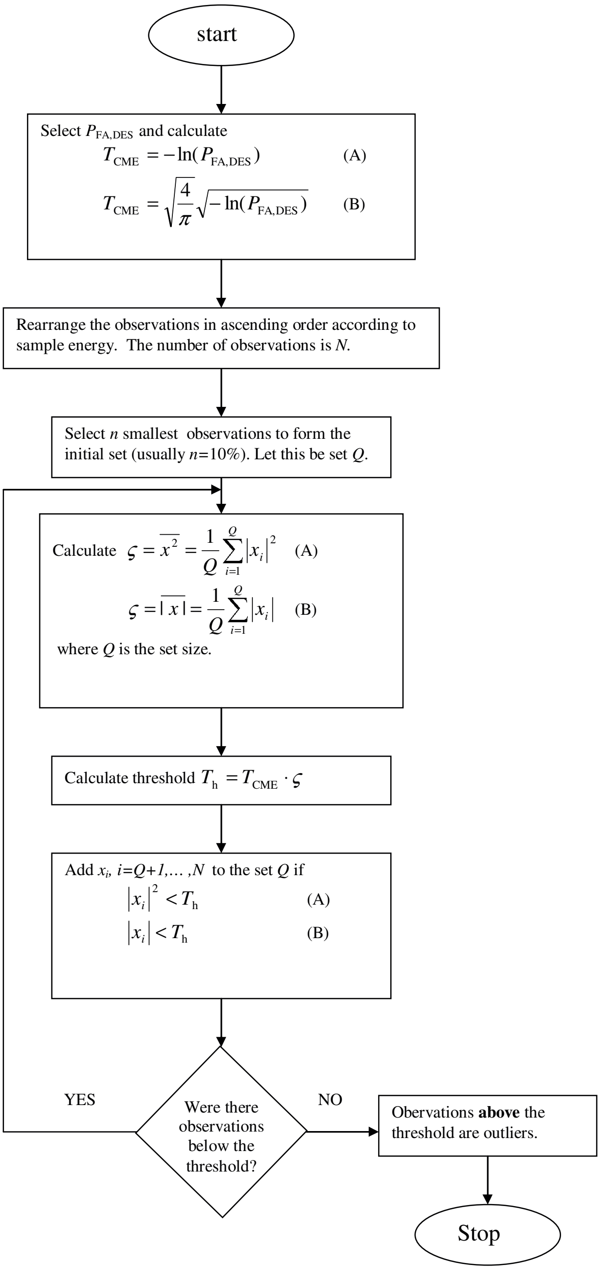

Fig. 14. The forward consecutive mean excision (FCME) algorithm. (A) chi-squared distribution (B) Rayleigh distribution.

domain processing. The computational complexity of FFT is $N \log_2 N$ [106]. In the FCME algorithm, the most complex parts are the Fourier transform, and rearranging the samples (sorting). The sorting can be done, for example, using Heapsort (average computational complexity $N \log_2 N$) or Quicksort (average computational complexity $2 \log_2 N$) [106]. Thus, the computational complexity of the CME algorithms is of the order of $N \log_2 N$.

The CME algorithms and their performance have been considered in several papers. In the supplementary paper [145], the CME algorithm was used as an interference suppression method in wideband signal detection. Therein, the detection of DS-CDMA signals under NB interference was considered. The interfering signals were 2-frequency shift keying (FSK), 4-FSK and off-center tone signals occupying 1.6% and 3.2% of the bandwidth. A Hann-256 window with 50% overlapping in the Welch power spectral density (PSD) was used. ISR was set to 20 dB. The CME threshold parameter was set to $\sqrt{3}$ and $\sqrt{4.5}$, because MFSK modulated signals have strong sidelobes. Radiometric detection was performed after the interference excision. The per bin probabilities of detection (P_{D}) and false alarm (P_{FA}) vs. SNR were simulated. The paper concluded that the loss caused by the IS was approximately $1-2$ dB depending on the SNR, and that the CME algorithm had good performance.

It is usually assumed that the signal arrives at the receiver from a single path. However, this is not necessarily a realistic assumption. In wireless channels, a signal may arrive at the receiver through various paths due to multipath propagation. In the supplementary paper [146], a frequency-selective Rayleigh fading channel model was used when studying the effects of multipath propagation on interference suppression. The Rayleigh fading channel is a channel without the line-of-sight (LOS) component, i.e., there is not a dominating path. The bit error rate (BER) performance of the FCME algorithm used for IS in a DS-CDMA system was considered. The interfering signals investigated were $1-5$ sinusoidal, bandlimited BPSK interfering signals with bandwidths up to 60% of the system's bandwidth, and chirp interference. A 4-term Blackman-Harris window was used before the Fourier transform. Absolute values of signal samples were used, and the FCME threshold parameter was 2.97. The BER performance vs. SNR and ISR were simulated as well as the effects of multipath interference on interference suppression. A frequency-selective Rayleigh fading channel model with two paths was used. It was assumed that the scattering was uncorrelated and that the path delays were multiples of the sampling interval. It was concluded that the FCME algorithm performed well. The narrower the bandwidth of the interfering signal, the smaller BER.

In addition, large ISR leads to a large BER value. The multipath interference caused performance degradation of the FCME algorithm only when the interfering signal was a chirp. This was mainly because the frequency domain is not the optimal excision domain for chirp signals, i.e., the chirp signal is not the narrowest in the frequency domain.

The threshold setting of the CME algorithms assumes that the noise is Gaussian. In practice, this is not necessarily true. The interference suppression ability of the CME, FCME and LCME methods for measured radio channel data was considered in the supplementary paper [140]. Therein, the data consisted of radio channel measurements performed in autumn 2004 in the city of Oulu, Finland, at 2.45 GHz with 200 MHz measurement bandwidth using the Elektrobit PropSound radio channel sounder [29, 70]. There was no interference-free reference data and the interfering signals were unknown to the receiver, so statistical analysis could not be performed. Instead, the aim was to show via examples that the CME algorithms are also able to operate in the case where the noise is not pure computer-generated Gaussian but from the real-world measurements. Both the channel transfer functions and impulse responses were studied. Receiver imperfections like nonlinearities were not studied. It was concluded that the CME algorithms are able to operate even though the noise is from real-life measurements.

Because the CME algorithms are blind, simple, low-complex and easy to implement – in other words, 'almost perfect' – an idea came to the mind: why not to use the CME algorithms to concentrated signal detection? As diagnostic outlier detection methods, the CME algorithms separate the noise-like samples and the samples caused by outliers, aka, concentrated signals. So, it should have no matter whether the concentrated signal is a desired signal or an interfering signal.

The above-mentioned idea was considered in the supplementary paper [144], which presented the idea of using the CME algorithm as a NB signal detection algorithm. The NB signal was a RC-BPSK signal with a bandwidth covering $5-40\%$ of the system bandwidth. The frequency samples caused by the NB signal were defined in two different ways, using 3 dB and 10 dB bandwidths of the signal. It was assumed that the received signal consisted only of the NB signal and the noise. Absolute values of signal samples were used. The CME algorithm with a threshold parameter of 2.42 was used for the NB signal detection. The number of samples was 512. The P_{D} and P_{FA} per frequency sample vs. SNR were demonstrated through simulations. The simulation results showed that the CME algorithm operated best when the signal bandwidth was narrow.

Both the CME and FCME algorithms were used as NB signal detection algorithms in Paper III. The paper compared a conventional notch filter, the CME and the FCME algorithms in the sense of correctness of the thresholds and probability of detection. The received signal consisted only of the NB signal and the noise. The narrowband signal consisted of adjacent off-center tone signals with a bandwidth (BW) covering $5-95\%$ of the receiver bandwidth. The phase of the narrowband signal was uniformly distributed on $[0,2\pi]$. The frequency samples caused by the NB signal were defined using 3 dB bandwidth of the signal. The number of samples was 512. Absolute values of signal samples were used. The threshold parameter was 2.42. The initial set size of the FCME algorithm was 9.8%. A channelized radiometer was used for comparison. The normalized mean square error (NMSE) between the theoretical and simulated thresholds was used to measure the correctness of the thresholds. The NMSE of the notch filter was poor even when the signal was very narrowband. The NMSE's of the CME and FCME algorithms were almost equal until the bandwidth of the narrowband signal was approximately 50%. After that, the NMSE of the CME algorithm started to degrade. Instead, the NMSE of the FCME algorithm was good even when the bandwidth of the narrowband signal was 80%. When the bandwidth of the narrowband signal was 95%, the NMSE of the FCME algorithm was poor because the initial set was not clean.

The probability of detection per frequency sample as a function of SNR was demonstrated via simulations. The results for the CME and FCME algorithms are presented in Figures 15 and 16. It was noticed that the FCME algorithm performed better than the CME algorithm and the performance of the notch filter was the worst. The paper concluded that the performance of the CME algorithm started to decrease when the signal bandwidth was more than 50% of the receiver bandwidth. Meanwhile, the FCME algorithm performed well even when the signal bandwidth was 85% of the receiver bandwidth. The performance of the conventional notch filter started to degrade after the signal bandwidth was more than 20% of the receiver bandwidth.

It was noticed in Paper III, that the FCME algorithm is better suited for detection than the CME algorithm. Although having good detection probabilities, the FCME algorithm was noticed not to be directly applicable for signal detection purposes. That was because statistical information such as bandwidth, center frequency and the number of detected signals is almost impossible to estimate properly due to problems in threshold setting that yield additional false alarms and needless signal separation. Something had to be done to fix the problem. Both low and high thresholds have good and poor detection properties. But how do they work together? This is discussed in more detail

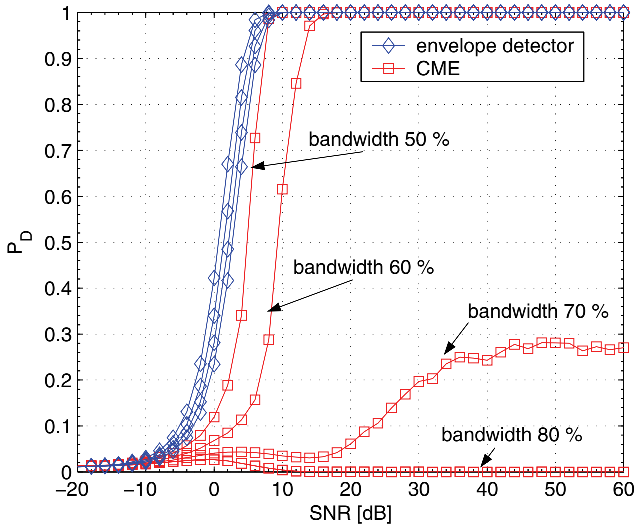

Fig. 15. Simulated P_D vs. SNR. The CME algorithm and the channelized radiometer (envelope detector) with signal BWs 50%, 60%, 70% and 80% of the receiver BW. (III, published by permission of IEEE).

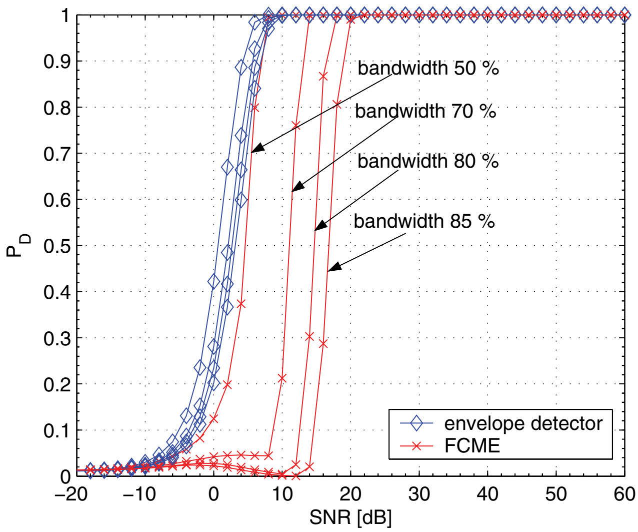

Fig. 16. Simulated P_D vs. SNR. The FCME algorithm and the channelized radiometer (envelope detector) with signal BWs 50%, 70%, 80% and 85% of the receiver BW. (III, published by permission of IEEE).

in Section 3.4, where one solution to this problem is given.

The threshold parameter values calculated from Eq. (8) and Eq. (12) are approximations which are used regardless of the number of samples and the size of the initial set. However, when the number of samples is small, the obtained false alarm does not equal to the desired false alarm. As a consequence, the false alarm rate is not properly controlled. The correctness of the false alarm rate is important in many applications. For example, in cognitive radios, a too high false alarm rate may lead to inefficient spectrum usage. For that reason, accurate false alarm probabilities were derived in Paper IV. The FCME algorithm and forward cell-averaging (CA) method [73, 76] were considered. Accurate false alarm probabilities of the FCME algorithm and, thus, the forward CA method were analytically studied. Accurate values of the threshold parameter as a function of number of signal samples N and the size of initial set were derived. First, the noise-only case was studied. The false alarm probabilities for the FCME and joint forward CA methods are presented in Figure 17 in the case of magnitude-squared values which correspond to the chi-squared distribution with 2 degrees of freedom. The simulations confirmed that the use of derived accurate threshold parameter values improved the false alarm probabilities, especially when N is small. It can be concluded that when the number of samples is at least 512, the desired false alarm probability $P_{\mathrm{FA,DES}} \leq 10^{-3}$, and the threshold parameter is calculated from Eq. (8), the desired and obtained false alarm rates are almost equal. In the presence of independent, noncentral chi-square distributed Rayleigh fading outliers covering approximately $31-62\%$ of the whole bandwidth, the obtained false alarm probabilities for the FCME algorithm were higher than the desired ones, even though accurate threshold parameter values were used. Instead, with the forward CA method the obtained and desired false alarm probabilities were approximately in the same level. However, the FCME algorithm had better detection rates than the forward CA method. The more outliers, the more the FCME algorithm outperformed the forward CA method.

The threshold parameter values in the case of chi-squared distribution with more than 2 degrees of freedom were also derived in Paper IV. In the noise-only case, the derived threshold parameter values had more precise false alarm probability when compared to the original threshold parameter values. It was noticed that by increasing the degrees of freedom, the effectiveness of the studied methods improved. In the presence of outliers, required SNR values for a given detection probability (0.9 and 0.99) were studied. It was noticed that in the studied cases, the required SNR values for the forward CA method were approximately 0.3 – 1.5 dB larger when compared to the ideal

		Desired false alarm probability $P_{\mathrm{FA,DES}}$							
		10^{-5}		10^{-4}		10^{-3}		10^{-2}	
N	I	A	B	A	B	A	B	A	B
16	4	22.6	1.17	9.00	1.25	5.16	1.5	5.03	2.47
16	8	1.14	**1.04**	1.20	**1.09**	1.42	1.24	2.26	1.87
···	···	↓ Region with acceptable performance ↓						↰↓ Poor ↑	
32	12	**1.01**	**1.01**	**1.03**	**1.03**	1.11	**1.10**	1.62	1.51
64	12	**1.0**	**1.0**	**1.0**	**1.0**	**1.1**	**1.1**	1.4	1.4
128	16	**1.0**	**1.0**	**1.0**	**1.0**	**1.1**	**1.1**	1.3	1.3
128	32	**1.0**	**1.0**	**1.0**	**1.0**	**1.1**	**1.1**	1.3	1.3
256	16	**1.0**	**1.0**	**1.0**	**1.0**	**1.1**	**1.1**	1.3	1.3
512	16	**1.0**	**1.0**	**1.0**	**1.0**	**1.1**	**1.1**	1.3	1.3

Fig. 17. False alarm probabilities in the noise-only case. A: The FCME algorithm and B: The forward CA method. I denotes the size of the initial set. Results are relative to the desired $P_{\mathrm{FA,DES}}$, i.e., 1 means that the desired false alarm probability is achieved. (IV, published by permission of IEEE).

NP detector.

Recently, the CME algorithms were analyzed in Paper V, and in the supplementary paper [148]. The presented analysis is based on the signals *shape* in the considered domain, e.g., spectrum in the frequency domain. The goal was to provide simple tools for checking whether a signal is detectable or not without the need for time-consuming simulations. The signal samples were re-ordered in a descending order according to their heights for the purposes of the analysis. The adjacent signal samples with equal heights were subsequently divided into different sets (*lobes*), so that one lobe consisted of signal samples with equal heights as illustrated in Figure 18. Because of the reordering, the first lobe consisted of the signal samples with the highest heights, as the last lobe consisted of the signal samples with the lowest heights. Based on Eq. (1) and using a geometrical approach to define the average sample mean, the limits of detection were derived for both the CME algorithms in terms of the heights of the lobes and the used threshold parameter (or threshold multiplier). In addition, different detection alternatives were also derived. From the results of the analysis, practical SNR limits at which the CME algorithms are able to find signals with different widths were derived. The detection limits are presented in Tables 3 and 4. It was noticed that the required SNR

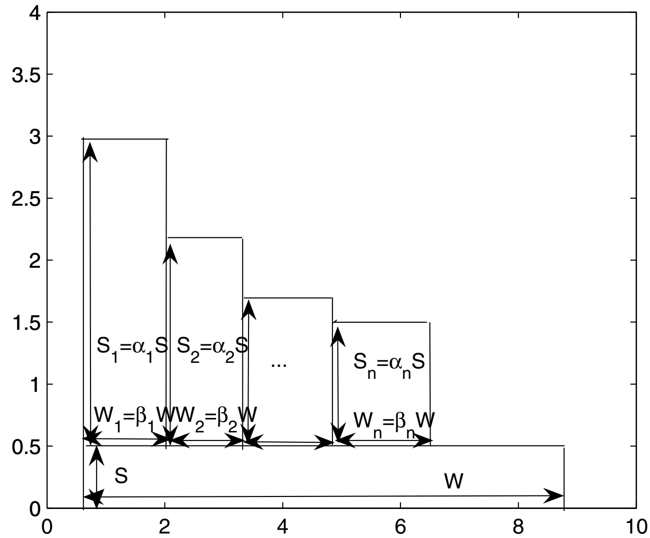

Fig. 18. An example of base signal SW and NB signal lobes (S_iW_i). S and W are the height and the width of the base signal, S_i and W_i are the height and the width of the ith signal lobe. (V, published by permission of IEEE).

Table 3. The values of SNR [dB] when the signal detection via the CME algorithm is possible with different values of threshold parameter $T_{\mathbf{CME}}$ and relative bandwidth of the signal β_1. The signal has only one lobe. SNR is defined per total bandwidth.

T_{CME}	$\beta_1 = 0.05$	$\beta_1 = 0.1$	$\beta_1 = 0.2$	$\beta_1 = 0.3$	$\beta_1 = 0.4$
2.3026	> -9 dB	> -6 dB	> -2 dB	> 2 dB	> 8 dB
4.6052	> -5 dB	> -1 dB	> 10 dB	$-^{*}$	$-^{*}$
6.9078	> -3 dB	> 3 dB	$-^{*}$	$-^{*}$	$-^{*}$

* detection is not possible

values for both CME algorithms are almost equal when the signal is very narrowband. When the bandwidth of the signal gets wider, the CME algorithm requires larger SNR for the detection when compared to the FCME algorithm. When the bandwidth of the signal was more than 40% of the total bandwidth, the CME algorithm does not operate at all. The obtained limits of detection were confirmed with simulations using random and OFDM signals. It was noticed that the analysis predicts well the detectability of signals.

Table 4. The values of SNR [dB] when the signal detection via the FCME algorithm is possible with different values of threshold parameter T and relative bandwidth of the signal β_1. The signal has only one lobe. SNR is defined per total bandwidth.

T	$\beta_1 = 0.05$	$\beta_1 = 0.1$	$\beta_1 = 0.2$	$\beta_1 = 0.3$	$\beta_1 = 0.4$
2.3026	> -9 dB	> -6 dB	> -3 dB	> -2 dB	> 0 dB
4.6052	> -6 dB	> -3 dB	> 0 dB	> 2 dB	> 3 dB
6.9078	> -5 dB	> -2 dB	> 1 dB	> 3 dB	> 4 dB

3.3 The transform selective interference suppression algorithm

While some interfering signals are best excised in the time domain, some are best excised in the frequency or some other domain. The optimal domain depends on the signal characteristics. Signals may be "broadband" in one domain but "narrowband" or concentrated in another domain. The CME algorithms discussed earlier in this chapter are able to excise interfering signals only in the considered domain, which is usually either the time domain or the frequency domain. The problem is that this type of IS methods are useless against interfering signals that are not "narrowband" or concentrated in the considered domain; for example the FCME algorithm in the time domain is effective against impulsive interfering signals while it is useless against other kind of interfering signals.

The transform selective interference suppression algorithm (TSISA) method is a computationally simple bank-type method for suppressing different types of time - varying and non-stationary interfering signals [3]. The TSISA method employs several transforms and makes the selection between the domains before the IS, which reduces the computational complexity considerably compared to other filter bank methods, for example, [17]. The most suitable transform is selected based on the simple compression gain (CG) metric. The IS is performed by the FCME algorithm. The block diagram of the TSISA is illustrated in Figure 7 c) on page 36.

The TSISA computes a number of transforms in parallel and selects the most suitable one for IS. The considered transform domains are the time domain, the ordinary Fourier domain and the fractional Fourier domain. However, an arbitrary number of transform domains may be used. The fractional Fourier transformation (FrFT) is a generalization of the ordinary Fourier transformation with an order parameter a [100]. When $a = 1$, the FrFT corresponds to the ordinary FT. When $a = 0$, the FrFT is the original signal itself in the time domain. So, the FrFT is able to make the transform to any intermediate domain between the time and frequency domains. The FT has sinusoids as basis functions. As a consequence, stationary NB interference is best excised in the frequency domain. The FrFT has frequency sweeping sinusoids, chirps, as basis functions. Therefore, it is theoretically possible to perfectly localize chirp interference in the FrFT domain. However, this requires that the order parameter of the FrFT has to be chosen properly. The optimal order depends on the sweep rate of the interfering signal. The order of the FrFT is defined by estimating the bandwidth of the interfering signal using the FCME algorithm in the FT domain. Hence, the FT and its CG are calculated before the calculation of the FrFT.

The used transform is selected based on the compression gain [100]

$$\varrho = \frac{\frac{1}{N}\sum_{n=1}^{N}|r(n)|^2}{\sqrt[N]{\prod_{n=1}^{N}|r(n)|^2}}, \tag{13}$$

where N and $r(n)$ are the used block length and the received signal sample at the appropriate transform domain, respectively. Theoretically, the CG is the ratio of the arithmetic mean M_a and the geometric mean M_g of the signal sample powers. The arithmetic mean is always larger than or equal to the geometric mean [13], so $\varrho \geq 1$. In its logarithmic form, the CG can be expressed as [161]

$$\ln \varrho = \ln \overline{|r(n)|^2} - \overline{\ln |r(n)|^2}, \tag{14}$$

where $\overline{(\cdot)}$ denotes the sample mean. Because $\varrho \geq 1$, it follows that $\ln \varrho \geq 0$ and $\ln \varrho = 0$ only if all the data values are equal.

The CG has been used previously, for example, in image processing, where it is known as a coding gain. In image processing, the CG measures how well a transform can compress the image data. In IS, the CG measures how well the interfering signal is compressed in the transform domain. The more the energy is concentrated in a smaller number of samples, the larger the CG is [3, 69] and the easier it is to detect and remove the interfering signal as already seen. It can be assumed that the concentrated energy is mostly from the interference, because the harmful interference is usually significantly stronger than the information signal or the noise.

The flatness of the spectrum has an influence on the CG. When the spectrum is totally flat, all the samples $r(n)$ have equal values, and the CG$= 1$. In such a case, the transform is not able to compress the signal. When the spectrum is not flat, $M_a > M_g$

and correspondingly CG>1. Unlike in the flat case, the transform is capable of compressing the signal. [13]

The performance of the TSISA [3] was considered in Paper I. Therein, the BER performance comparisons of the TSISA to pure FCME algorithm based IS and recursive least squares (RLS) based IS were presented in every considered transform domain. The received signal consisted of a DS spread spectrum wideband information signal, interfering signal and noise. Three types of interfering signals – impulses, multiple sinusoids and chirps – were considered. Impulses had random or constant pulse repetition rate, and the frequency-offset of the sinusoidal interference was random. The chirp swept the predetermined frequency band during one bit duration. Three transform domains for IS were considered: the time domain, the Fourier domain and the fractional Fourier domain. With both the Fourier transforms, a 4-term Blackman-Harris window was used. The SNR was set to 15 dB and the ISR to 30 dB per interfering signal. Absolute values of signal samples were used. The FCME algorithm with threshold parameter 2.97 and with the initial set size of 10% was used. The length of the RLS filter was 8 taps. Both the domain selection process and BER were evaluated. It was assumed that the time domain is the most suitable domain for impulsive interference, the Fourier domain is the most suitable domain for sinusoids, and the fractional Fourier domain is the most suitable domain for chirp interfering signals.

In the case of constant and random impulse interference, the TSISA was able to select the time domain even when the contamination ratio was approximately 80% of the samples. The BER performance of the TSISA was superior when compared to the performance of the RLS filter as can be seen from Figures 19 and 20. The BER performance of the TSISA and that of the time domain FCME algorithm were almost in the same level. In the case of sinusoids, the TSISA started to select the Fourier domain when ISR was 10 dB, or when the number of sinusoids was 3. It was noticed that when there were only few sinusoidal signals, the bandwidth was narrow, and the order of the FrFT was close to one, corresponding the FFT. For that reason, the selection rate of the FrFT was almost equal to that of the FFT. The BER results for sinusoidal signals are presented in Figures 21 and 22. The BER performance of the TSISA was equal to that of the Fourier domain FCME algorithm but better than that of the RLS filter regardless of the number of sinusoids. When the interfering signal was a chirp, the TSISA started to select the FrFT domain when the ISR was 15 dB, or when the relative bandwidth of the chirp was 20%. This is because the selection rates of the FrFT and FFT are almost equal when the bandwidth of the chirp is narrow. At low ISR, the signal is so weak

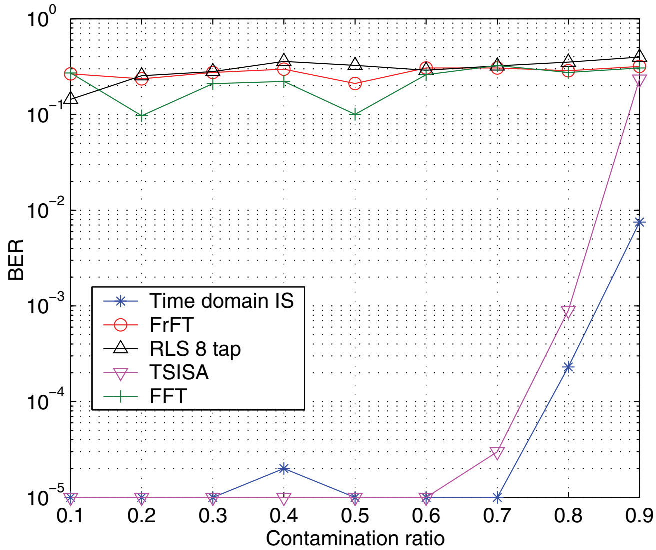

Fig. 19. BER vs. contamination ratio with constant impulse interference. ISR=30 dB. (I, published by permission of IEEE).

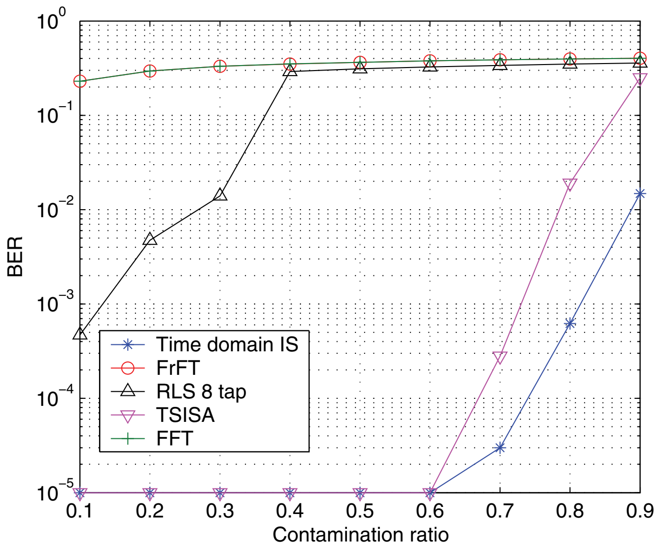

Fig. 20. BER vs. contamination ratio with random impulse interference. ISR=30 dB. (I, published by permission of IEEE).

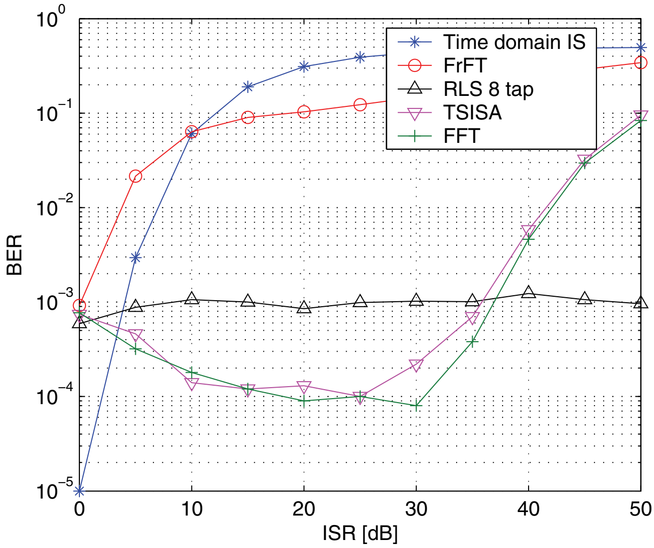

Fig. 21. BER vs. ISR with sinusoidal interference. The number of sinusoids is five. SNR=15 dB. (I, published by permission of IEEE).

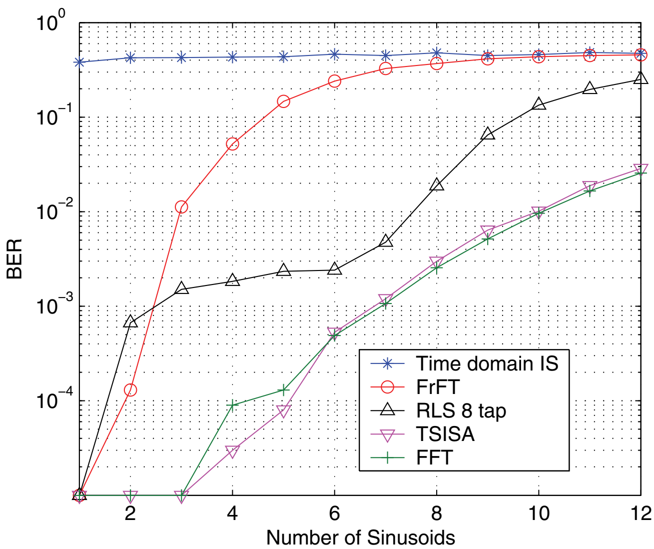

Fig. 22. BER vs. number of sinusoids. SNR=15 dB and ISR=30 dB. (I, published by permission of IEEE).

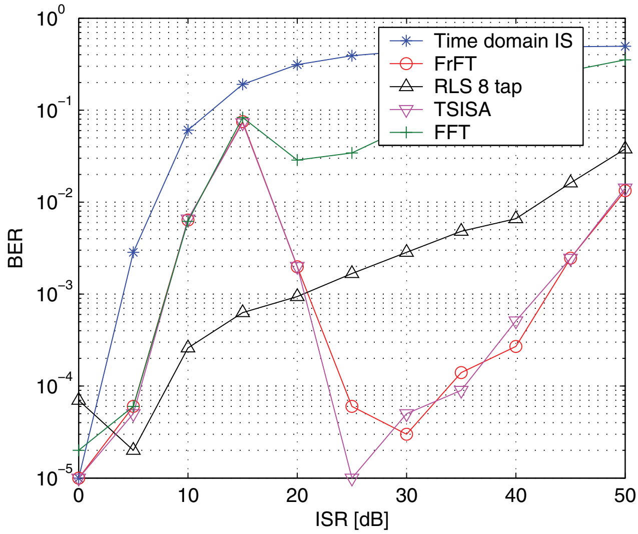

Fig. 23. BER vs. ISR with chirp interference. Chirp sweeps the whole frequency band in one bit duration. SNR=15 dB. (I, published by permission of IEEE).

that the FCME algorithm does not find it. In addition, at large ISR value, raising sidelobes decrease the performance. The BER performance of the TSISA was better than that of the RLS filter when the ISR was 20 dB or more (Figure 23). Again, the performance of the TSISA and FrFT domain FCME were almost equal. The domain selection procedure of the TSISA in the presence of above-mentioned interfering signals has also been considered in the supplementary paper [141].

According to the simulation results it can be concluded that the TSISA has an excellent BER performance. The performance of the TSISA was superior to the RLS based IS, and a pure FCME algorithm also outperformed the RLS based IS. In addition, the performance loss between the TSISA and the FCME interference suppression in the best suitable domain was small. It was also observed that the computational complexity of the TSISA was low. It can be concluded that when there exists interfering signals that are concentrated in different transform domains, or it is not known in which transform domain the interfering signals are the most concentrated, the TSISA could be a reasonable choice for IS. The question which came up was that could there be any other simple transform selection methods?

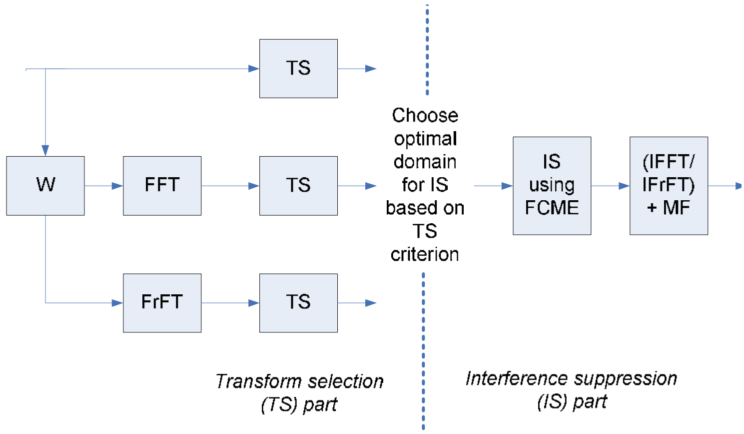

Fig. 24. Interference suppression with transform selection (TS). W denotes a window.

3.3.1 Other transform selection metrics

In addition to the compression gain, the domain selection in the TSISA can be done using, for example, percentiles (PRC), maximum or coefficient of variation (CV) (Paper II, supplementary paper [147]). The block diagram of this extended TSISA system is illustrated in Figure 24.

A PRC is a value that indicates the percentage of the values which are below or equal to the PRC. For example, 25th percentile means that 25% of the values are below it. The method operates as follows. First, the energies of samples are rearranged in an ascending order in every transform domain [106]. The number of extra sorting operations is $M-1$, where M denotes the number of transform domains. Note that the sorting has already been done in the Fourier domain because of the FCME algorithm, so that does not increase additive sorting. Then, the 25% PRCs (quartile) are calculated. The sum of energies have to be normalized in all the transform domains that use windowing because it reduces the energy. The normalization coefficient ρ is given by

$$\rho \sum |r_f(n)|^2 = \sum |r_t(n)|^2, \tag{15}$$

where $r_t(n)$ and $r_f(n)$ are the time domain samples and windowed samples in the transform domain, respectively. From that, ρ may be written as

$$\rho = \frac{\sum |r_t(n)|^2}{\sum |r_f(n)|^2}. \tag{16}$$

Because it can be assumed that most of the energy is from the interfering signal, the relatively largest value in each transform domain (maximum) can also be used as a metric for selecting the best transform domain for IS. The relatively largest value, i.e., the ratio of the largest value to the smallest value, can be expressed as

$$\max_{k=1,\ldots,M} \left(\frac{\max_{n=1,\ldots,N}(|r_k(n)|^2)}{\min_{n=1,\ldots,N}(|r_k(n)|^2)} \right). \tag{17}$$

This method is called the maximum (metric) hereafter.

The coefficient of variation measures the deviation of a variable from its mean. When the variation is small, also the CV is small. It does not depend on the mean intensity. The CV can be expressed as [161]

$$\epsilon = \hat{\sigma}/\overline{|r(n)|^2}, \tag{18}$$

where

$$\hat{\sigma} = \sqrt{\frac{1}{N-1}\sum_{i=1}^{N}(|r(n)|^2 - \overline{|r(n)|^2})^2} \tag{19}$$

is the estimate of the standard deviation. In other words, the CV is the ratio of the standard deviation and the mean of the data. The transform domain with the largest CV is chosen.

The percentile was first used with the FCME algorithm in the supplementary paper [78], where the domain selection was performed between the time and frequency domains. An extension of the TSISA was considered in Paper II. There, two novel transform domain selection methods, namely the maximum and the CV, were proposed and evaluated. The percentile and CG were used as points of comparison. The system was assumed to consist of a wideband BPSK DS spread spectrum signal with Gold spreading codes, an interfering signal and Gaussian noise. Sinusoidal, impulsive, chirp and BPSK signals were used as interfering signals. Two or three transform domains for IS were considered, namely, the time domain, the Fourier domain, and, in some simulations, the fractional Fourier domain. ISR was set to 30 dB whereas SNR was set to 5 or 15 dB. The frequency domain samples were calculated with the windowed 64-point FFT. The 4-term Blackman-Harris window was used. Absolute values of signal samples were used. The FCME threshold parameter was chosen to be 2.97. The uncoded BER performance of the considered methods was evaluated via simulations. When the selection was done between the time and Fourier domains, impulses, multiple sinusoids and

RC-BPSK signals were considered. In the case of impulsive interference and SNR=15 dB, the BER as a function of the contamination ratio was studied. The CG and PRC had almost equal performance. CV performed slightly worse as the performance of the maximum was the worst. The CG, PRC and CV are able to operate even when slightly more than half of the samples are corrupted. When there were multiple sinusoids present and SNR=15 dB, the BER as a function of the number of sinusoidal signals was simulated. The maximum performed the worst. Instead, all other methods offered decent performance, the BER less than 10^{-3}, when there were less than seven sinusoids. In the case of RC-BPSK signal with 10% bandwidth and SNR=15 dB, the BER as a function of ISR was considered. The FCME algorithm started to operate properly when ISR=10 dB. It was noticed that the CG and CV had the best performance while the maximum had the worst performance. In the case of the CG, CV and the PRC, the BER was less than 10^{-3} when ISR was less than 40 dB.

When the selection was done between all the three domains, impulses, multiple sinusoids and chirps were considered. It was noticed that in the case of impulses and multiple sinusoids, the BER results were almost equal when compared to the BER results where the domain selection was done between only the time and Fourier domains (Figures 25 and 26). In the case of chirp interference, the BER as a function of ISR was studied. The results are presented in Figure 27. The FCME algorithm started to operate properly right after ISR=15 dB. This is because at lower ISR, the signal is so weak that the FCME algorithm does not find it. In addition, at large ISR value, raising sidelobes decrease the performance. The maximum performed the worst, as CV, CR and PRC offered almost equal performance. The BER less than 10^{-3} was achieved when ISR was between 20 and 40 dB and SNR=15 dB.

It was also noticed that when the SNR=5 dB, the BER was in all of the studied cases at its best 10^{-2}. According to the simulations, the CG was able to offer the best performance in most of the cases. However, the performance of the CV was almost as good as the performance of the CG. The maximum method performed the worst. The simulations indicated that the proposed CV-based domain selection provided good performance against all studied interfering signals. In addition, it was noticed that the CV is simple to implement and has a low computational complexity. The domain selection process of the proposed methods was considered in the supplementary paper [147]. Therein, it was noticed that CV and CG had almost equal performance, and the maximum method performed the worst.

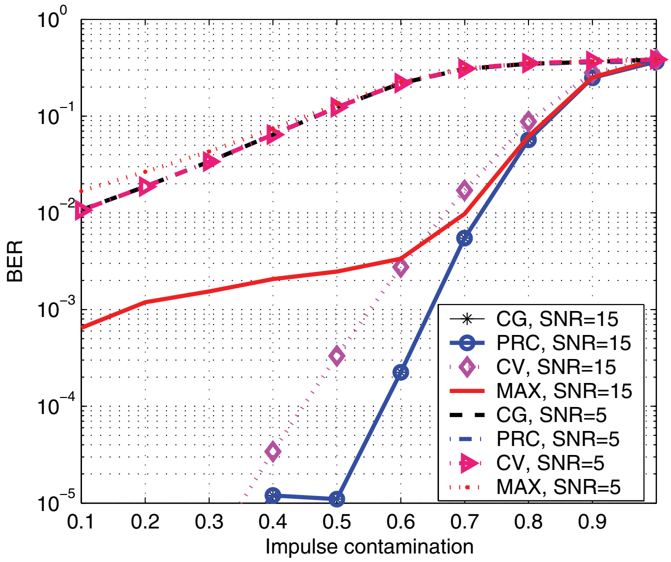

Fig. 25. BER vs. contamination ratio with Gaussian impulsive interference. ISR$=$ 30 dB. (II, published by permission of IEEE).

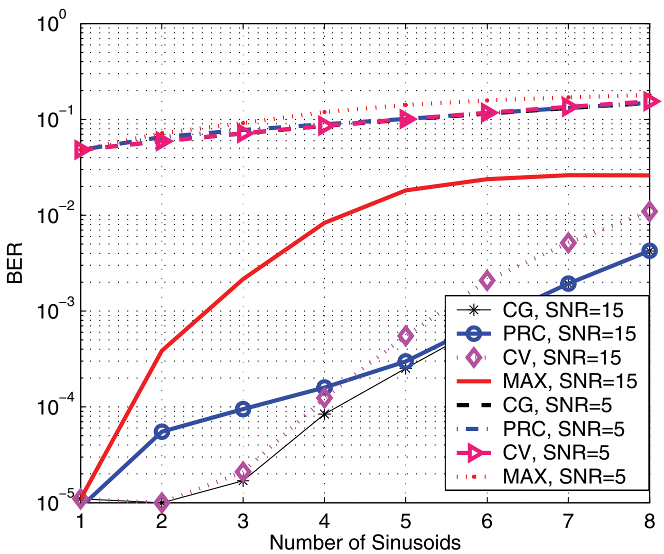

Fig. 26. BER vs. number of sinusoidal signals. ISR$=$ 30 dB. (II, published by permission of IEEE).

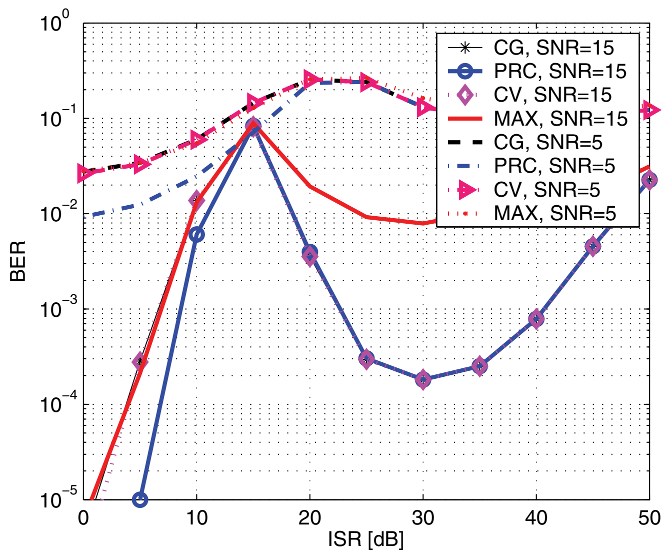

Fig. 27. BER vs. ISR with chirp interference. (II, published by permission of IEEE).

3.4 The localization algorithm based on double-thresholding

The localization algorithm based on double-thresholding (LAD) method was proposed in Paper VI, and in the supplementary paper [143]. The purpose of the LAD method is to reduce the problems of falsely separated and detected signals. The LAD method is based on the usage of two thresholds, the upper and lower thresholds. The LAD thresholds can be calculated with the FCME algorithm, for example. The FCME algorithm is run twice with two threshold parameters, which are called the upper (T_1) and lower (T_2) threshold parameters, $T_1 > T_2$, to have two thresholds, which are called the upper (T_u) and lower (T_l) thresholds. After the threshold calculation, the LAD method groups the adjacent samples above the lower threshold T_l into the same group called a *cluster*. The largest element of a cluster is compared to the upper threshold. If it exceeds the upper threshold T_u, it is decided that the cluster corresponds to a concentrated signal. If the largest sample is below the upper threshold, it is decided that the cluster corresponds to the noise and possible wideband information signal.

Blind SNR estimation discussed, for example, in [8, 85, 101, 121], is useful when *a priori* knowledge of the signal(s) and/or the noise is not available. The LAD method can be extended to estimate the SNR values of several unknown narrowband signals as illustrated in Figure 28. After running the LAD method, there are m' estimated sets of narrowband signals and one noise set. The SNR estimate for the kth estimated narrowband signal is then given by

$$\hat{\gamma}_k = \frac{\frac{1}{N_k}\sum |I_k(n)|^2}{\frac{1}{K}\sum |W(n)|^2} = \frac{\hat{P}_k^i}{\hat{P}_w}, \tag{20}$$

where $\{I_k\}, k = 1, \cdots, m'$, means the received frequency domain samples belonging to the kth estimated narrowband signal set, N_k is the number of those samples, $\{W(n)\}$ is the received frequency domain samples belonging to the noise + possible wideband signal set, and K is the noise set size. The complexity cost of the SNR calculation is low, because all the samples are already in the Fourier domain and also squared.

The LAD method has several advantages. First, it does not need *a priori* knowledge of the signal to be detected, because the threshold calculation via the FCME algorithm is done blindly. Second, the computational complexity of the LAD method is low. This is due to the simple threshold computation. There are also some problems. The LAD method is not always capable of separating two adjacent signals and it is not able to localize weak signals accurately. High sidelobes also cause problems when estimating the (band)width of a signal.

A flowchart of the LAD method is presented in Figure 29. In Figure 30, the threshold setting of the LAD method is compared to that of the FCME algorithm and the advantages of the LAD method are illustrated.

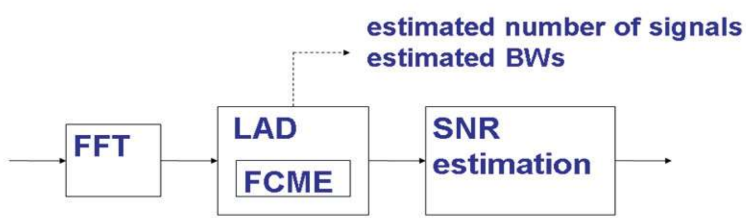

Fig. 28. A blind SNR estimation scheme.

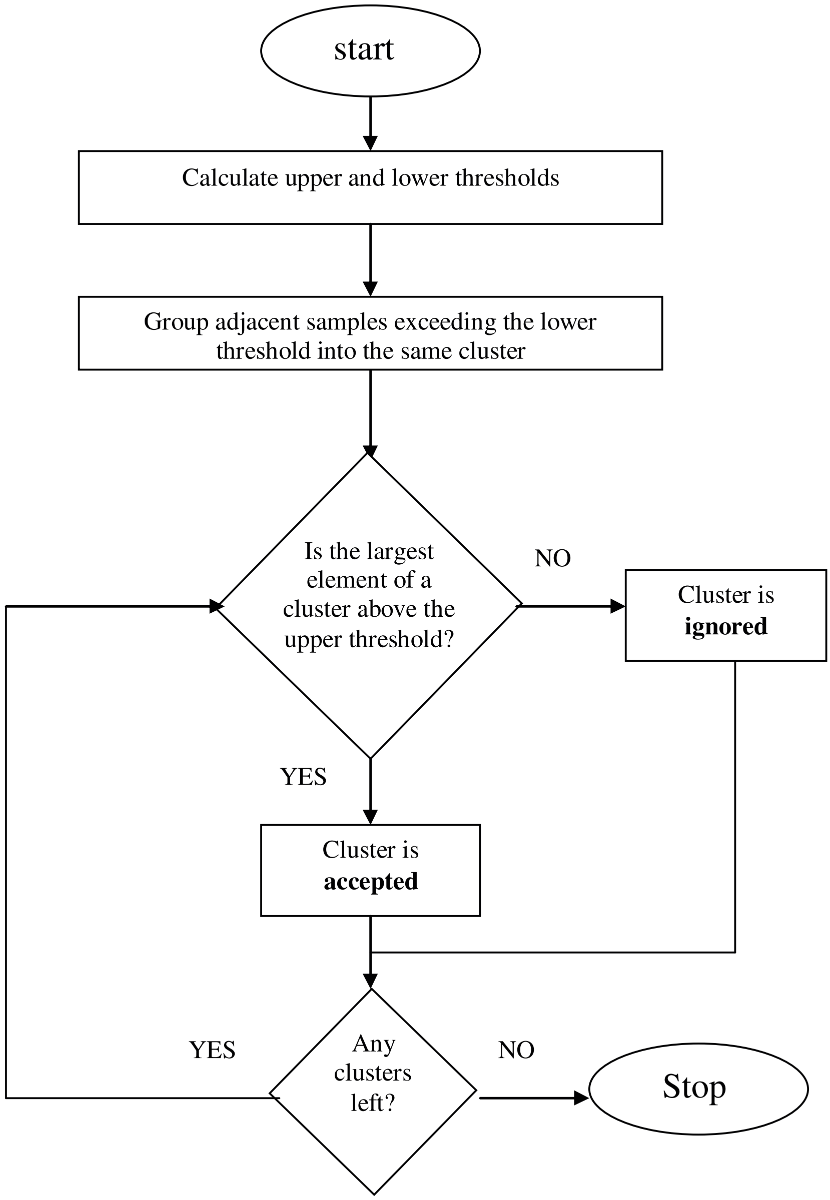

Fig. 29. The localization algorithm based on double-thresholding (LAD). The thresholds can be calculated with the FCME algorithm, for example. "Cluster is ignored" means that the cluster corresponds to noise (and possibly a wideband signal). "Cluster is accepted" means that the cluster corresponds to a concentrated signal.

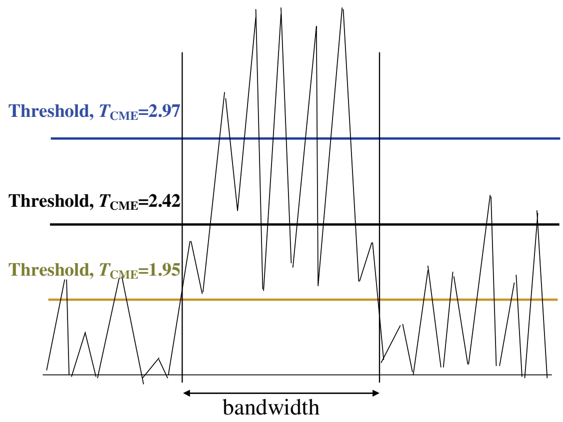

(a)

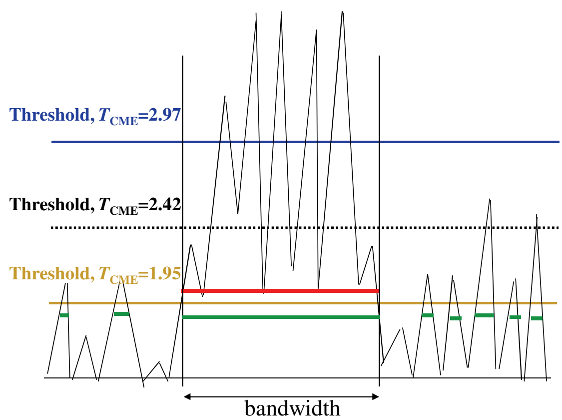

(b)

Fig. 30. A RC-BPSK signal in the frequency domain. (a) The FCME algorithm with threshold parameters 2.97, 2.42 or 1.95. The uppermost threshold finds 5 signals, the middle threshold finds 6 signals and the lowest threshold 8 signals. (b) The LAD with upper (threshold parameter 2.97) and lower (threshold parameter 1.95) thresholds. The LAD finds 8 groups, i.e., peaks above the lower threshold, but only one group is accepted as a signal, i.e., if a peak of the cluster exceeds the upper threshold. (VI, published by permission of IEEE)

3.4.1 The LAD with normalized thresholds

The LAD threshold calculation can be simplified as proposed in Paper VIII. In the LAD NT method, the threshold is calculated only once, and the upper and lower thresholds are derived from that. This reduces the computational complexity. First, one threshold is calculated using some threshold parameter T_x, $T_2 \leq T_x \leq T_1$. Thus, the last threshold is $T_{\mathrm{new}} = T_x \zeta_{\mathrm{new}}$, where ζ_{new} is the mean after the last iteration. Second, two fixing coefficients

$$P_{\mathrm{up}} = (T_1/T_x)a \tag{21}$$

and

$$P_{\mathrm{lo}} = (T_2/T_x)b, \tag{22}$$

$a \geq 1$ and $b \leq 1$, are used to get the upper and lower thresholds

$$T'_{\mathrm{u}} = T_{\mathrm{new}} P_{\mathrm{up}} \tag{23}$$

and

$$T'_{\mathrm{l}} = T_{\mathrm{new}} P_{\mathrm{lo}}. \tag{24}$$

Coefficients a and b are used to correct the mean values. The mean of the set with less samples is smaller than the mean of the set with more samples because the samples are sorted in an ascending order according to their energies [118]. However, without coefficients a and b, $\zeta_u = \zeta_{\mathrm{new}}$ and $\zeta_l = \zeta_{\mathrm{new}}$ which are not true. Thus, a proper choice for a and b is $a = \mathrm{E}[\zeta_u/\zeta_{\mathrm{new}}]$ and $b = \mathrm{E}[\zeta_l/\zeta_{\mathrm{new}}]$. However, the means ζ_u and ζ_l are usually unknown. So, a and b can be selected to be, for example, the statistical means in extensive computation simulations. The means depend on the actual realizations, so T_{u} and T'_{u} as well as T_{l} and T'_{l} do not exactly correspond to each other. It follows that the desired and obtained false alarm rates are not equal. For that reason, the NT method is a so called *ad hoc* method. However, the thresholds are close enough as noticed in VIII.

The threshold parameter T_x can be selected in different ways. In case (a), the lower threshold parameter T_2 is used as a threshold parameter T_x. Thus, $T_{\mathrm{l}} = T'_{\mathrm{l}}$. In case (b), the used threshold parameter T_x is in the middle of the upper and lower threshold parameters, i.e., $T_x = (T_1 + T_2)/2$. The LAD NT method is illustrated in Figures 31 and 32.

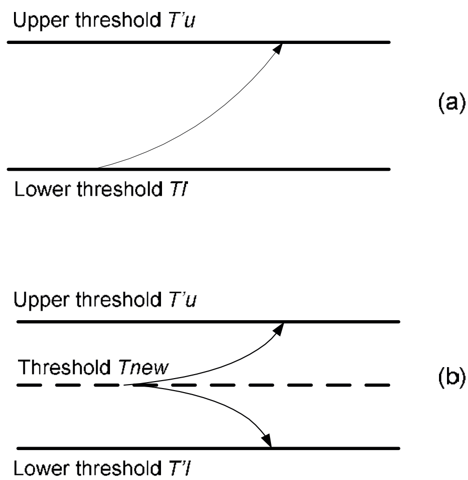

Fig. 31. The LAD NT method. (a) The upper threshold is calculated from the lower threshold. (b) The upper and lower thresholds are calculated from a threshold which is in the middle of the thresholds.

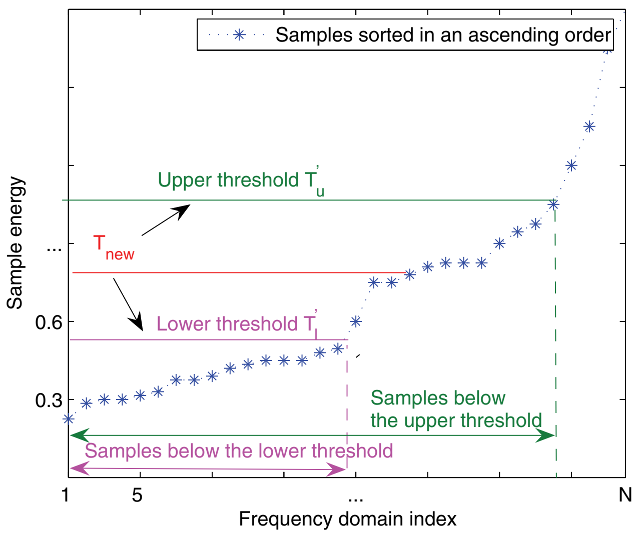

Fig. 32. LAD with normalized thresholds (LAD NT). The original LAD method calculates the upper (T_{u}) and the lower (T_{l}) thresholds separately. Instead, the LAD NT method calculates only one threshold, T_{new}, and derives the corresponding upper and lower thresholds by multiplying the threshold T_{new}. [149]

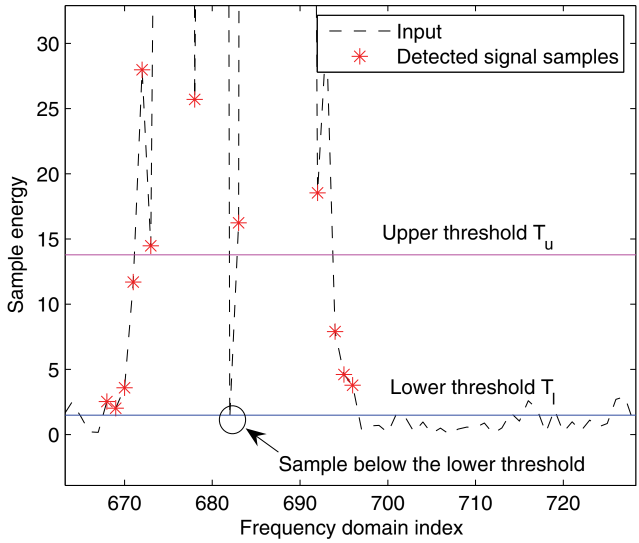

Fig. 33. LAD with adjacent cluster combining (LAD ACC). The original LAD method separates the signal into two parts because of the occasional signal sample below the lower threshold during the signal. Instead, the LAD ACC method makes the decision that there is only one signal. [149]

3.4.2 The LAD with adjacent cluster combining

The performance of the original LAD method in the sense of estimating the correct number of signals can be enhanced. In the original LAD method and especially at low SNR values, the signal can be separated into several signals due to the fluctuation as can be seen in Figure 33. In spectrum sensing applications, this phenomena may lead to the illusion of unoccupied frequencies inside the signal, as in signal detection, the parameter (bandwidth, etc.) estimation of the signal fails. This problem can be solved using the LAD with adjacent cluster combining (ACC) proposed in Paper VIII. The LAD ACC method uses an extra condition after the LAD processing. Therein, if accepted clusters are separated only by at most n samples below the lower threshold, these accepted clusters are decided to be from one signal. So, these clusters and separating samples are joined together into one signal. In other words, two distinct signals can be separated if there is $n+1$ or more adjacent samples between the signals that are below the lower threshold. The value n can be, for example, 1 or more.

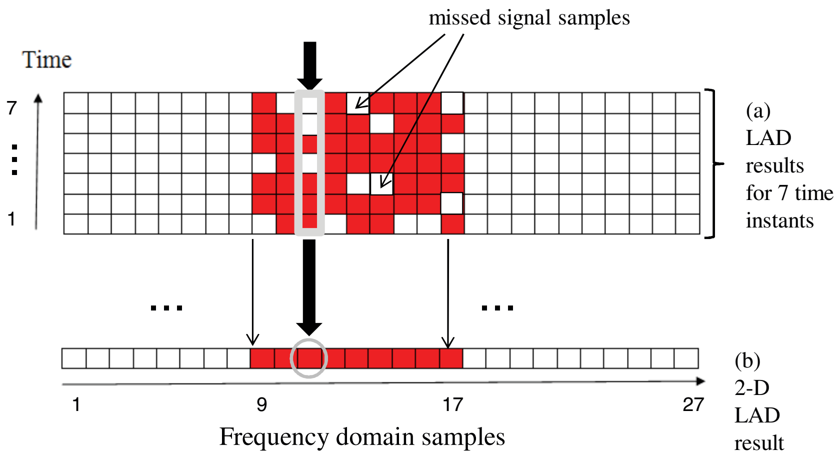

Fig. 34. Illustration of the 2-D LAD method. Time is in the vertical axis and frequency in the horizontal axis. Dark blocks present the detected signal samples and white blocks present the missed signal samples inside the signal and noise samples outside the signal. $p = 4$ and $r = 7$. (a) LAD results for 7 consecutive time intervals. (b) Combined results (the 2-D LAD method). For example in column 11, there are 3 missed signal samples (white blocks) and 4 signal samples (dark blocks) in (a). So, the 2-D LAD decides that the frequency domain sample is caused by the signal in (b). (Revised from IX).

3.4.3 Two-dimensional LAD

The problem with the LAD ACC method is that the parameter n has to be rather large to avoid separating the signal. This may lead to a situation where two closely separated signals may be classified as one single signal. To overcome this problem, an extension of the LAD method that utilizes both time and frequency domain processing was proposed in Paper IX. The proposed two-dimensional (2-D) LAD method that coincides with binary detection in radar systems [124] helps to reduce the number of missed signal samples, i.e., samples from the signal that are below the threshold. That is, after the original LAD processing in the frequency domain, time domain processing is performed: r consecutive time intervals are considered to decide if the samples are caused by a signal or not. If a specific frequency domain sample is reported to belong to the signal at least p times out of r time instants, that frequency domain sample is decided to belong to the signal (Figure 34). A sliding window is used. It means that the first examination period consists of time intervals $1, \ldots, p$, the second examination period

Table 5. The LAD-based NB signal detection methods. T_1 **is the upper and** T_2 **is the lower threshold parameter.**

LAD	two-threshold based detection method: T_1, T_2	original
LAD ACC	LAD with adjacent cluster combining: T_1, T_2	enhanced version
LAD NT	LAD with normalized thresholds	simplified version
-case (a)	One threshold parameter, $T_x = T_2$	
-case (b)	One threshold parameter, $T_x = (T_1 + T_2)/2$	
2-D LAD	two-dimensional LAD with time domain processing: T_1, T_2	enhanced version

consists of time intervals $2, \ldots, p+1$, etc. The 2-D LAD method is illustrated in Figure 34 where a simplified example is presented. There are 27 frequency domain samples (columns), and LAD results for 7 consecutive time intervals (rows) are considered. In the 2-D LAD method, $p = 4$ and $r = 7$. The signal is located at frequencies $9 - 17$. Frequencies $1 - 8$ and $18 - 27$ denote noise samples. It can be seen from (a) that after the original LAD processing, there are missed signal samples (white blocks) among the signal samples $9 - 17$ at every time instant. For example, at time instant one (first row), there are 4 missed signal samples inside the signal. Because every column $9 - 17$ consisted of at least 4 signal samples, the 2-D LAD method decided that the frequencies $9 - 17$ consist of a signal (b).

In Table 5, the LAD, LAD ACC, LAD NT and 2-D LAD methods are presented. A flowchart of the LAD, LAD ACC, LAD NT and 2-D LAD methods is presented in Figure 35.

The performance of the LAD methods has been studied in several papers. The LAD method was proposed and its detection performance was considered in the supplementary paper [143] and Paper VI. Both the BER performance and the number of correctly detected signals were studied in the Fourier domain in Paper VI. The FCME algorithm was used as a point of comparison. In the simulations, there was a BPSK-DS spread spectrum signal among the NB signals and noise. A 4-term Blackman-Harris window was used. The simulated NB signals were RC-BPSK signals and 1 or 3 sinusoidal signals. In the case of multiple sinusoids, there was a fixed signal separation of 15% or 30% between the center frequencies of the sinusoids. Absolute values of signal samples were used. The LAD threshold parameters were selected to be 1.95 ($P_{\mathrm{FA,DES}} = 5\%$) for the lower threshold and 2.97 ($P_{\mathrm{FA,DES}} = 0.1\%$) for the upper threshold. The FCME algorithm was used as a point of comparison with the threshold parameter 1.95, 2.42

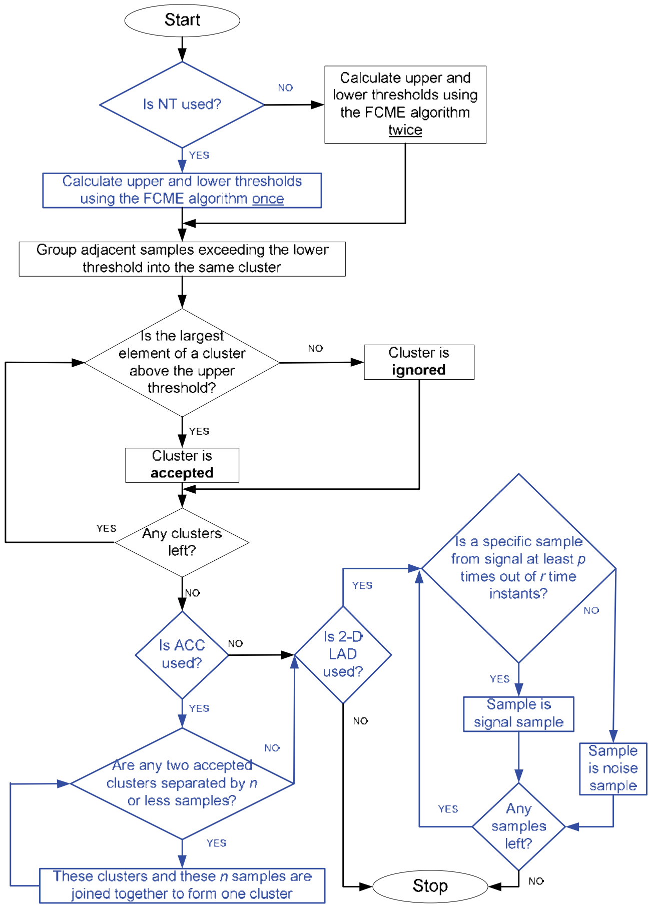

Fig. 35. **LAD, LAD with normalized thresholds (NT), LAD with adjacent cluster combining (ACC) and two-dimensional (2-D) LAD. "Cluster is ignored" denotes that the cluster corresponds to noise (and possibly a wideband signal), as "Cluster is accepted" denotes that the cluster corresponds to a signal.**

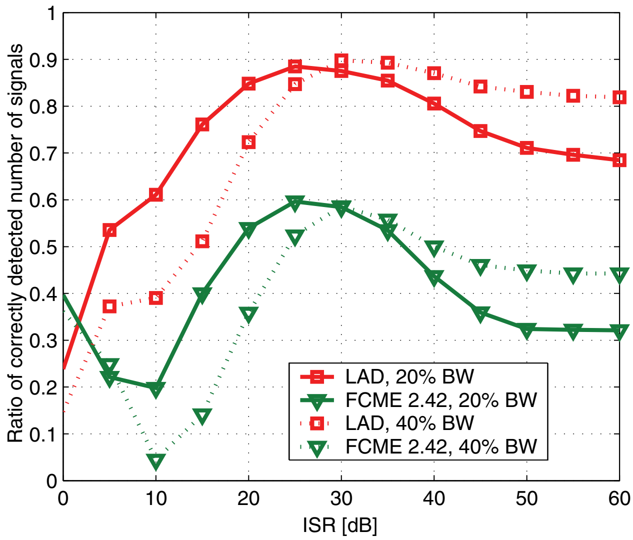

Fig. 36. The LAD and FCME methods. Number of correctly detected signals vs. ISR with RC-BPSK signal. SNR= 15 dB. (VI, published by permission of IEEE).

or 2.97. In the RC-BPSK signal scenario, the ratio of the correctly detected number of signals was simulated as a function of ISR (Figure 36). In addition, the bandwidth estimation success rate as a function of the relative bandwidth of the RC-BPSK signal was simulated. The LAD was able to determine the correct number of NB signals even in 90% of the cases. By comparison, the original FCME algorithm defined the correct number of NB signals at its best only in approximately 60% of the cases. However, with a large ISR, the bandwidth definition was not accurate because of the large sidelobes that partially rise above the threshold. At low ISR values, the signal is so weak that the methods are not able to find it. Because the LAD method is able to find weaker signals than the FCME algorithm, the LAD method starts to operate properly at a lower ISR value than the FCME algorithm. In the BER simulations, the BER was simulated as a function of SNR and ISR. The performance of the LAD method was almost equal to that of the FCME algorithm with threshold parameter 2.42 or only slightly worse. In the sinusoidal signal scenario, the ratio of the correctly detected number of signals was simulated as a function of ISR (Figure 37). The LAD method clearly outperformed the FCME algorithm. The performance of the LAD method in the means of a correctly detected number of signals was excellent. When 15% signal separation was used, the sinusoids fused together at large ISR values causing performance loss. As in the pre-

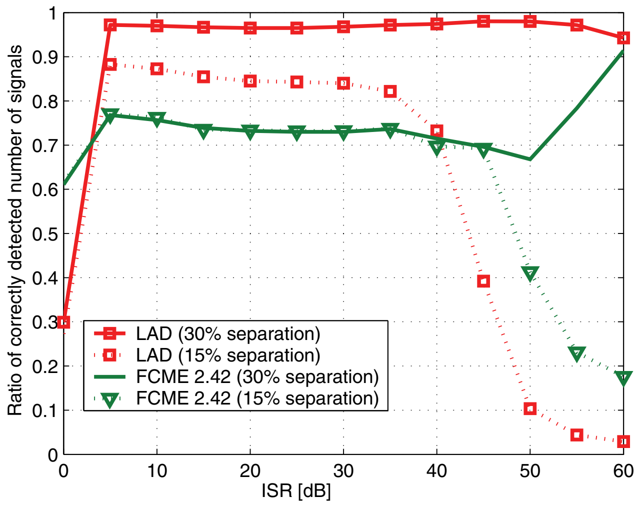

Fig. 37. The LAD and FCME methods. Number of correctly detected signals vs. ISR with three sinusoidal signals. SNR= 15 dB. (VI, published by permission of IEEE).

vious case, the LAD method was able to find the correct number of NB signals more accurately than the FCME algorithm. In the BER simulations, the BER was simulated as a function of ISR (Figure 38). Again, the performance of the LAD method was almost equal to or only slightly worse than that of the FCME algorithm with threshold parameter 2.42.

It was concluded that the LAD method has a good performance in terms of detecting the correct number of signals. In addition, the BER performance is good. In the bandwidth estimation, large sidelobes cause problems, and, thus, some performance degradation. It was also noticed that the LAD method is not able to separate two closely spaced signals or weak signals accurately. The LAD method has also been considered in the supplementary paper [143]. Therein, a DS spread spectrum signal was within the noise. The LAD method was performed in the Fourier domain. The number of correctly detected signals was studied in the presence of RC-BPSK and multiple sinusoidal signals. It was concluded that the LAD method outperformed the FCME algorithm.

The LAD method was extended to compute SNR values of several unknown narrowband signals in Paper VII. Both the SNR and bandwidth estimation accuracies were studied in the Fourier domain. The bias and NMSE of the SNR were used to measure the performance of the extended method. There were at most five off-center si-

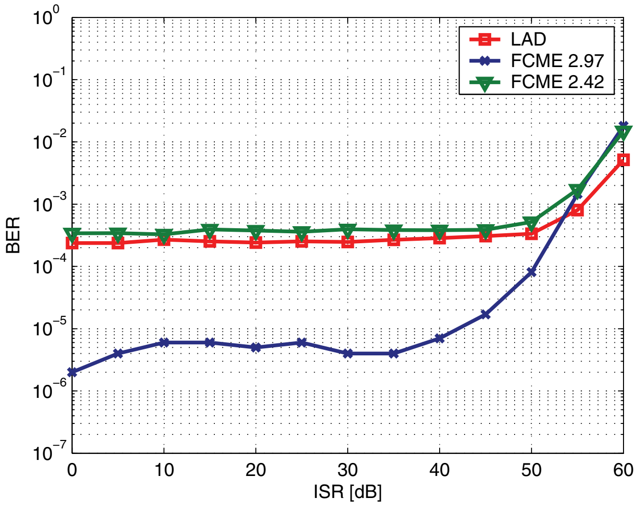

Fig. 38. The LAD and FCME methods. BER vs. ISR, with one sinusoidal signal. SNR= 15 dB. (VI, published by permission of IEEE).

nusoidal or at most two BPSK signals with bandwidths of $2-10\%$ of the system's bandwidth and noise. The received samples were magnitude squared. The LAD parameters were selected to be 13.814 ($P_{\mathrm{FA,DES}} = 10^{-6}$) for the upper threshold and 2.66 ($P_{\mathrm{FA,DES}} = 7 \cdot 10^{-2}$) for the lower threshold. This selection seemed to be a good choice and this assumption was analytically confirmed later in the supplementary paper [77]. There were 1024 samples and the FFT length was 1024. No windowing was used. In the bandwidth estimation simulations, one or two RC-BPSK signals were considered with bandwidths 5 or 10% of the system's bandwidth. The numerical bandwidth estimation results are presented in Table 6. Figure 39 presents one bandwidth and SNR estimation example for single realization. It was noticed that at low SNR values, the LAD method had problems when defining the correct number of BPSK signals because of the separation of the signal. Instead, large SNR values raise the sidelobes thus leading to too wide estimated bandwidths. The latter phenomena is illustrated in Figure 40, where NMSE of the estimated noise mean vs. SNR is presented in the case of different signals. In the simulations it was noticed that the LAD method is able to estimate the SNR values well. However, at low SNR values, NMSE is large. In addition, with large SNR values, the number of estimation errors increases because of the rising sidelobes.

The LAD method was also tested with real-life radio channel measurement data where the noise was from the reality instead of being computer-generated. There were

Table 6. Bandwidth estimation accuracy of the LAD method.

	Estimated BWs					
	SNR [dB]					
	0	5	10	15	20	25
BPSK, BW 5%	5.0	5.6	6.1	6.9	8.6	11.9
BPSK, BW 10%	7.7	10.3	11.3	11.9	12.7	14.6
BPSK #1, BW 5%	4.8	5.0	5.8	6.5	7.9	9.8
BPSK #2, BW 5%	3.9	4.7	5.9	6.6	7.8	10.0
BPSK #1, BW 10%	5.9	6.6	9.1	10.0	11.4	12.5
BPSK #2, BW 10%	3.6	6.3	8.6	10.5	11.2	12.5

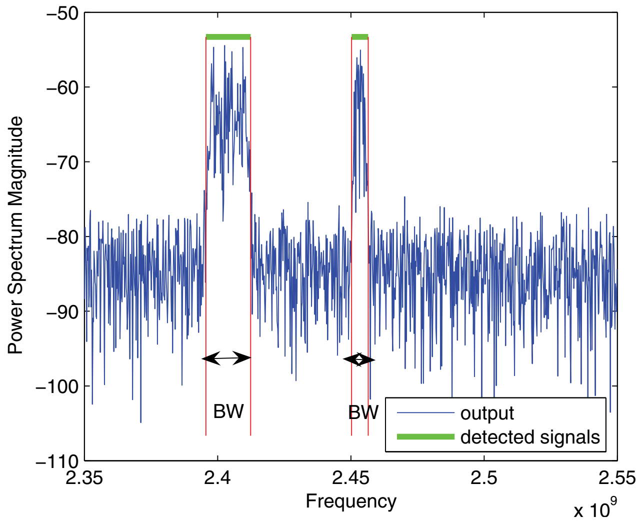

Fig. 39. THe LAD method, one bandwidth and SNR estimation example based on single realization. Two RC-BPSK signals. Actual BWs 8 and 2%, estimated BWs 8.5 and 3.2%. Actual SNR=10 and 7 dB, estimated SNR=9.7 and 6.4 dB. (VII, published by permission of IEEE).

some realizations (measured "snapshots") from the data measured using the Elektrobit PropSound multidimensional radio channel sounder [29] in the city of Oulu, Finland, in autumn 2004 at 2.45 GHz with 200 MHz receiver bandwidth [70]. Because the measured signals were unknown to the receiver and clean data was not available as a reference, only some example realizations were presented as an example. Statistical analysis was not possible. However, it was noticed that both the bandwidth and SNR estimation realizations seem to be successful even though the noise is from real-life

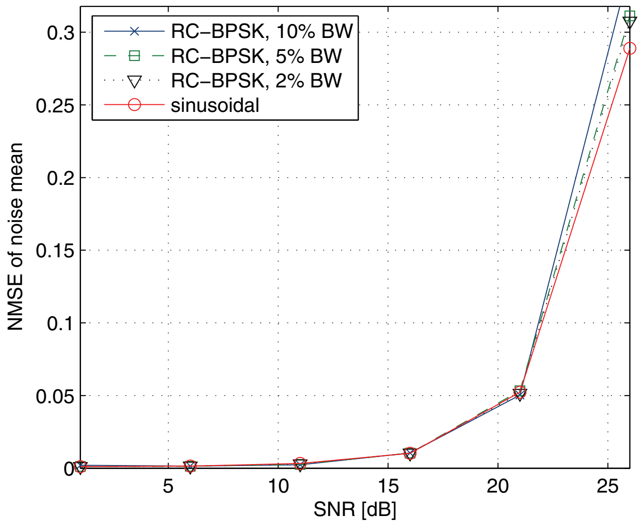

Fig. 40. The LAD method. NMSE of the estimated noise mean vs. SNR. (VII, published by permission of IEEE).

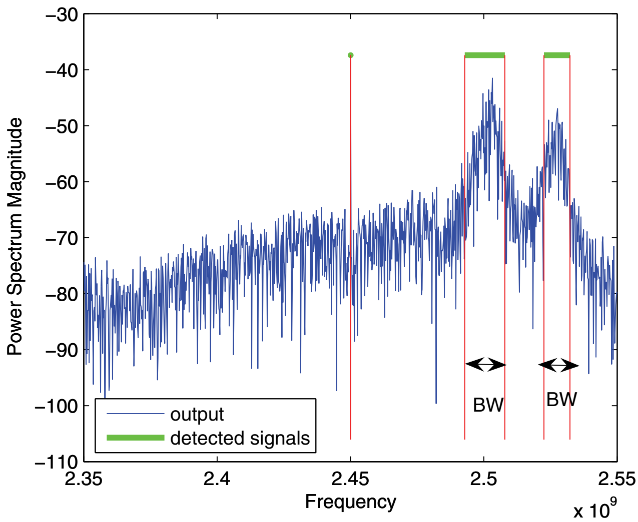

Fig. 41. The LAD method. BW and SNR estimation example for real-life radio channel measurement. DC-component at 2.45 GHz. Estimated center frequencies 2.45, 2.5 and 2.53 GHz. Estimated BWs 0.19, 15.04 and 9.77 MHz. Estimated SNR values 30.74, 18.39 and 15.97 dB. (VII, published by permission of IEEE).

radio channel measurements. One example "snapshot" is illustrated in Figure 41.

It was concluded that if the number of narrowband signals was estimated correctly, the LAD method was able to estimate the SNR values reliably. The problem was that even though the LAD method clearly outperformed the FCME algorithm as a detection method, the detection capability of the LAD method still had a room for improvements.

The LAD ACC and NT methods were proposed in VIII. Therein, the LAD system was also proposed to be used for spectrum sensing purposes in cognitive radios. The proposed methods were studied in the Fourier domain in the presence of $2-4$ BPSK signals in the AWGN channel. The BPSK signals had bandwidths of $2-10\%$ of the system's bandwidth. The SNR per signal was between 0 and 25 dB. There were $N = 1024$ samples and the FFT length was also 1024. Windowing was not used. The received samples were magnitude squared. The LAD parameters were selected to be 13.814 ($P_{\mathrm{FA,DES}} = 10^{-6}$) for the upper threshold and 2.66 ($P_{\mathrm{FA,DES}} = 7 \cdot 10^{-2}$) for the lower threshold. As mentioned earlier, this selection was justified later in the supplementary paper [77]. In the case of the LAD ACC method, $n = 1$. The detection performance as well as bandwidth estimation accuracy of the LAD ACC method were simulated. The NT was applied to both the LAD and LAD ACC methods. When considering the ratio of correctly detected number of signals as a function of SNR, it was noticed that the LAD ACC was able to perform much better than the original LAD method. The difference was the biggest with low SNR values. At its best, the LAD ACC method was able to find the correct number of signals even more often than in 95% of the cases. In contrast, the original LAD method was able to find the correct number of signals at most in 60% of the cases. In addition, it was noticed that the LAD ACC started to operate properly at a lower SNR level than the original LAD method. In most of the cases, the LAD ACC method operated well when the SNR was 5 dB or more, whereas the original LAD method required at least $10-15$ dB SNR. In general, the difference in the performance was huge: when SNR was 5 dB or more, the best performance of the original LAD method was still worse than the worst performance of the LAD ACC method. In all the studied cases, NT only had a slight effect on the performance of the LAD and LAD ACC methods, meaning that in practice, the threshold needs to be computed only once instead of twice. Figure 42 presents the ratio of correctly detected number of signals in the presence of two RC-BPSK signals relating to the discussion above.

The bandwidth estimation accuracies were also studied. With low (0 dB) SNR values, bandwidth estimation performance was not good. When the SNR was higher,

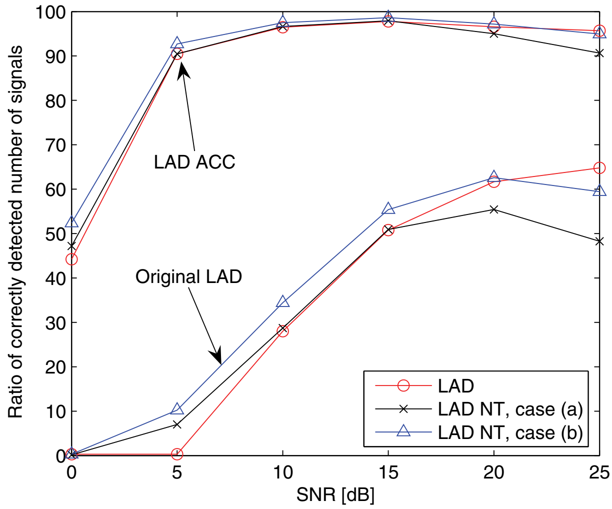

Fig. 42. The LAD, LAD NT and LAD ACC methods. The ratio of correctly detected signals vs. SNR. Two RC-BPSK signals with BWs 5%. (VIII, published by permission of IEEE).

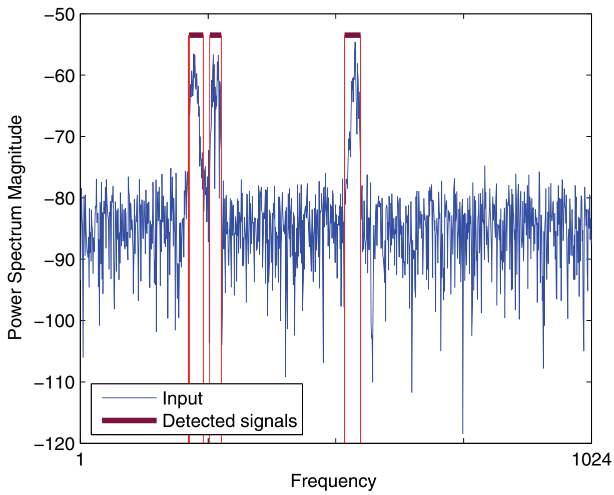

Fig. 43. The LAD ACC method. One bandwidth estimation example in the presence of three RC-BPSK signals with SNR values 5dB. Actual BWs 2%, estimated BWs 2.9, 2.3 and 3.2%. (VIII, published by permission of IEEE).

the LAD ACC method was able to offer good bandwidth estimation accuracy. When

Table 7. Bandwidth estimation accuracy of the LAD ACC method.

	Estimated average BWs					
	SNR [dB]					
	0	5	10	15	20	25
2 BPSK signals, BWs 5%	4.9	5.5	5.9	6.6	7.8	9.8
2 BPSK signals, BWs 7%	5.7	7.0	7.6	8.2	9.1	10.4
2 BPSK signals, BWs 10%	1.7	9.4	10.9	11.7	12.4	13.4
3 BPSK signals, BWs 2%	2.3	2.6	3.1	4.1	5.5	7.4
3 BPSK signals, BWs 5%	4.6	5.4	5.9	6.5	7.3	8.6
4 BPSK signals, BWs 2%	2.3	2.6	3.1	4.0	5.2	6.6

the SNR was high, the bandwidth estimates were too wide because of rising sidelobes. In Figure 43, one bandwidth estimation example is illustrated in the case of three RC-BPSK signals. The bandwidth estimation results for the LAD ACC method are presented in Table 7. With NT, the estimates were approximately in the same level. It was concluded that both the LAD ACC and NT methods had a good performance, and the LAD ACC method is able to estimate the number of detected signals much better than the original LAD method. However, the problem with the LAD ACC method is that two signals located close to each other may be classified as one signal. In that case, the estimation of signal parameters such as the number of signals and their bandwidths fails.

The cognitive radio approach was also used in the supplementary paper [149], where the LAD methods were also used for detecting signals from real-life radio channel measurement data [29, 70]. In the measurements, the signals were unknown to the receiver. In addition, there were no clean reference measurements. For those reasons, only some example results were presented. The main point was to show that the LAD methods are also able to operate in the case when the noise is from the reality and, thus, not computer-generated Gaussian. According to the considered examples it was noticed that the LAD methods are able to detect measured real-life signals.

The performance analysis of the LAD method was considered in the supplementary paper [77]. Therein, both the clean sample rejection and detection rates were analyzed. According to the analysis, it was confirmed that the P_{FA} values 10^{-6} and $7 \cdot 10^{-2}$ used in the Papers VII and VIII are good choices when defining the upper and lower thresholds, respectively. It was noted that the P_{FA} value in the case of the lower threshold has to be as high as possible but less than 10^{-1}. In other words, the lower threshold should be as low as possible, but not too low or the sidelobes will rise above the threshold and the rejection rate will rise remarkably. It was also noticed that in the case of the LAD ACC method, the setting of the lower threshold was not so critical a task.

Usually, the periodogram has been used with the CME and LAD methods. In the supplementary paper [71], the LAD ACC method was used with the Welch spectrum estimator. First, an asymptotic approach for obtaining the proper threshold parameter for the FCME algorithm with the Welch spectrum estimator was presented. The threshold parameter cannot be calculated based on chi-squared (Eq. 8) or Rayleigh (Eq. 12) distribution, because the distribution of the desired signal is distorted due to windowing and overlapping. It was noticed that the asymptotic approach was sufficient when the desired clean sample rejection rate was less than 0.01. Second, the performance of the LAD ACC method in the presence of real-life signals was considered. The probability of detection as a function of SNR was studied. Laboratory measurements were performed using BPSK and recorded FM signals generated by Agilent E4438C signal generator. A cable was used between the signal generator and spectrum analyzer. In the field measurements, a real wireless microphone signal generated by Sony UTX-B1 wireless microphone was used. The field measurements were performed in the University of Oulu, Finland, in December 2008. Silence, speech and pop music were studied. In the Welch estimator, 50% overlapping and averaging was used. The LAD ACC method was able to detect the studied signals. The narrower the BPSK signal the better the performance of the LAD ACC method was. The FM signal was detected when SNR was larger than -20 dB. Wireless microphone signals were detected when the signal (+ noise) power was as weak as approximately -110 dBm. Because the lowest signal power at which the wireless microphone was able to operate was approximately -80 dBm, it was discovered that when using the LAD ACC method, the safeguard for the wireless microphone signal is approximately 30 dB. It was concluded that the gain from the Welch detector was approximately 10 dB when compared to the conventional periodogram. It means that when the Welch detector is used, approximately 10 dB weaker narrowband signals can be found than when using the periodogram.

The 2-D LAD method that operates both in time and frequency domains was proposed and its detection performance was considered in Paper IX. Therein, the probability of detecting a correct number of signals was studied. The main goal was to enhance the signal detection probability of the LAD and LAD ACC methods. Both the LAD and LAD ACC methods were used as a point of comparison. In the simulations, there was one measured BPSK signal and measured thermal noise. The signal was generated using the Agilent E4438C signal generator as the measurements were performed using

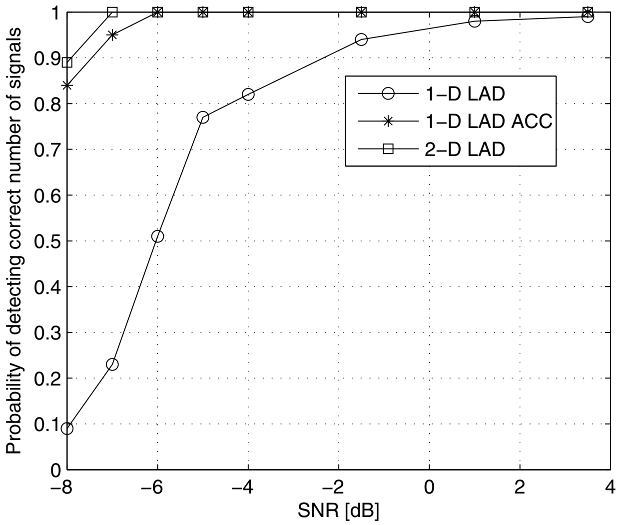

Fig. 44. The probability of detecting one signal vs. SNR. A BPSK signal with bandwidth of 12.5% of the system bandwidth. The original LAD (1-D) method, LAD ACC (1-D LAD ACC) method and 2-D LAD method. (IX, published by permission of IEICE).

an Agilent E4446A spectrum analyzer. The total bandwidth was 8 MHz and the bandwidth of the signal was either 25%, 19% or 12.5% of the total bandwidth. SNR was defined to be the ratio of the signal power to the noise power in the system's bandwidth. There were ten overlapping blocks and 50% overlap. The FFT size was 1024. In the simulations, the LAD threshold parameters were calculated using $P_{\mathrm{FA,DES}} = 10^{-5}$ and 10^{-1}, which in the case of the Welch spectrum estimate method yield to the threshold parameters 3.07 and 1.54, respectively [71]. With the ACC processing, $n = 8$ samples. First, the values of p and r used in the simulations were selected. The smaller the p, the higher the probability is. A small value of p, however, increases the probability of false alarm. A large value of r increases the need of memory. Values of $p = 5$ and $r = 10$ were selected to be used in the simulations based on the values used in the literature and several example scenarios. Figure 44 presents the probability of detecting the correct number of signals vs. SNR. One signal with the bandwidth of 12.5% is present. The LAD, LAD ACC and 2-D LAD methods were used. As can be seen, the performance of the original LAD method is rather poor when SNR is low. The proposed 2-D LAD method is able to perform well even when SNR is low. In addition, the 2-D LAD

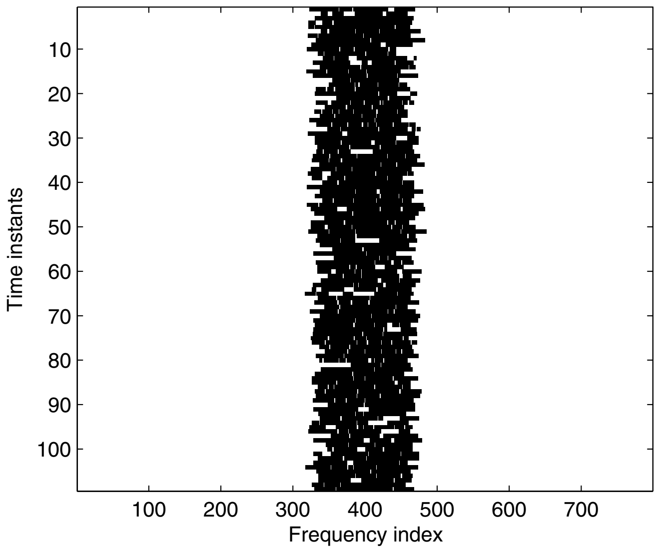

Fig. 45. A BPSK signal with bandwidth of 25% of the system bandwidth and with SNR=−4 dB after the original LAD method. (IX, published by permission of IEICE).

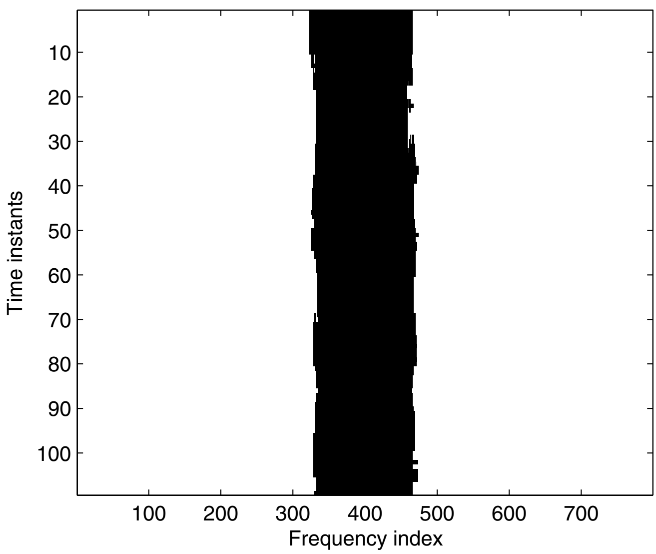

Fig. 46. A BPSK signal with bandwidth of 25% of the system bandwidth and with SNR=−4 dB after the 2-D LAD method. (IX, published by permission of IEICE).

method slightly outperforms the LAD ACC method. Note that because of the Welch spectrum estimate, the LAD methods are able to operate at low SNR values. According to the supplementary paper [71], the gain due to averaging is approximately 10 dB. Figures 45 and 46 present the detection performance difference between the original LAD and 2-D LAD methods. Therein, the bandwidth of the signal is 25% and SNR$= -4$ dB. Figure 45 shows that the original LAD method splits the signal into several parts. The probability of detecting one signal is 4%. In Figure 46 it can be seen that the 2-D LAD method detects the signal almost perfectly, that is, the probability of detecting one signal is 87%. One time instant (row) in Figure 46 includes the combined results of 10 time intervals from Figure 45. According to Paper IX, the 2-D LAD method offers better detection performance especially at low SNR values when compared to the LAD and LAD ACC methods. The lower the SNR, the more gain was achieved. The 2-D LAD method and ACC can also be combined to achieve better performance. In addition, the computational complexity of the 2-D LAD method remains at a reasonable level, that is, of the order of $N \log_2 N$.

Hänninen implemented the LAD method on the wireless open-access research platform (WARP) in 2009 [48], supplementary paper [49]. The goal was to study spectrum sensing in OFDM communication systems in the Fourier domain. The LAD method was configured to the WARP using Xilinx Platform Studio (XPS). Because of the limited resources of the field-programmable gate array (FPGA) chip on WARP, the FFT length of the implemented LAD method was only 64. Averaging or overlapping were not used. In the simulations, the thresholds calculated by digital logic and Matlab were compared. The narrowband signal was a BPSK signal and the noise was Gaussian. The error between the thresholds was at most 2%. This error was partially explained by the fact that the Matlab uses round operation as Xilinx blocks use truncate operation. It was noticed that the 64-point LAD method is able to find signals with the bandwidth of at most 10/20/40% of the system's bandwidth when SNR$\geq 5/10/20$ dB, respectively. It was also noticed that with high bandwidth and low SNR, the 64-point LAD was not able to find signals. In the real-life demonstrations, a signal with 2 MHz (5%) bandwidth was created using a signal generator. Commercial spectrum analyzer which was used as a reference listened to the same band as the WARP board. The demonstration setup is presented in Figure 47. It was noticed that the LAD method was able to find the signal. However, it was noticed that taking only 64 samples from 40 MHz band was not enough. The initial set contained only 6 samples, so the size of the initial set was too small. Therefore, the resulting thresholds were often either too low or too high.

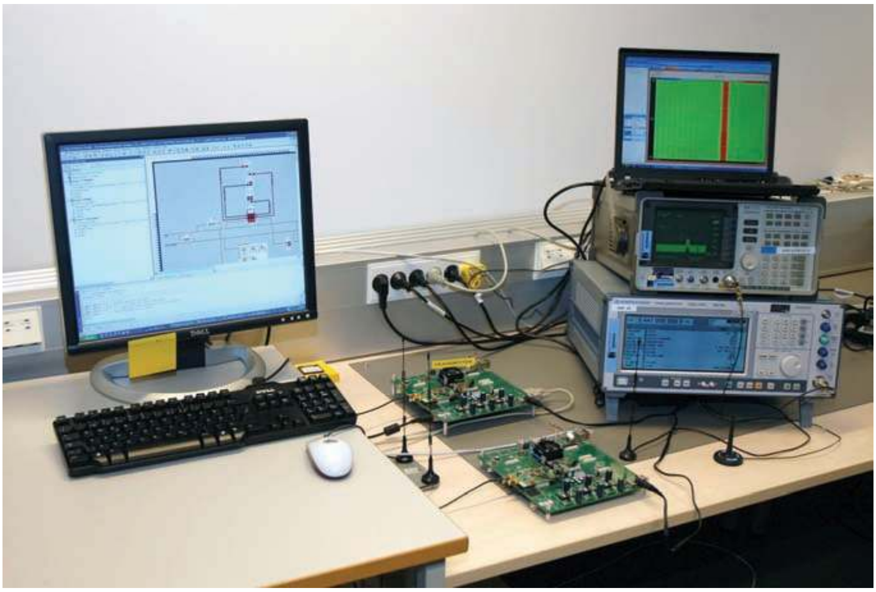

Fig. 47. Demonstration setup. © Hänninen 2009 [48]

Table 8. Summary of assumptions in original publications; DET = detection, RCDNS = ratio of correctly detected number of signals, BWEA = bandwidth estimation accuracy and SIN = sinusoidal signal.

	Description	Performance measure	Methods used	Transform domain(s)	Threshold parameter(s)	Signals
Paper I	IS	Selection rate, BER	TSISA, FCME, RLS	time, FT, FrFT	2.97	SIN, impulse, chirp
Paper II	IS	BER	extended TSISA, TSISA, FCME	time, FT, FrFT	2.97	SIN, impulse, RC-BPSK, chirp
Paper III	DET	NMSE, P_D	notch filter, CME, FCME	FT	2.42	SIN
Paper IV	Analysis	P_D, P_{FA}	FCME, forward CA	FT	Varies	noncentral chi-squared NB signals
Paper V	Analysis	limits of detection	CME, FCME	Generic	2.3, 4.6, 6.9	random
Paper VI	DET	RCDNS, BWEA, BER	FCME, LAD	FT	FCME: 1.95, 2.42, 2.97 LAD: 1.95 and 2.97	SIN, RC-BPSK
Paper VII	DET	BWEA, SNR, Bias, NMSE	LAD	FT	2.66 and 13.81	SIN, RC-BPSK
Paper VIII	DET	RCDNS, BWEA	LAD, LAD ACC, LAD NT	FT	2.66 and 13.81	RC-BPSK
Paper IX	DET	RCDNS	LAD, LAD ACC, 2-D LAD	FT	1.54 and 3.07	RC-BPSK

4 Discussion and summary

This thesis studied the problem of outlier detection in wireless communications. Two areas of outlier detection were studied. The first research area considered the concentrated interference suppression, and the second area studied the concentrated signal detection focused on spectrum sensing in cognitive radios. Chapter 2 reviewed the literature in the research areas related to the thesis. The studied methods and an overview of the achieved research results was presented in Chapter 3.

Three existing outlier detection methods were considered closer, namely, the CME and FCME algorithms and the TSISA method. In addition, new methods called as the extended TSISA and the LAD methods were introduced. Besides being blind and computationally attractive, all these methods are applications of the CME algorithm.

The iterative CME algorithms are blind IS methods in the sense that they do not need to know the noise level. Due to computational reasons, it was noticed that it could be appropriate to use the same algorithm for both IS and narrowband signal detection. Hence, the CME algorithms were studied as narrowband signal detection and localization algorithms. The per bin probabilities of detection were studied in the frequency domain. As in the IS case, the FCME algorithm outperformed the original CME algorithm. The FCME algorithm performed well even when the bandwidth of the signal was large. However, the CME algorithms were not able to estimate the number of narrowband signals nor their parameters such as the bandwidth.

The threshold parameter of the CME algorithms is calculated based on the desired false alarm rate. The equations commonly used in the calculation give only approximations of the threshold parameter, so the desired and obtained false alarm rates are not necessarily equal. This may cause problems in the applications where it is desired that the false alarm rate is controlled. To overcome this problem, accurate threshold parameters for the FCME algorithm were defined. It was noticed that in the noise-only case, when the number of samples is 512 or more, the approximation of the threshold parameter leads to accurate false alarm rate. Instead, when the number of samples is smaller, an accurate threshold parameter value improved the false alarm probability.

The detection capabilities of the CME algorithms were also theoretically analyzed. The generic analysis was based on the shape on the signal, and was not restricted to any transform domain. The effects of the threshold parameter used as well as the width and height of the signal to the detection were considered. Moreover, SNR values at which the signals can be detected using the CME or the FCME algorithm were found. The resulting limits of detection were confirmed via computer simulations. These limits can be used for fast checking whether the signal can be detected or not without computer simulations, so they are applicable both in IS and signal detection purposes.

Because interfering signals may also be concentrated on a domain other than the frequency domain, the CME algorithms are not optimal methods for IS as such. The TSISA method is a bank-type method that performs IS using the FCME algorithm in several transform domains. The CG metric which defines how well the interfering signal is concentrated on the transform domain is used to select the optimal transform domain. The optimal domain depends on the characteristics of the interfering signals and is, for example, time domain for impulses, Fourier domain for sinusoids and fractional Fourier domain for chirps. The BER performance of the TSISA method and the FCME-based IS in the optimal domain were almost equal. That is, the performance loss caused by the domain selection operation was negligible. The simulations on the selection process confirmed that the TSISA method is able to select the optimal domain for IS in all considered interfering signal cases. Also, the computational complexity was low. The TSISA seems, therefore, to be an attractive IS method when it is not known in which domain the interfering signal is the most concentrated. The TSISA method was also extended to contain other transform selection methods, namely the percentile, coefficient of variation and maximum. It was noticed that the coefficient of variation is not only simple to implement but also has a good performance. The percentile metric also operated rather well, as the maximum metric had the worst performance.

The FCME algorithm was noticed to be able to localize narrowband signals, but not accurately. A needless separation of the signal as well as falsely detected signals lead to an inaccurate estimation of signal parameters such as the number of the signals and their bandwidths. In applications like signal detection and spectrum sensing, the accuracy of these estimations is important to enable correct decisions. To solve these problems, a new method for unknown narrowband signal detection and localization called the LAD was introduced. Whereas the FCME algorithm uses one threshold, the LAD method uses two thresholds to achieve better performance. The performance of the LAD method was studied and compared to the FCME algorithm. The simulations confirmed that the LAD method has a better localization ability than the FCME algorithm, and the LAD method is able to estimate the number of narrowband signals and their parameters including, for example, center frequencies and bandwidths. The

LAD method was extended to estimate the SNR values of several unknown narrowband signals. The SNR estimation accuracy was noticed to be highly dependent on the bandwidth estimation accuracy, at which the LAD method had problems especially with low SNR values.

The LAD ACC method was introduced to enhance the bandwidth estimation accuracy of the LAD method. It was noticed that the LAD ACC method has a much better localization ability than the original LAD method, especially when the bandwidth of the detected signal is wide and the SNR is low. The drawback is that two signals located close to each other may be classified as one signal. The computation of the LAD method was simplified with the LAD NT method. It was noticed that the LAD NT method is able to offer a good performance. However, the false alarm rate is not controlled, i.e., the desired false alarm rate is not equal to the obtained one. It depends on the application whether this causes problems or not. The LAD methods were also investigated as spectrum sensing methods in cognitive radios. Although concentrated in narrowband signal detection, the LAD methods are also applicable for concentrated signal detection in other transform domains.

The 2-D LAD method that utilizes time domain processing after the original frequency domain LAD method was proposed to enhance the performance of the LAD and LAD ACC methods. It was noticed that the 2-D LAD method is able to operate at lower SNR values than the original LAD and LAD ACC methods. The 2-D LAD method helps to reduce the number of missed signal samples and prevents two closely spaced signals from being classified as one signal. At the same time, the low computational complexity was maintained. The proposed 2-D LAD method can also be used together with the ACC method.

There are still some open problems and interesting questions without answers. For example, it could be interesting to study if it is possible to enhance the interference suppression performance of the CME algorithms and/or detection performance of the LAD methods. The proposed methods have only been studied in the presence of one type of concentrated signal. It could be interesting to study cases when there are several types of concentrated signals simultaneously, for example, impulsive and sinusoidal signals. In that case, either both signals should be suppressed, or the impulsive signal should be suppressed before detecting the sinusoidal signal. There are several possible applications in several fields of wireless communications for which the blind and computationally simple CME-based methods can be used. In addition to the spectrum sensing in cognitive radios, promising cognitive-based applications include, for example, cognitive radio based femtocells, i.e., small base stations inside a building. In the military applications, LAD-based methods could be used for detecting signals and estimating their parameters like center frequencies and bandwidths. Furthermore, this detection information could be used to aid interference suppression methods, for example, the CME algorithms, or jamming.

References

1. Ahnström U, Falk J, Händel P & Wikström M (2003) Detection and direction-finding of spread spectrum signals using correlation and narrowband interference rejection. Proc. Nordic Matlab Conference, Copenhagen, Denmark.
2. Akay O & Boudreaux-Bartels GF (1998) Broadband interference excision in spread spectrum communication systems via fractional Fourier transform. Proc. Conference Record on the 32nd Asilomar Conference on Signals, Systems and Computers 1: 823–837.
3. Aromaa S, Henttu P & Juntti M (2005) Transform selective interference suppression algorithm for spread spectrum communications. IEEE Signal Processing Letters 12(1): 49–51.
4. ATSC (2006) Digital television standard. Revision E with Amendments No. 1 and No. 2, ANNEX D.
5. Aysal TC, Kandeepan S & Piesiewicz R (2009) Cooperative spectrum sensing with noisy hard decision transmissions. Proc. IEEE International Conference on Communications, Dresden, Germany: 1–5.
6. Barboy B, Lomes A & Perkalski E (1986) Cell-averaging CFAR for multiple-target situations. IEE Communications, Radar and Signal Processing 133(2): 176–186.
7. Barkat M, Himonas SD & Varshney PK (1989) CFAR detection for multiple target situations. IEE Proceedings F Radar and Signal Processing 136(5): 193–209.
8. Benedict TR & Soong TT (1967) The joint estimation of signal and noise from the sum envelope. IEEE Transactions on Information Theory 13(3): 447–454.
9. Biesecker K (2000) The promise of broadband wireless. IT Professional 2(6): 31–39.
10. Bin S, Kyung SK, Longyang H & Zheng Z (2008) Improved consecutive mean excision algorithm based spectrum sensing for dynamic spectrum access. Proc. IEEE International Conference on Communications Workshops: 513–517.
11. Braga-Illa A (1964) A simple approach to the Bayes choice criterion: The method of critical probabilities. Journal of the American Statistical Association 59(308): 1227–1230.
12. Brown TX (2005) An analysis of unlicensed device operation in licensed broadcast service bands. Proc. IEEE International Symposium on Dynamic Spectrum Access Networks, Baltimore, Maryland: 11–29.
13. Bullen PS, Mitrinovic DS & Vasic PM (1988) Means and Their Inequalities. D. Reidel Publishing Company, Dordrecht, the Netherlands.
14. Cabric D, Mishra SM & Brodersen RW (2004) Implementation issues in spectrum sensing for cognitive radios. Proc. Annual Asilomar Conference on Signals, Systems and Computers, Pacific Grove, CA, 1: 772–776.
15. Canny J (1986) A computational approach to edge detection. IEEE Transactions on Pattern Analysis and Machine Intelligence 8(6): 679–698.
16. Capozza PT, Holland BJ, Hopkinson TM & Landrau RL (2000) A single-chip narrow-band frequency-domain excisor for a global positioning system GPS receiver. IEEE Journal of Solid-State Circuits 35(3): 401–411.
17. Carlemalm C, Poor HV & Logothetis A (2000) Suppression of multiple narrowband interferers in a spread-spectrum communication system. IEEE Journal on Selected Areas in Communications 18(8): 1365–1374.

18. Chakravarthy V, Shaw A, Temple M & Stephens J (2005) Cognitive radio - an adaptive waveform with spectral sharing capability. Proc. IEEE Wireless Communications and Networking Conference, New Orleans, LA, USA: 724–729.
19. Chen HS, Gao W & Daut DG (2009) Spectrum sensing for OFDM systems employing pilot tones. IEEE Transactions on Wireless Communications 8(12): 5862–5870.
20. Cooper GR & McGillem CD (1986) Modern communications and spread spectrum. McGraw-Hill, Singapore, 1st edition.
21. Cordeiro C (2005) A cognitive PHY/MAC proposal for IEEE 802.22 WRAN systems. IEEE 802.22-05/0105r1 (Jan 26, 2010).
22. Cordeiro C, Challapali K, Birru D & Shankar SN (2005) Spectrum agile radios: Utilization and sensing architectures. Proc. IEEE International Symposium on Dynamic Spectrum Access Networks, Baltimore, USA, 1: 328–337.
23. Cordeiro C, Challapalli K & Birru D (2006) IEEE 802.22: An introduction to the first wireless standard based on cognitive radios. Journal of Communications 1(1): 38–47.
24. Davidovici S & Kanterakis EG (1989) Narrowband interference rejection using real-time Fourier transforms. IEEE Transactions on Communications 37(7): 713–722.
25. Davidovici S & Kanterakis EG (1989) Radiometric detection of direct-sequence spread-spectrum signals using interference excision. IEEE Journal on Selected Areas In Communications 7: 576–589.
26. Delic H & Hocanm A (2002) Robust detection in DS-CDMA. IEEE Transactions on Vehicular Technology 51(1): 155–170.
27. Dillard RA (1979) Detectability of spread-spectrum signals. IEEE Transactions on Aerospace and Electronic Systems 15: 526–537.
28. Dixon RC (1994) Spread spectrum systems - with commercial applications. John Wiley & Sons, New York, NY, USA, 3rd edition.
29. Elektrobit Ltd (2006) Propsound multidimensional channel sounder. http://www.propsound.com (Mar. 2, 2006).
30. Enserink S & Cochran D (1994) A cyclostationary feature detector. Proc. 28th Asilomar Conference on Signals, Systems, and Computers, Monterey, CA, USA: 806–810.
31. Eschbach R, Fan Z, Knox KT & Marcu G (2003) Threshold modulation and stability in error diffusion. IEEE Signal Processing Magazine 20(4): 39–50.
32. ETSI (2008) Frame structure channel coding and modulation for a second generation digital terrestrial television broadcasting system. European Telecommun. Standard DTV Doc. A122.
33. FCC (2002) Spectrum policy task force report. Tech. Rep. TR 02-155.
34. FCC (2003) FCC makes additional spectrum available for unlicensed use. http://wireless.fcc.gov/ (21.06.2004).
35. FCC (2003) Notice for proposed rulemaking: Facilitating opportunities for flexible, efficient, and reliable spectrum use employing cognitive radio technologies. ET Docket No. 03-108.
36. FCC (2004) First report and order and further notice for proposed rulemaking. ET Docket 06-156.
37. FCC (2004) Notice of proposed rule making: Unlicensed operation in the TV broadcast bands. ET Docket No. 04-186.
38. FCC (2008) Second report and order and memorandum opinion and order. ET Docket No. 08-260.

39. FCC (2010) FCC frees up vacant tv airwaves for super Wi-Fi technologies. http://www.fcc.gov (Sep. 24, 2010)
40. Finnish Communications Regulatory Authority (FICORA) (2006) Use of radio frequencies. http://www.ficora.fi/englanti/radio/index.htm.
41. Gandhi PP & Kassam SA (1988) Analysis of CFAR processors in nonhomogenous background. IEEE Transactions on Aerospace and Electronic Systems 24(4): 427–445.
42. Gardner WA (1988) Signal interception: a unifying theoretical framework for feature detection. IEEE Transactions on Communications 36(8): 897–906.
43. Garth J & Poor HV (1992) Narrowband interference suppression in impulsive channels. IEEE Transactions on Aerospace and Electronic Systems 28(1): 15–34.
44. Gevargiz J, Das PJ & Milstein LB (1989) Adaptive narrowband interference rejection in a DS spread-spectrum intercept receiver using transform domain signal processing techniques. IEEE Transactions on Communications 37(12): 1359–1366.
45. Ghasemi A & Sousa ES (2005) Collaborative spectrum sensing for opportunistic access in fading environments. Proc. IEEE International Symposium on Dynamic Spectrum Access Networks, Baltimore, USA, 1: 131–136.
46. Goldsmith A, Jafar SA, Maric I & Srinivasa S (2009) Breaking spectrum gridlock with cognitive radios: An information theoretic perspective. IEEE 97(5): 894–914.
47. Hadi AS (1992) Identifying multiple outliers in multivariate data. Journal of the Royal Statistical Society 54(3): 761–771.
48. Hänninen T (2009) Implementation of spectrum sensing on wireless open-access research platform. Master's thesis, Department of Electrical and Information Engineering, Faculty of Technology, University of Oulu, Finland.
49. Hänninen T, Vartiainen J, Juntti M & Raustia M (2010) Implementation of spectrum sensing on wireless open-access research platform. Proc. 3rd International Workshop on Cognitive Radio and Advanced Spectrum Management COGART (in press), Rome, Italy.
50. Hardin J & Rocke DM (2005) The distribution of robust distances. Journal of Computational and Graphical Statistics 14: 1–19.
51. Harris FJ (1978) On the use of windows for harmonic analysis with the discrete Fourier transform. IEEE 66(1): 51–83.
52. Haykin S (1996) Adaptive filter theory. Prentice Hall, Upper Saddle River (N.J.), USA, 3rd edition.
53. Haykin S (2005) Cognitive radio: Brain-empowered wireless communications. IEEE Journal in Selected Areas in Comm 23(2): 201–220.
54. Hazmi A (2007) Studies in digital TV signal processing: impulse noise mitigation, repeater loop interference cancellation, and DVB-T transmission in CATV networks. Ph.D. thesis, Publication 668. Tampere University of Technology.
55. Henttu P (2000) A new interference suppression algorithm against broadband constant envelope interference. Proc. Military Communication Conference MILCOM, Los Angeles, CA, USA, 2: 742–746.
56. Henttu P (2003) Blind Interference Suppression in FH/DS Communication System. Licentiate thesis, University of Oulu, Finland.
57. Henttu P & Aromaa S (2002) Consecutive mean excision algorithm. Proc. IEEE 7th International Symposium on Spread Spectrum Techniques and Application, Praha, Czech Republic: 450–454.

58. Henttu P, Saarnisaari H & Aromaa S (2001) Interference suppression in DS/FH system using modified two sided adaptive filter. Proc. Military Communication Conference MILCOM, McLean, USA, 2: 1429–1433.
59. Himonas SD & Barkat M (1992) Automatic censored CFAR detection for nonhomogeneous environments. IEEE Transactions on Aerospace and Electronic Systems 28(1): 286–304.
60. Howard SJ (1992) Narrowband interference rejection using small FFT block sizes. Proc. IEEE Military Communications Conference MILCOM 1992, San Diego, USA: 608–612.
61. Höyhtyä M, Vartiainen J, Sarvanko H & Mämmelä A (2010) Combination of short term and long term database for cognitive radio resource management. Proc. 3rd International Workshop on Cognitive Radio and Advanced Spectrum Management COGART 2010, Rome, Italy. Invited paper (in press).
62. Huber PJ (1964) Robust estimation of a location parameter. The Annals of Mathematical Statistics 35: 73–101.
63. Juntti M, Saarnisaari H, Vartiainen J, Lehtomäki J & Myllylä M (2005) Diagnostic methods: General purpose tools for concentrated signal processing. Proc. International Workshop on Convergent Technologies IWCT, Oulu, Finland. Invited paper.
64. Kassam S & Poor HV (1985) Robust techniques for signal processing: A survey. IEEE 73(3): 433–481.
65. Kay SM (1998) Fundamentals of statistical signal processing: Detection theory. Prentice Hall, Upper Saddle River (NJ.), USA.
66. Keane HG (1991) A new approach to frequency line tracking. Proc. 25th Asilomar Conference on Signals, Systems and Computers, Monterey, California, USA, 2: 808–812.
67. Ketchum JW & Proakis JG (1982) Adaptive algorithms for estimating and suppressing narrow-band interference in PN spread-spectrum systems. IEEE Transactions on Communications COM-30(5): 913–924.
68. Khan Z, Lehtomäki J, Umebayashi K & Vartiainen J (2010) On the selection of the best detection performance sensors for cognitive radio networks. IEEE Signal Processing Letters 17(4): 359–362.
69. Kok CW & Nguyen TQ (1998) Multirate filter banks and transform coding gain. IEEE Transactions on Signal Processing 46(7): 2041–2044.
70. Laselva D, Zhao X, Meinilä J, Jämsä T, Nuutinen JP, Kyösti P & Hentilä L (2005) Empirical large-scale characterization of the received power for rural, suburban and indoor environments at 2.45 and 5.25 GHz. Proc. European cooperation in the field of scientific and technical research, Euro-Cost, Bologna, Italy.
71. Lehtomäki J, Salmenkaita S, Vartiainen J, Mäkelä JP, Vuohtoniemi R & Juntti M (2009) Measurement studies of a spectrum sensing algorithm based on double thresholding. Proc. 2nd International Workshop on Cognitive Radio and Advanced Spectrum Management COGART, Aalborg, Denmark: 69–73.
72. Lehtomäki J, Vartiainen J & Juntti M (2009) Combined wideband and narrowband signal detection for spectrum sensing. Proc. 2nd International Workshop on Cognitive Radio and Advanced Spectrum Management COGART, Aalborg, Denmark: 91–95.
73. Lehtomäki J, Vartiainen J, Juntti M & Saarnisaari H (2006) Spectrum sensing with forward methods. Proc. Military Communications Conference MILCOM, Washington DC, USA.
74. Lehtomäki J, Vartiainen J, Khan Z, & Bräysy T (2010) Selection of cognitive radios for cooperative sensing. Proc. 3rd International Workshop on Cognitive Radio and Advanced Spectrum Management COGART 2010, Rome, Italy. Invited paper (in press).

75. Lehtomäki J, Vartiainen J, Pyhtilä J & Saarnisaari H (2003) Energy detection of DS-CDMA signals with jammer excision in first stage. Proc. Signal Processing, Pattern Recognition, and Applications SPPRA 2003, Rhodes, Greece: 143–146.
76. Lehtomäki JJ, Juntti M & Saarnisaari H (2005) CFAR strategies for channelized radiometer. IEEE Signal Processing Letters 12: 13–16.
77. Lehtomäki JJ, Vartiainen J, Juntti M & Saarnisaari H (2008) Analysis of the LAD methods. IEEE Signal Processing Letters 15: 237–240.
78. Lehtomäki JJ, Vartiainen J & Saarnisaari H (2004) Domain selective interference excision and energy detection of direct sequence signals. Proc. 6th Nordic Signal Processing Symposium NORSIG 2004, Espoo, Finland.
79. Li C, Hu G & Liu M (2000) Narrow-band interference excision in spread-spectrum systems using self-orthogonalizing transform-domain adaptive filters. IEEE Journal on Selected Areas in Communications 18(3): 403–406.
80. Liang YZ & Kvalheim OM (1996) Robust methods for multivariate analysis - a tutorial review. Chemometrics and Intelligent Laboratory Systems 10: 1–10.
81. Lunden J, Koivunen V, Huttunen A & Poor HV (2009) Collaborative cyclostationary spectrum sensing for cognitive radio systems. IEEE Transactions on Signal Processing 57(11): 4182–4195.
82. Mahalanobis P (1936) On the generalized distance in statistic. Nat. Inst. Sci. India, Calcutta 2(1): 49–55.
83. Masreliez CJ (1975) Approximate non-Gaussian filtering with linear state and observation relations. IEEE Transactions on Automatic Control 20(2): 107–110.
84. Masry E & Milstein LB (1995) Enhanced signal interception in the presence of interference. IEEE Transactions on Communications 43: 1089–1096.
85. Matzner R & Englberger F (1994) An SNR estimation algorithm using fourth-order moments. Proc. Proceedings of the IEEE International Symposium on Information Theory, Trondheim, Norway: 119.
86. Middleton D (1999) Non-Gaussian noise models in signal processing for telecommunications: New methods and results for class A and B noise models. IEEE Transactions on Information Theory 45(4): 1129–1149.
87. Miller KS (1969) Complex Gaussian processes. SIAM Review 11: 544–567.
88. Milstein LB (1988) Interference rejection techniques in spread spectrum communications. IEEE 76: 657–671.
89. Milstein LB & Das PK (1977) Spread spectrum receiver using surface acoustic wave technology. IEEE Transactions on Communications COM-25: 841–847.
90. Milstein LB & Das PK (1980) An analysis of a real-time transform domain filtering digital communication system -part I: Narrowband interference rejection using real-time Fourier transforms. IEEE Transactions on Communications COM-28: 816–824.
91. Mishra SM, Sahai A & Brodersen R (2006) Cooperative sensing among cognitive radios. Proc. IEEE International Conference on Communications, Istanbul, Turkey.
92. Mitola III J (1999) Cognitive radio for flexible mobile multimedia communications. Proc. IEEE International Workshop on Mobile Multimedia Communications MoMuC 99, San Diego, CA, USA: 3–10.
93. Mitola III J (2009) Cognitive radio architecture evolution. IEEE 97(4): 626–641.
94. Mitola III J & Jr GQM (1999) Cognitive radio: making software radios more personal. IEEE Personal Communications 6(4): 13–18.

95. Mustafa H, Doroslovacki M & Deng H (2003) Algorithms for emitter detection based on the shape of power spectrum. Proc. Conference on Information Sciences and Systems, The Johns Hopkins University, Baltimore, MD, USA.
96. Neeser FD & Massey JL (1993) Proper complex random processes with applications to information theory. IEEE Transactions on Information Theory 39: 1293–1302.
97. Nicholson DL (1998) Spread spectrum signal design, LPE & AJ systems. Computer Science Press, USA.
98. Ofcom (2007) Digital dividend review: a statement on our approach to awarding the digital dividend.
99. Ollila E (2010) Contributions to independent component analysis, sensor array and complex-valued signal processing. Ph.D. thesis, Report 14. Department of Signal Processing and Acoustics. Faculty of Electronics, Communications and Automation. Helsinki University of Technology.
100. Ozaktas HM, Zalevsky Z & Kutay MA (2001) The Fractional Fourier Transform with Applications in Optics and Signal Processing. John Wiley & Sons, Chichester, England.
101. Pauluzzi DR & Beaulieu NC (2000) A comparison of SNR estimation techniques for the AWGN channel. IEEE Transactions on Communications 48: 1681 – 1691.
102. Peterson RL, Ziemer RE & Borth DE (1995) Introduction to spread spectrum communications. Prentice-Hall, Englewood Cliffs, HNJ, USA.
103. Poor HV (1998) An introduction to signal detection and estimation. Springer-Verlag, Berlin, Germany, 2nd edition.
104. Poor HV & Ruch LA (1998) Blind adaptive interference suppression of narrowband digital interferences from spread-spectrum signals. Wireless Personal Communications 6: 69–96.
105. Pouttu A, Raustia M, Henttu P, Saarnisaari H & Lahtinen T (2002) Method selection diversity approach to interference suppression. Proc. IEEE 7th International Symposium on Spread Spectrum Techniques and Application, Prague, Czech Republic: 623–627.
106. Press W, Vetterling W, Teukolsky S & Flannery B (1992) Numerical Recipes in C. Cambridge University Press, New York, USA, 2nd edition.
107. Proakis J (1995) Digital Communications. McGraw-Hill, New York, USA.
108. Puska H, Saarnisaari H & Iinatti J (2005) Comparison of antenna array algorithms in DS/SS code acquisition with jamming. Proc. Military Communications Conference MILCOM, Atlantic City, USA.
109. Puska H, Saarnisaari H & Iinatti J (2005) Comparison of matched filter acquisition using beamforming and CME algorithm in impulsive interference. Proc. IEEE 61st Vehicular Technology Conference VTC, Stockholm, Sweden.
110. Quan Z, Cui S & Sayed AH (2008) Optimal linear cooperation for spectrum sensing in cognitive radio networks. IEEE Journal on Selected Areas in Signal Processing 2(1).
111. Renzo MD, Imbriglio L, Graziosi F & Santucci F (2009) Distributed data fusion over correlated log-normal sensing and reporting channels: application to cognitive radio networks. IEEE Transactions on Wireless Communications 8(12): 5813–5821.
112. Rifkin R (1991) Comments on narrowband interference rejection using real-time Fourier transforms. IEEE Transactions on Communications 39(9): 1292–1293.
113. Rocke DM (1996) Robustness properties of S-estimators of multivariate location and shape in high dimension. The Annals of Statistics 24(3): 1327–1345.
114. Rocke DM & Woodruff DL (1996) Identification of outliers in multivariate data. Journal of the American Statistical Association 91(435): 1047–1061.

115. Rusch LA & Poor HV (1994) Narrowband interference suppression in CDMA spread spectrum communications. IEEE Transactions on Communications 42(2/3/4): 1969–1979.
116. Saarnisaari H (2004) Consecutive mean excision algorithms in narrowband or short time interference mitigation. Proc. Position Location and Navigation Symposium PLANS 2004, Monterey, CA, USA: 447–454.
117. Saarnisaari H & Henttu P (2003) Impulse detection and rejection methods for radio systems. Proc. IEEE Military Communications Conference MILCOM 2003, Boston, MA, USA. CD-rom.
118. Saarnisaari H, Henttu P & Juntti M (2005) Iterative multidimensional impulse detectors for communications based on the classical diagnostic methods. IEEE Transactions on Communications 53(3): 395–398.
119. Sahai A, Cabric D, Hoven N, Tandra R, Mishra S & Brodersen R (2005) Spectrum sensing: fundamental limits and practical challenges (tutorial). Proc. IEEE International Symposium on Dynamic Spectrum Access Networks, Baltimore, Maryland.
120. Saulnier GJ (1992) Suppression of narrowband jammers in a spread spectrum receiver using transform domain adaptive filtering. IEEE Journal on Selected Areas in Communications 10: 742–749.
121. Shah B & Hinedi S (1990) The split symbol moments SNR estimator in narrow-band channels. IEEE Transactions on Aerospace and Electronic Systems 26(5): 737–747.
122. Shankar SN, Cordeiro C & Challapali K (2005) Spectrum agile radios: Utilization and sensing architectures. Proc. IEEE International Symposium on Dynamic Spectrum Access Networks, Baltimore, USA, 1: 160–169.
123. Simon MK, Omura JK & Levitt BK (1994) Spread spectrum communications handbook. McGraw-Hill, USA.
124. Skolnik MI (2001) Introduction to Radar Systems. McGraw-Hill, NY, USA.
125. Sonnenschein A & Fishman PM (1992) Radiometric detection of spread-spectrum signals in noise of uncertain power. IEEE Transactions on Aerospace and Electronic Systems 28: 654–660.
126. Spaulding A & Middleton D (1977) Optimum reception in an impulsive interference environment-part i: Coherent detection. IEEE Transactions on Communications 25(9): 910–923.
127. Spaulding A & Middleton D (1977) Optimum reception in an impulsive interference environment-part ii: Incoherent detection. IEEE Transactions on Communications 25(9): 924–934.
128. Stevenson CR (2006) IEEE p802.22 wireless RANs: Initial TV band comments text from .22 to .18. IEEE 802.22-06/-247r0.
129. Stitz T & Renfors M (2004) Filter-bank-based narrowband interference detection and suppression in spread spectrum systems. EURASIP Journal on Applied Signal Processing: 1163–1176.
130. Stoica P & Moses RL (1997) Introduction to Spectral Analysis. Prentice Hall, Upper Saddle River, NJ, USA.
131. Thompson WR (1935) On a criterion for the rejection of observations and the distribution of the ratio of deviation to sample stantard deviation. The Annals of Mathematical Statistics 6(4): 214–219.
132. Tian Z & Giannakis GB (2006) A wavelet approach to wideband spectrum sensing for cognitive radios. Proc. 1st International Conference on Cognitive Radio Oriented Wireless

Networks and Communications CrownCom, Greece: 1–5.
133. Torrieri DJ (1992) Principles of secure communication system. Artech House, Norwood, MA, USA, 2nd edition.
134. Trees HLV (1968) Detection, estimation, and modulation theory, Part I. John Wiley, New York, USA.
135. Trees HLV (1992) Detection, estimation, and modulation theory, Part 3: Radar-Sonar Signal Processing and Gaussian Signals in Noise. John Wiley, New York, USA.
136. Tsakalides P & Nikias C (1995) Maximum likelihood localization of sources in noise modeled as a stable process. IEEE Transactions on Signal Processing 43(11): 2700–2713.
137. Urkowitz H (1967) Energy detection of unknown deterministic signals. IEEE 55(4): 523–531.
138. Vartiainen J (2005) Concentrated signal extraction using consecutive mean excision algorithms. Proc. Finnish Signal Processing Symposium FINSIG, Kuopio, Finland. CD-rom.
139. Vartiainen J (2007) Localization of narrowband signals. Patent granted, US Pat. 7231194, Jun. 12, 2007.
140. Vartiainen J, Alatossava M, Lehtomäki JJ & Saarnisaari H (2006) Interference suppression for measured radio channel data at 2.45 GHz. Proc. IEEE International Symposium on Personal, Indoor, and Mobile Radio Communications PIMRC, Helsinki, Finland.
141. Vartiainen J, Aromaa S, Saarnisaari H & Juntti M (2004) Selection process of a transform selective interference suppression algorithm. Proc. 6th Nordic Signal Processing Symposium NORSIG 2004, Espoo, Finland: 220–223. CD-rom.
142. Vartiainen J, Höyhtyä M, Lehtomäki J & Bräysy T (2010) Priority channel selection based on detection history database. Proc. 5th International Conference on Cognitive Radio Oriented Wireless Networks and Communications CrownCom 2010, Cannes, France.
143. Vartiainen J, Lehtomäki J, Aromaa S & Saarnisaari H (2004) Localization of multiple narrowband signals based on the FCME algorithm. Proc. Nordic Radio Symposium NRS 2004 including the Finnish Wireless Communications Workshop FWCW 2004, Oulu, Finland. CD-rom.
144. Vartiainen J, Lehtomäki JJ, Henttu P & Raustia M (2003) A narrowband signal detection algorithm in wideband receivers. Proc. XXVIII Convention on Radio Science and IV Finnish Wireless Communications Workshop URSI/FWCW 2003, Oulu, Finland.
145. Vartiainen J, Lehtomäki JJ & Saarnisaari H (2003) Detection of DS-CDMA signals under narrowband interference. Proc. XXVIII Convention on Radio Science and IV Finnish Wireless Communications Workshop URSI/FWCW 2003, Oulu, Finland.
146. Vartiainen J, Lehtomäki JJ & Saarnisaari H (2004) Performance of forward consecutive mean excision interference suppressor in direct sequence systems. Proc. Nordic Radio Symposium NRS 2004 including the Finnish Wireless Communications Workshop FWCW 2004, Oulu, Finland. CD-rom.
147. Vartiainen J, Lehtomäki JJ, Saarnisaari H & Juntti M (2005) Transform selection metrics for interference suppression. Proc. Finnish Signal Processing Symposium FINSIG, Kuopio, Finland. Cd-rom.
148. Vartiainen J, Lehtomäki JJ, Saarnisaari H & Juntti M (2010) Analysis of the consecutive mean excision algorithms. Journal of Electrical and Computer Engineering (submitted).
149. Vartiainen J, Sarvanko H, Lehtomäki J, Juntti M & Latva-Aho M (2007) Energy detection based spectrum sensing methods in cognitive radios. Proc. Wireless World Research Forum WWRF, Espoo, Finland.

150. Veeravalli VV & Poor HV (1991) Quadratic detection of signals with drifting phase. Journal of the Acoustical Society of America 89(2): 811–819.
151. Vijayan R & Poor HV (1990) Nonlinear techniques for interference suppression in spread spectrum systems. IEEE Transactions on Communications 38(7): 1060–1065.
152. Visotsky E, Kuffner S & Peterson R (2005) On collaborative detection of TV transmissions in support of dynamic spectrum sensing. Proc. IEEE Symposium on New Frontiers in Dynamic Spectrum Access Networks, Baltimore, USA.
153. Wang H, Yang E, Zhao Z & Zhang W (2009) Spectrum sensing in cognitive radio using goodness of fit testing. IEEE Transactions on Wireless Communications 8(11): 5427–5430.
154. Wang KJ & Yao Y (1999) New nonlinear algorithms for narrowband interference suppression in CDMA spread-spectrum systems. IEEE Journal on Selected Areas in Communications 17(12): 2148–2153.
155. Wang S, An JP, Wang AH & Bu XY (2010) A minimum value based threshold setting strategy for frequency domain interference excision. IEEE Signal Processing Letters 17(5): 501–504.
156. Wang S, Patenaude F & Inkol R (2007) Computation of the normalized detection threshold for the FFT filter bank-based summation CFAR detector. Journal of Computers 2(6): 35–48.
157. Wang X & Poor V (1999) Robust multiuser detection in non-Gaussian channels. IEEE Transactions on Signal Processing 47(2): 289–305.
158. Widrow B *et al* (1975) Adaptive noise cancelling: Principles and applications. IEEE 63: 1692–1716.
159. Wiley RG (1993) Electronic intelligence: the analysis of radar signals. Artech House, London, 2nd edition.
160. Wisnowski JW, Montgomery DC & Simpson JR (2001) A comparative analysis of multiple outlier detection procedures in the linear regression model. Computational Statistics & Data Analysis 36(3): 351–382.
161. Woodhouse IH (2001) The ratio of the arithmetic to the geometric mean: A cross-entropy interpretation. IEEE Transactions on Geoscience and Remote Sensing 39(1): 188–189.
162. Young JA & Lehnert JS (1998) Analysis of DFT-based frequency excision algorithms for direct-sequence spread-spectrum systems. IEEE Transactions on Communications 46(8): 1076–1087.
163. Young JA & Lehnert JS (1999) Performance metrics for windows used in real-time DFT-based multiple-tone frequency excision. IEEE Transactions on Signal Processing 47(3): 800–812.
164. Yücek T & Arslan H (2006) Spectrum characterization for opportunistic cognitive radio systems. Proc. IEEE Military Communications Conference MILCOM, Washington DC, USA.
165. Zeng Y & Liang Y (2009) Eigenvalue-based spectrum sensing algorithms for cognitive radio. IEEE Transactions on Communications 57(6): 1784–1793.
166. Zhang W, Mallik RK & Letaief KB (2009) Optimization of cooperative spectrum sensing with energy detection in cognitive radio networks. IEEE Transactions on Wireless Communications 8(12): 5761–5766.
167. Zhang X, Luo L & Zhou Y (2005) Consecutive mean excision based signal existence detection in AWGN. Proc. 5th International Wireless Communications, Networking and Mobile Computing WiCom, Shanghai, China.

168. Zheng X, Cui L, Chen J, Wu Q & Wang J (2008) Cooperative spectrum sensing in cognitive radio systems. Proc. Congress on Image and Signal Processing CISP, Sanya, Hainan, China, 262–266.
169. Zheng Y, Xie X & Yang L (2009) Cooperative spectrum sensing based on blind source separation for cognitive radio. Proc. 1st International Conference on Future Information Networks ICFIN, Beijing, China, 398–402.
170. Ziemer RE & Peterson RL (1985) Digital communications and spread spectrum systems. Macmillan Publishing, USA.

Original articles

I Vartiainen J, Aromaa S, Saarnisaari H & Juntti M (2004) Performance Evaluation of Transform Selective Interference Suppression. IEEE Military Communications Conference MILCOM 2004, Monterey, CA, USA.

II Vartiainen J, Lehtomäki J, Saarnisaari H & Juntti M (2005) Interference Suppression in Several Transform Domains. IEEE Military Communication Conference MILCOM 2005, Atlantic City, USA.

III Vartiainen J, Lehtomäki J, Saarnisaari H & Henttu P (2004) Estimation of Signal Detection Threshold by CME algorithms. IEEE Vehicular Technology Conference VTC 2004 spring, Milan, Italy.

IV Lehtomäki J, Vartiainen J, Juntti M & Saarnisaari H (2007) CFAR Outlier Detection with Forward Methods. IEEE Transactions on Signal Processing 55(9): 4702–4706.

V Vartiainen J, Lehtomäki J, Saarnisaari H & Juntti M (2010) Limits of Detection for the Consecutive Mean Excision Algorithms. 5th International Conference on Cognitive Radio Oriented Wireless Networks and Communications CrownCom 2010, Cannes, France.

VI Vartiainen J, Lehtomäki J & Saarnisaari H (2005) Double-Threshold based Narrowband Signal Extraction. IEEE 61st Semiannual Vehicular Technology conference VTC 2005 spring, Stockholm, Sweden.

VII Vartiainen J, Saarnisaari H, Lehtomäki J & Juntti M (2006) A Blind Signal Localization and SNR Estimation Method. IEEE Military Communication Conference MILCOM 2006, Washington DC, USA.

VIII Vartiainen J, Sarvanko H, Lehtomäki J, Juntti M. & Latva-aho M (2007) Spectrum Sensing with LAD based Methods. IEEE International Symposium on Personal, Indoor and Mobile Radio Communications PIMRC 2007, Athens, Greece.

IX Vartiainen J, Lehtomäki J, Saarnisaari H, Juntti M & Umebayashi K (2010) Two-Dimensional Signal Localization Algorithm for Spectrum Sensing. IEICE Transactions on Communications E93-B(11).

Original publications are not included in the electronic version of the dissertation.

351. Haverinen, Hanna (2010) Inkjet-printed quantum dot hybrid light-emitting devices—towards display applications

352. Bykov, Alexander (2010) Experimental investigation and numerical simulation of laser light propagation in strongly scattering media with structural and dynamic inhomogeneities

353. Kannala, Juho (2010) Models and methods for geometric computer vision

354. Kela, Lari (2010) Attenuating amplitude of pulsating pressure in a low-pressure hydraulic system by an adaptive Helmholtz resonator

355. Ronkainen, Sami (2010) Designing for ultra-mobile interaction : experiences and a method

356. Loikkanen, Mikko (2010) Design and compensation of high performance class AB amplifiers

357. Puikko, Janne (2010) An exact management method for demand driven, industrial operations

358. Ylioinas, Jari (2010) Iterative detection, decoding, and channel estimation in MIMO-OFDM

359. Tervonen, Pekka (2010) Integrated ESSQ management : as a part of excellent operational and business management—a framework, integration and maturity

360. Putkonen, Ari (2010) Macroergonomic approach applied to work system modelling in product development contexts

361. Ou, Zhonghong (2010) Structured peer-to-peer networks: Hierarchical architecture and performance evaluation

362. Sahlman, Kari (2010) Elements of strategic technology management

363. Isokangas, Ari (2010) Analysis and management of wood room

364. Väänänen, Mirja (2010) Communication in high technology product development projects : project personnel's viewpoint for improvement

365. Korhonen, Esa (2010) On-chip testing of A/D and D/A converters : static linearity testing without statistically known stimulus

366. Palukuru, Vamsi Krishna (2010) Electrically tunable microwave devices using BST-LTCC thick films

367. Saarenpää, Ensio (2010) Good construction quality : the realisation of good construction quality in Finnish construction regulations

Book orders:
Granum: Virtual book store
http://granum.uta.fi/granum/

UNIVERSITY OF OULU P.O.B. 7500 FI-90014 UNIVERSITY OF OULU FINLAND

ACTA UNIVERSITATIS OULUENSIS

ISBN 978-951-42-6348-4 (Paperback)
ISBN 978-951-42-6349-1 (PDF)
ISSN 0355-3213 (Print)
ISSN 1796-2226 (Online)

UNIVERSITY of OULU
OULUN YLIOPISTO